K.S. RANGASAMY COLLEGE OF TECHNOLOGY

TIRUCHENGODE 637215

DEPARTMENT OF TEXTILE TECHNOLOGY

COURSE MATERIAL

Subject code : 50TT 302

Subject name : Structure and Properties of Fibers

Year / Semester : II / IV

K.S. Rangasamy College of Technology - Autonomous **R 2018**

50 TT 302 - Structure and Properties of Fibers

B.Tech. Textile Technology

Semester	Hours / Week			Total hrs	Credit	Maximum Marks		
	L	T	P		C	CA	ES	Total
III	4	0	0	60	4	50	50	100

Objective(s)	• To expose the students to the various methods in structural investigation of fibres. • To enable the students to understand the moisture absorption properties of fibres. • To enable the students to understand the mechanical properties of fibres. • To enable the students to understand the optical and frictional properties of fibres. • To enable the students to understand the thermal and electrical properties of fibres.
Course Outcomes	**At the end of the course, the students will be able to** 1. Review the different methods in the investigation of fibres. 2. Describe the moisture absorption properties of fibres. 3. Discuss the concepts of mechanical properties of fibres. 4. Explain the optical and frictional properties of fibres. 5. Outline the thermal and electrical properties of fibres.

Note: Hours notified against each unit in the syllabus are only indicative but are not decisive. Faculty may decide the number of hours for each unit depending upon the concepts and depth. Questions need not be asked based on the number of hours notified against each unit in the syllabus.

Structural Investigation of Fibres

Basic requirements for fibre formation; Models of fibre structure-fringed micelle, fringed fibril and fringed lamellar models. Investigation of fibre structure by X-ray diffraction, SEM, TEM, STEM, FTIR and NMR. [10]

Moisture Absorption Properties of Fibres

Definitions- humidity, relative humidity, standard testing atmosphere, moisture content and regain; hysteresis in moisture absorption; moisture absorption behaviour of textile fibres; Influence of various factors on regain; absorption in crystalline and amorphous regions.

Heats of sorption-Integral and differential, measurement, effects of heats of sorption; Conditioning of fibres, mechanism of conditioning, factors influencing the rate of conditioning; swelling of fibres, types of swelling and its measurement. [12]

Mechanical Properties of Fibres

Tensile property- definitions related to tensile property; stress strain curves of various textile fibres and its importance, influence of moisture and temperature on tensile characteristics, Weak- link effect.

Elastic recovery and its relation to stress and strain of various textile fibres; Mechanical conditioning of fibres.

Time dependent effects- creep and stress relaxation phenomena; Directional effects – Brief study on flexural and torsional rigidity of fibres. [14]

Optical and Frictional Properties of Fibres

Optical property - Refractive index and its measurement; Birefringence and its measurement; Absorption and dichroism; reflection and lustre of fibres.

Frictional property - Amonton's and Bowden's law of friction, various influencing factors- load, area of contact, speed of sliding, state of surface and regain; directional frictional effect of wool. [12]

Thermal and Electrical Properties of Fibres

Thermal property- structural changes in fibres on heating, thermal transitions and melting; heat setting of fibres and its importance. Electrical property- mass specific resistance; influence of moisture, temperature and impurities on resistance; Dielectric properties-factors influencing dielectric properties of fibre; Static electricity – introduction, problems and elimination techniques. [12]

Total Hours: 60

Text book(s):

1. Morton W.E. and Hearle J.W.S., "Physical properties of textile fibres", published by The Textile Institute Manchester,U.K., 4th Edition, 2008.ISBN 978-1-84569-220-9.
2. Meredith R. and Hearle J.W.S., "Physical methods of investigation of textiles", Wiley Publications, Newyork, 1989.

Reference(s) :

1. Meredith R., "Mechanical Properties of Textile Fibres", North Holland, Amsterdam, 1986.
2. Mukhopadhyay S.K., "Advances in fibre science", The Textile Institute, Manchester, U.K., 1992.
3. Gordon cook. J,"Hand book of textile fibres –Vol.I - Natural fibers", Wood Head Publishing Limited, Cambridge-England, 2006.
4. Sreenivasa Murthy.H.V, "Introduction to Textile Fibers", Revised Edition, Wood Head Publishing India Private Limited, New Delhi.

Dr. G. KARTHIKEYAN, B.E., M.Tech., Ph.D
Professor and Head
Department of Textile Technology

UNIT : I

STRUCTURAL INVESTIGATION OF FIBERS

Basic Requirement of Fiber Forming Polymers

a) Long chain molecules ,corresponding to the long fibers that make up yarns: if the molecules or fibers are too short, There will be a loss of strength as illustrated in diagram.

b) A More or less parallel arrangement of the molecules.

c) Laternal forces to hold the molecules together and give cohesion to the structure.

d) Some measure of freedom of molecules movement in order to give necessary extensibility to the fiber and some openness to give room for moisture absorption and uptake of dyes.

ESSENSIAL REQUIREMENT OF FIBER FORMING POLYMERS

.

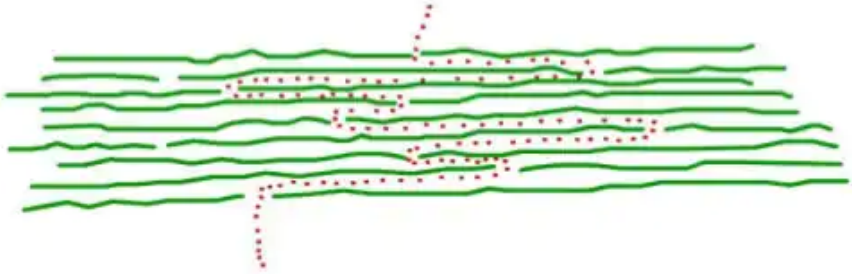

Fig 4: A figure shows strong fiber as it has long 'path of break' [1].

Figure 5 shows polymers of low molecular weight. Although they are well oriented, the shortness of its 'path of break' tends to make it weak fiber and polymers with high molecular weight results in long 'path of break' results in the strong fibers with well orientation.

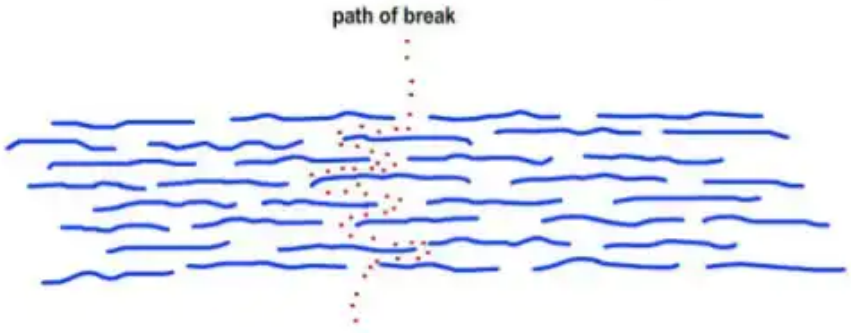

Fig 5: Weak fiber as it has short 'path of break' [1].

vi. **Orientation**

Fiber polymers should be capable of being oriented. The polymers are aligned into more or less parallel order in the direction of the longitudinal axis of the fiber or filament. The orientation of

SEM-Scanning Electron Microscope

Scanning Electron Microscope is an improved model of an electron microscope. SEM is used to study the three dimensional image of the specimen.

Working Principle:

When the accelerated primary electrons stricks the sample, it produces secondary electrons. These secondary electrons are collected by a positive charged electron detector which in turn gives a 3-dimensional image of the sample.

Construction:

- **It consists of an electron gun to produce high energy electron beam. A magnetic condensing lens is used to condense the electron beam and a scanning coil is arranged in between magnetic condensing lens and the sample.**
- **The electron detector (Scintillator) is used to collect the secondary electrons and can be converted into electrical signal. These signals can be fed into CRO drogh video amplifier as shown in fig.**

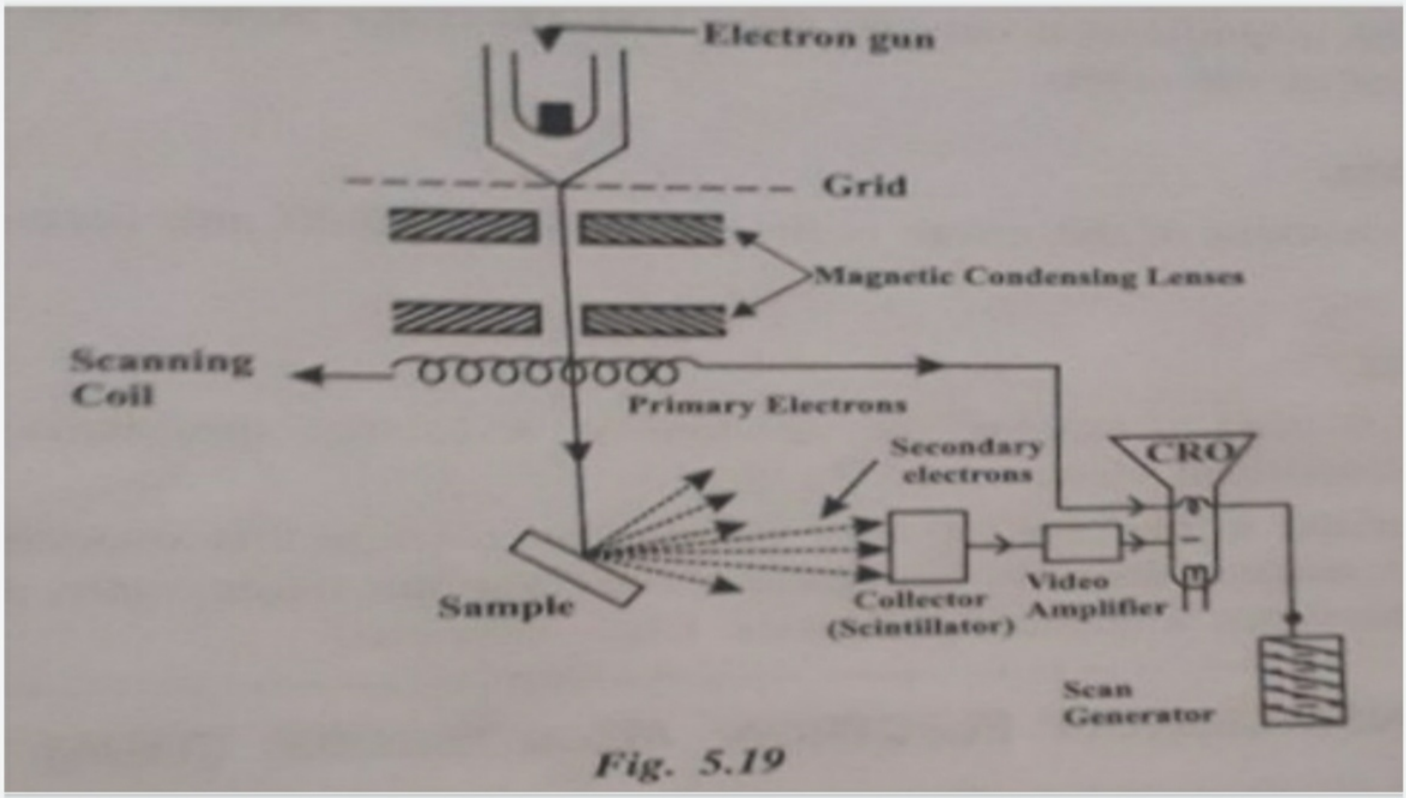

Fig. 5.19

Working:

- Stream of electrons are produced by the electron gun and these primary electrons are accelerated by the grid and anode. These accelerated primary electrons are made to incident on the sample through condensing lenses and scanning coil.

- These high speed primary electrons on falling over the sample produces low energy secondary electrons. The collection of secondary electrons are very difficult because of their low energy. Therefore, to collect these secondary electrons, a very high voltage is applied to the collector

- These collected electrons produce scintillatons on photo-multplier tube (detector) and are converted into electrical signals. These signals are amplified by the video amplifier and is fed to the CRO.

- By similar procedure the electron beam scans he sample from lef to right and again from left to right etc.. rad a book (fig. 5.20), and the whole picture

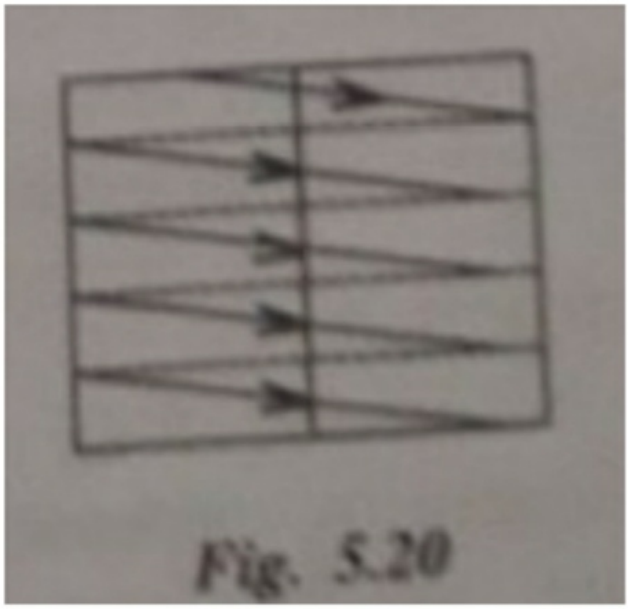

Fig. 5.20

SEM IMAGE

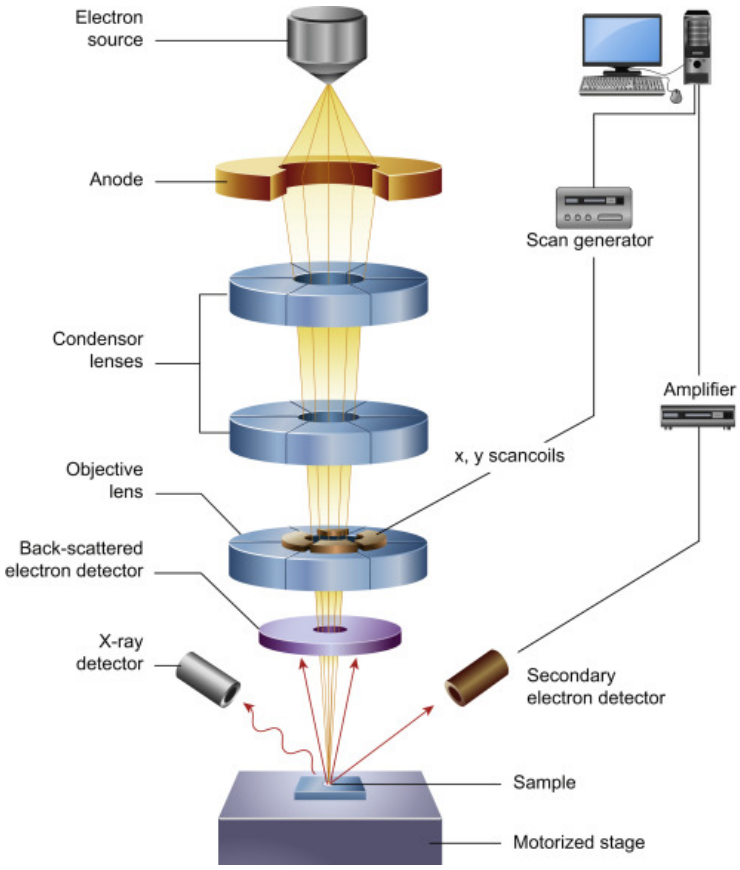

Advantages

(i) It can be used to examine specimens of large thickness.
(ii) It has large depth of focus.
(iii) It can be used to get a three dimensional image of the object.
(iv) Since the image can be directly viewed in the screen, structural details can be resolved in a precise manner.
(v) The magnification may be upto 3,00,000 times greater than that of the size of the object.

Disadvantage

The resolution of the image is limited to about 10-20 nm, hence it is very poor

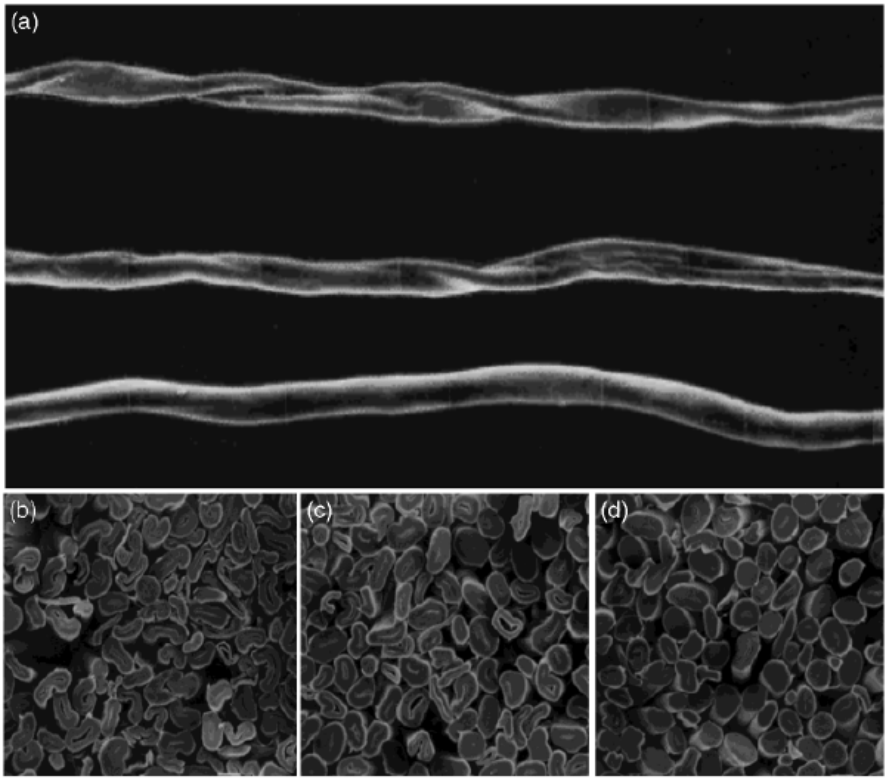

SEM images of cotton fibers.

(a) Side view of cotton fibers from top to bottom: bleached, mercerized, and liquid ammonia treated.

Cross-section views of
(b) bleached cotton,
(c) mercerized cotton, and
(d) liquid ammonia-treated cotton fabric.

TEM - Transmission Electron Microscope

We know in scanning electron microscope the resolution of the image is limited only upto 10-20 nm. This will not be useful to view the internal features of an atom (or) the morphology of a sample of size say 0.2 nm.

Thus to examine the sample of size upto 0.2 nm, the transmission electron microscope can be used. In this microscope the image is obtained by transmitting the electrons through the specimen.

Principle

Electrons are made to pass through the specimen and the image is formed in the fluorescent screen, either by using transmitted beam (Bright field image) on by using diffracted beam (Dark field image).

Construction

It consists of an electrorgun to produce electrons. Magnetic condensing lens is used to condense the electrons and is also used to adjust the size of the electron that falls onto the specimen.

The specimen is placed in between the condensing lens and objective lens as shown in fig 5.21. The magnetic objective lens is used to block the high angle di fracted beams and the aperature is used to eliminate the di fracted beam (if any) and in turn it increases the contrast of the image.

The magnetic projector lens is placed above the fluorescent screen inorder to achieve higher magnification. The image can be recorded by using a fluorescent (phosphor) screen or (CCD) (charged coupled device) also.

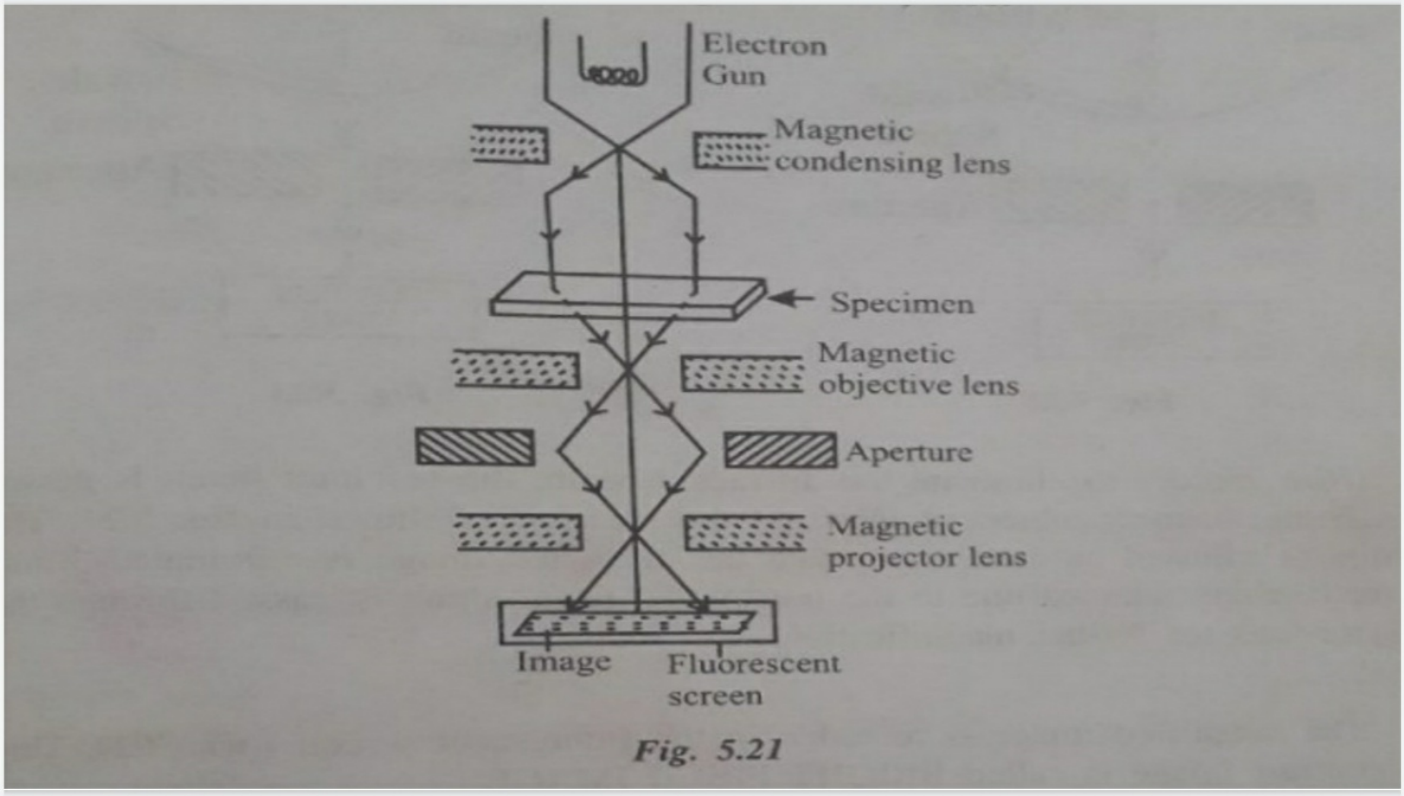

Fig. 5.21

Working

• Stream of electrons are produced by the electron gun and is made to fall over the specimen using the magnetic condensing lens.

• Based on the angle of incidence, the beam is partly transmitted and partly diffracted, as shown in fig 5.22. Both the transmitted beam and the diffracted beams are recombined at the E-wald sphere (sphere of reflection which encloses all possible reflections from the crystal/specimen, satisfying Bragg's law), to form the image as shown in fig 5.2 The combined image is called the phase contrast image.

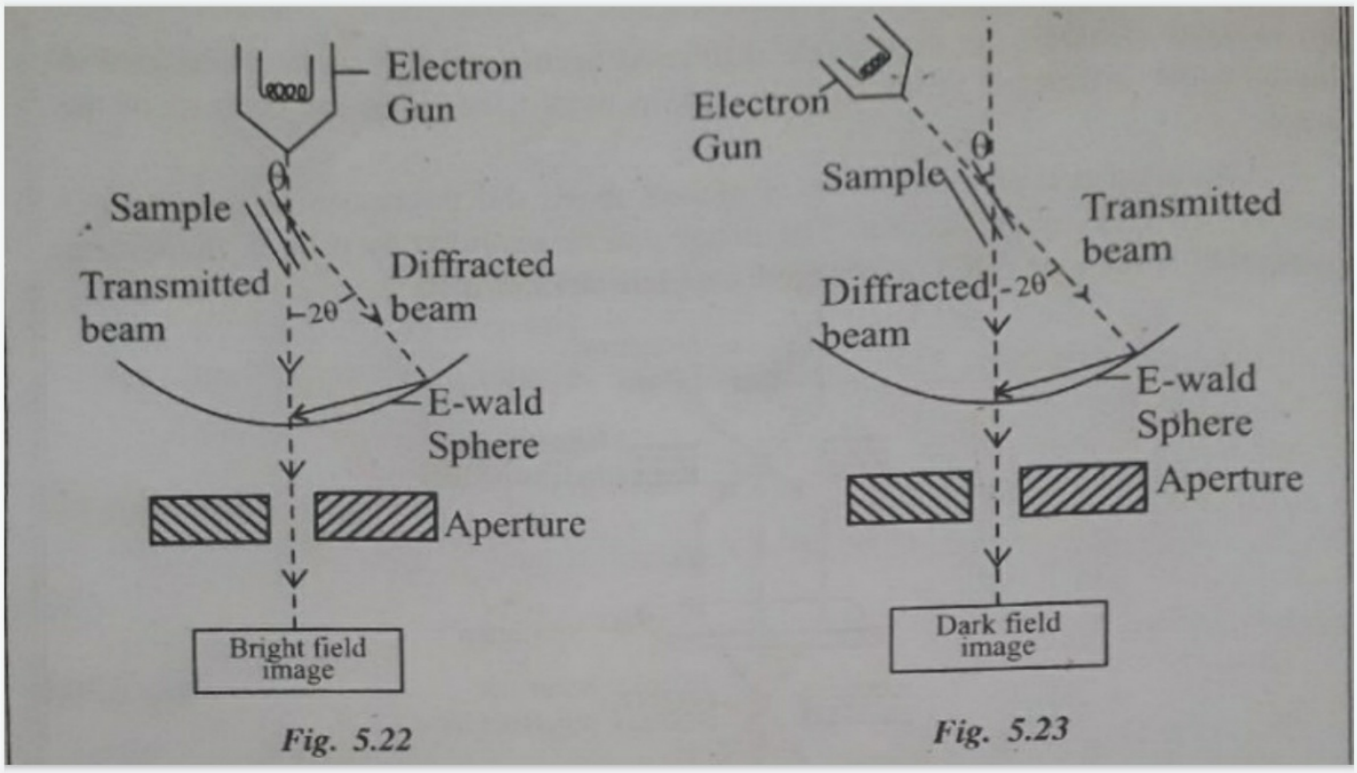

Fig. 5.22 *Fig. 5.23*

TEM IMAGE

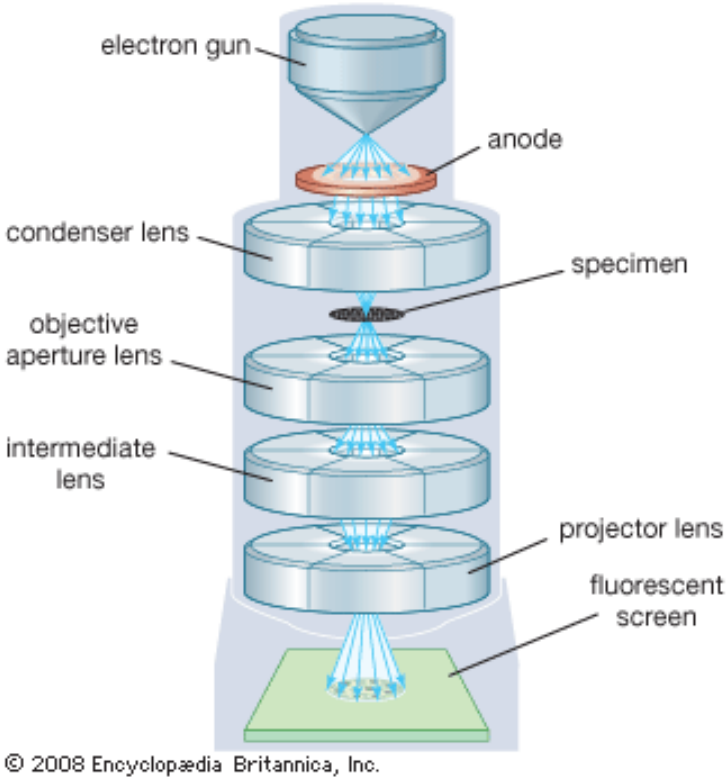

The magnified image is recorded in the fluorescent screen (or) CCD. This high contrast image is called BRIGHT FIELD IMAGE.

Also, it has to be noted that the bright field image obtained is purely due to the elastic scattering (no energy change) i.e., due to transmitted beam alone.

Advantages

1. It can be used to examine the specimen of size upto 0.2 nm.
2. The magnification is 1,000,000 times greater than the size of the object.
3. It has high resolution.
4. The resolving power is 1 A to 2 Å.
5. We can get high contrast image due to both transmitted beams (bright field) and diffracted beam (dark field)

Disadvantages

1.The specimen should be very thin.
2. It is not suitable for thick samples.
3. There are chances for the structural change, during sample preparaton.
4. 3-dimensional image cannot be obtained.
5. In case of biological samples, the electrons may interact with the samples, which may even damage the sample

Applications

1. The main application of TEM is in nano-sciences (nano-tubes, micro machines etc), used to find the internal structures of nano-materials.
2. It is used to find the 2-dimensional image of very small biological cells. virus, bacteria etc.
3. It is used in thin-film technology, metallurgy, bio-chemistry, micro-biology etc.
4. It is used to study the compositions of paints, papers, fibers, composite materials, alloys etc.,

Scanning transmission electron microscope(STEM)

Scanning transmission electron microscope (STEM) is designed with the features of both the scanning electron microscope (SEM) and transmission electron microscope (TEM).

STEM=TEM+SEM

We know in transmission electron microscope, we can get bright field image due to elastic scattering i.e., transmission of electrons and dark field image due to inelastic scattering i.e., diffraction of electrons. The same principle is used in STEM along with a scanning process and hence this microscope is called scanning TEM

Principle

Electrons are made to pass through the specimen and the specimen is scanned using scanning coils. The transmitted beam is used to produce 3-dimensional bright field image and the diffracted beam can be used to produce the 3-dimensional dark field image in the CRO (cathode ray oscilloscope).

Construction

It consists of an electron gun to produce sam of electrons. Three types of lenses were used at various sectors viz.

(i) Magnetic condensing lens: To condense the electron beams and to effectively focus those electrons onto the specimen

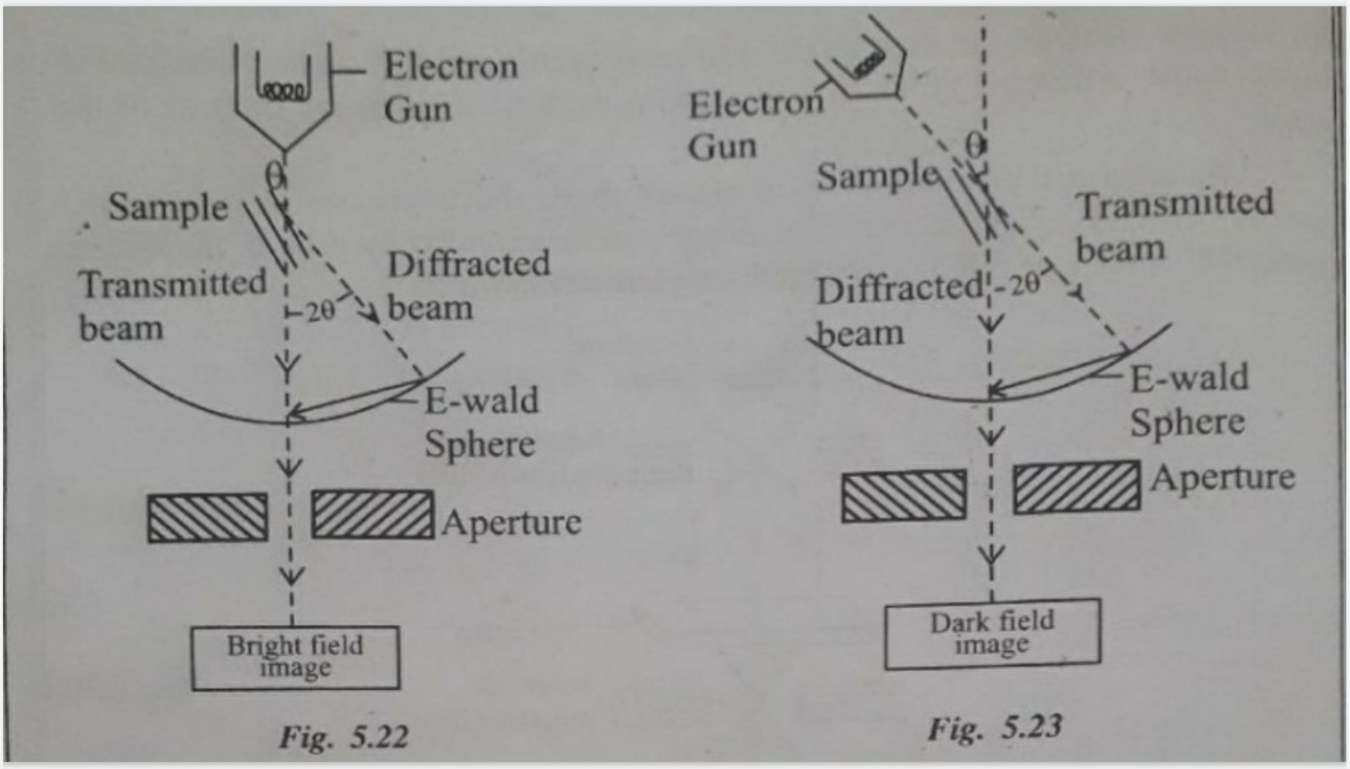

Fig. 5.22 *Fig. 5.23*

ii) Objective lens: Here we have two types of objective lenses viz (a) Objective ens-1, with a scanning coil as shown in fig 5.24 and (b) objective lens-2 to increase the contrast of the image.

iii) Intermediate lens: It is similar to a projector lens, which is used to magnify the image produced. The final image can be amplified using an amplifier.

The scanning coil and the detector is connected to the CRO in order to scan and view the image on the screen, respectively

Working

- Stream of electrons are produced by the electron gun. These electrons are made to fall on the objective lens scanning coil, with the help of a magnetc condensing lens.
- The electron beam is effectively focussed onto the specimen with the help of the scanning coil, by step by step procedure. The positons of the scanning coil is recorded in the CRO.
- The electron beam after a passing through the specimen produces a diffraction pattern, so called nano diffraction. Also a part of the beam is transmitted through the specimen (without energy loss), similar to that in the TEM.
- We can get the required image pattern, either by adjusttng the angle of incidence (or) by adjusting the apertures in the instrument.

Now by properly adjusting the apertures we can get any one of the following images viz.

(i) Bright field image (Due to elastic scattering)

(ii) Dark field image (Due to inelastic scattering

Advantages

1. It has high resolution (0.1 nm) and high contrast.
2.It is used to examine the nano materials of size 1 nm.
3. It is used to produce a 3-dimensional image of the specimen.
4. All kinds of materials such as crystalline, amorphous and biological materials can be investigated.

Disadvantages

1. Cost is very high
2. Sample preparation is tedious.
3. Some specimen can loss its structural property due to the interaction of electrons with the sample.
4. The procedure for the elimination of unwanted beams using aperture is complicated

Applications

1. STEM is used in finding the nano-structures.
2. It is used to get the 3-dimensional image of plant cells, biological cells. DNA, bacteriophages etc.
3. In Engineering they are used in thin-film technology, quantum physics, nano sciences etc.
4. They are used to find the structural composition of paper pulps, ceramic materials, polymer etc.
5. They are also used in mass mapping (mass determination process).

STEM mode

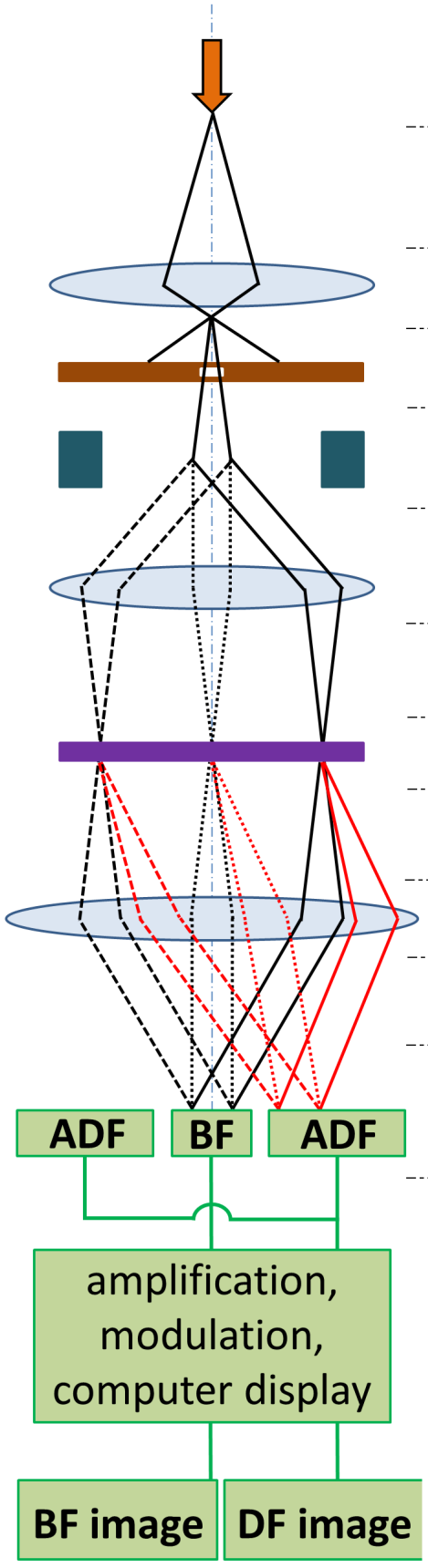

Electron Gun

System of condenser lenses

Condenser aperture

Deflection scan coils

Upper-objective polepiece

Specimen

Lower-objective polepiece

STEM detector
(back focal plane of objective lens)

AIM: X-Ray Diffraction (XRD)

To determine the particle size of the given sample by Powder XRD and Debye-scherrer formula

EQUIPMENT'S NEEDED:

XRD – data of the sample.

PRINCIPLE:

Using scherrer formula in X - ray pattern surface area measured in an instrument based on this principle is in excellent agreement with that measured by the gas adsorption technique has a number of advantages over the gas adsorption technique.

METHOD I:

Fig 1 shows the X-ray diffraction pattern of nano crystalline silicon which exhibits significant line broadening shown for comparison is the diffraction pattern from bulk size with a particle size greater than 20 nm. Note that the ka2 line is well resolved in the bulk sample but indistinguishable in the n – Si case. The extent of broadening is described by b, which is the full width at half maximum intensity of the peak.

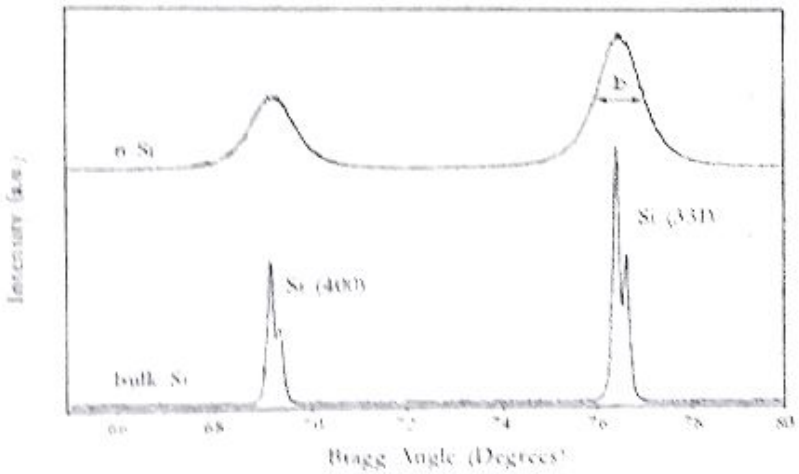

After the value of b is corrected for the instrumental contribution, it can be substituted into scherrer's equation

$$D = \frac{K\lambda}{\beta \cos\theta}$$

$$\text{The pure width, } \beta = \sqrt{B_M^2 - B_S^2}$$

where ,

35

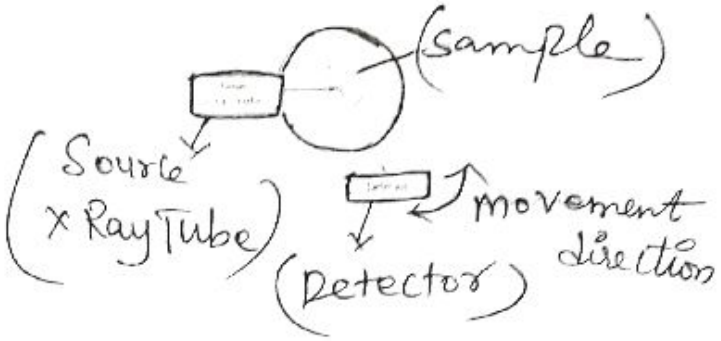

D = Crystallite size, Å

K = Crystallite-shape factor = 0.9

λ = X-ray wavelength, 1.5418 Å for CuKα

θ = Observed peak angle, degree

β = X-ray diffraction broadening, radian

BM = The measured peak width in radians at half peak height.

BS = The corresponding width of the standard material.

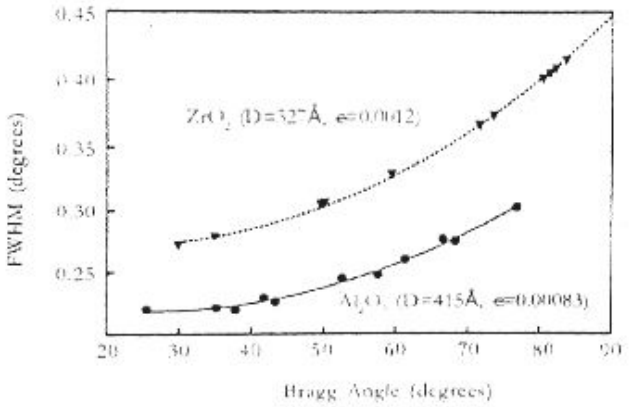

An example of this method is shown in fig 2. for a nano scale Al_2O_3 / ZrO_2 composite. After partial sintering, the broadening of each diffraction peak was measured and plotted as a function of the Bragg angle. From this data it was possible to determine the strain and particle size for each phase.

This method can also be used to study many other phenomena such as stacking fault density and non uniform deformation. Where λ is the wavelength and θ is the diffraction angle. For the diffraction pattern shown above, $\theta = 38.226^0$, $b = 0.0190^0$ red (after correction) and $\lambda = 1054178\ A^0$ yielding a particle size D of $93A^0$

METHOD 2:

The simple method based upon scherrer's formula described in method 1 is only valid when the diffracting material is stress free in these cases where both stress and particle size lead to broadening of the diffraction peaks, a more comprehensive method must be used to separate the contributors.

The most common method of strain / size analysis utilizes the fact that the broadening from the two different sources has different angular relationships. For instance, the size broadening as described earlier has a λ / Cos θ relationship while the strain follows a tan θ function. Finally, the instrument also contributes to the broadening.

Thus, the total broadening b_t can be described by

$$\beta_t^2 = \left\{\frac{0.9\,\lambda}{D\cos\Theta}\right\}^2 + \left\{4\varepsilon\tan\Theta\right\}^2 + \beta_i^2$$

Where ,

e – is the strain

b_o – is the instrumental broadening

by least squares method, the experimentally observed broadening of several peaks can be used to compute the average particles size D and the strain e simultaneously.

Calculation of the crystallite size by Debye-Scherrer equation:

The crystallite size was calculated from the Full Width Half-Maximum (FWHM) of the diffraction Peak of XRD pattern using the Debye-Scherrer equation.

From Scherrer equation:

$$D = \frac{K\lambda}{\beta\cos\theta} \qquad \text{(B.1)}$$

Where,

D = Crystallite size, Å

K = Crystallite-shape factor = 0.9

λ = X-ray wavelength, 1.5418 Å for CuKα

θ = Observed peak angle, degree

β = X-ray diffraction broadening, radian

The X-ray diffraction broadening (β) is the pure width of powder diffraction free from all broadening due to the experimental equipment. α-Alumina is used as a standard sample to observe the instrumental broadening since its crystallite size is larger than 2000 Å. The X-ray diffraction broadening (β) can be obtained by using

Warren's formula.

From Warren's formula:

$$\beta = \sqrt{B_M^2 - B_S^2} \qquad \text{(B.2)}$$

Where BM = The measured peak width in radians at half peak height.

BS = The corresponding width of the standard material.

Example:

Calculation of the crystallite size of Pd/γ-Al2O3-com.

The FWHM of (111) diffraction peak = 0.89º (from the figure B.1)

= (0.89xπ)/180

= 0.0155 radian

The corresponding half-height width of peak of α-Alumina (from the Bs value at the 2θ of 34.08º in figure B.2) = 0.00405 radian.

$$\text{The pure width, } \beta = \sqrt{B_M^2 - B_S^2}$$

$= \sqrt{(0.0155^2 - 0.00405^2)}$

= 0.0151 radian

B = 0.0151 radian

2θ = 34.08º

θ = 17.04º

λ = 1.5418 Å

$$\text{The crystallite size} = (0.9 \times 1.5418) \div (0.0151 \cos 17.04)$$

= 96.04 Å

= 9.6 nm

Figure B.1 The diffraction peak of Pd/Al_2O_3 for calculation of the crystallite Size

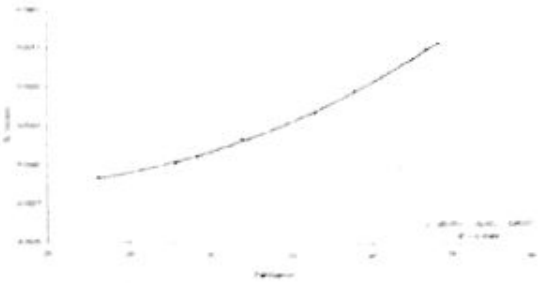

Figure B.2 The plot indicating the value of line broadening due to the equipment. Thedata were obtained by using α-alumina as a standard

AIM: FTIR

To identify the functional group of given sample using FTIR Spectroscopy.

EQUIPMENT'S NEEDED:

Potassium bromide (KBr), Pellet maker, Pestle & mortar, Sample, FTIR Spectroscopy.

PRINCIPLE:

Fourier transfer infrared spectroscopy involves the absorption of electromagnetic radiation in the infrared region of the spectrum which results in changes in the vibrational energy of molecule. Since, usually all molecules will be having vibrations in the form of stretching, bending, etc., the absorbed energy will be utilised in changing the energy levels associated with them. It is a valuable and formidable tool in identifying organic compounds which have polar chemical bonds (such as OH, NH, CH, etc.) with good charge separation (strong dipoles).

INSTRUMENT DESIGN:

The Schematic design of FTIR spectroscopy instrument is shown below

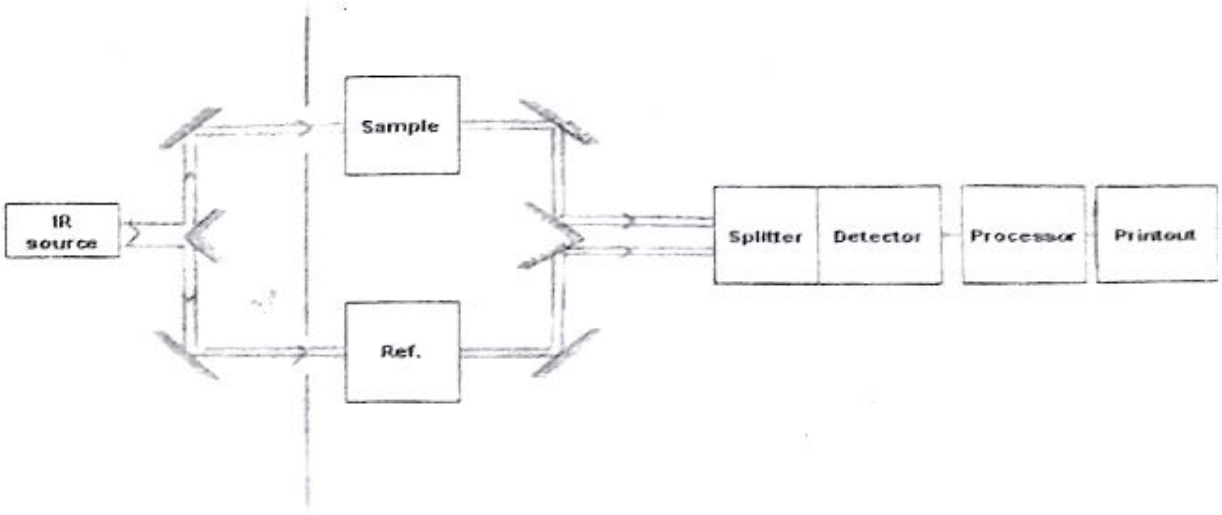

A beam of infrared light is produced and split into two separate beams. One is passed through the sample, the other passed through a reference which is often the substance the sample is dissolved in. The beams are both reflected back towards a detector, however first

they pass through a splitter which quickly alternates which of the two beams enters the detector. The two signals are then compared and a printout is obtained.

A reference prevents fluctuations in the output of the source affecting the data. The reference also allows the effects of the solvent to be cancelled out (the reference is usually a pure form of the solvent the sample is in).

1. **The Source:** Infrared energy is emitted from a glowing black-body source. This beam passes through an aperture which controls the amount of energy presented to the sample (and, ultimately, to the detector).
2. **The Interferometer:** The beam enters the interferometer where the "spectral encoding" takes place. The resulting interferogram signal then exits the interferometer.
3. **The Sample:** The beam enters the sample compartment where it is transmitted through or reflected off of the surface of the sample, depending on the type of analysis being accomplished. This is where specific frequencies of energy, which are uniquely characteristic of the sample, are absorbed.
4. **The Detector:** The beam finally passes to the detector for final measurement. The detectors used are specially designed to measure the special interferogram signal.

SAMPLE PREPERATION:

The pellet for FTIR measurement was prepared by mixing the sample (2 mg) with 200 mg of IR-grade KBr. The mixed powder was pressed in a stainless steel pellet die for 1 min at a pressure of 125 kg cm^{-2} to obtain a translucent disc. The transmission spectra were measured from 4,000 to 400 cm^{-1} at a resolution of 1 cm^{-1} using spectrum 100 (Perkin Elmer, USA) spectrometer.

PROCEDURE:

Clean the sample holder by acetone with Kimwipes, make sure not to splash the acetone on the instrument.

Launch the "spectrum" software it will initialize the instrument for analysis with the scan range of 650-4500 cm^{-1}).

After the back round run of the sample holder the sample was placed on the sample holder and the analysis was started.

Then the spectrum was analyzed using Std. FTIR library.

EXAMPLE:

FTIR – Standard Data

S.No	Wave number (cm^{-1})	Bonding
1	470, 1200	Si-O-Si bending mode
2	958	Si-O-Ca vibration band
3	1070, 607, 567	Stretching vibration of phosphate group
5	3610	Free OH stretching
6	3432-3233	H- bonded OH
7	2960	C-H asymmetric Stretching
8	2700-2560	OH associated phosphoric acids
9	1630-1650	Deformation vibration of H-O-H
10	1175-710	SiO_4^{4-} orthosilicate
11	1120-940	PO_4^{3-} orthophosphate
12	1089-1080	Asymmetric vibration of the Sio_4^{4-}
13	1060-1020	P-O stretching bend
14	650-540	PO_4^{3-} orthophosphate
15	540-470	SiO_4^{4-} orthosilicate

Models of fibers - Fringed micelle, Fringed fibril and Fringed lamellar models

Two Phase Structure: 2-

* The crystallite morphology of manufactured cellulose fibres is similar to that of synthetic polymer fibres since both are man-made spun fibres.

Two basic models often are used for manufactured cellulose fibres: (i) Fringed micelle model (ii) Fringed fibril model.

In both cases, polymer chains are more (or) less aligned along the fibres axis.

* The fringed fibril model with fringe chains connecting the crystallites is the more appropriate model for most manufactured cellulose fibres.

Fig shows a fringed fibril model proposed describing the crystalline structure of manufactured cellulose fibres.

Although the fringed fibril model is more desirable The fringed micelle model still is suitable for a few manufactured cellulose fibres such a rayon.

model representations of fibre fine structure

Starch and certain vegetable materials comprised extremely small crystalline particles which are called micelles.

These particles were bound together with other substances such as gums, giving an over all structure conclude to that bricks in mortar.

The fringed micelle concept:

* One of the salient features of most commodity fibres is their ability to withstand quite large relative extensions (50%) without significant loss of physical form(or) elasticity.
* This range of deformation is quite unusual the majority of non-polymeric solids fracture a considerably lower strain - generally a few percent at most.
* It is difficult to envisage how a simple micellar structure could retain continuity at large deformations.
* It is likely that delamination would occur between the micellas leading to voids, cracks

and other gross damage at comparatively small extensions.

* A further and more damning, criticism arose once better estimates of molecular length became available. It is now known, for example that cellulose molecules are actually 400 – 1000nm long, which is ten to twenty times longer than the early data suggested.

* Who were studying gelatin and collagen at the time, suggested that individual molecules might pass alternately through several micelles, and through several intervening regions, to produce a structure similar to ~~show~~ in figure (a)

This view is known as the fringed micelle concept.

(Fig(a))

The fringed micelle model: an individual chain molecule may pass alternately through ordered and disordered regions.

Advantages of this model:

* This model was that is provided the structural continuity which was absent from those proposed earlies.

* Several alternative two-phase models lates emerged, togethes with a good deal of controversy about which most closely described true fibre structu

* The precise details of these vary, but most share the basic characteristic of two continuously linked, but geometrically separate, crystalline & non-crystalline regions.

II The fringed fibril concept:

Two phase structure which differed from previous models in an important respect:

All Previous fringed micelle variants showed chain molecules emerging exclusively from the ends of the crystallites is show fig(b) pointed lack of rotionale for this assumption and proposed that chains could be expected to enter (or) leave a crystal at essentially

any position along its length.

The author view of structure of the fibre incorporated continuous fringed fibrils giving rise to an arrangement simplified form.

Advantages:

This model had the advantage that it could be applied to fibres which various techniques revealed to possess long, needle-like features (fibrils) as distinct from approximately cuboidal micelles.

---

commonly held view of the interface between ordered and disordered Structural phases; chains emerge exclusively from the ends of crystallites.

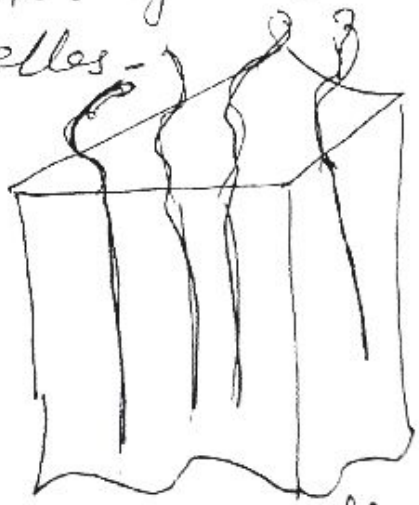

micelle

Unit : II

MOISTURE ABSORPTION PROPERTIES OF FIBERS

Unit – II MOISTURE ABSORPTION PROPERTIES OF FIBRES

Definitions: regain, humidity, moisture content. Moisture hysteresis. Moisture absorption behaviour of natural & manmade fibres. Influence of fibre structure, humidity & temperature. Relation between regain & relative humidity. Effect of hydrophilic groups. Absorption in crystalline & amorphous region. Hysteresis: molecular explanation.

Heat of sorption: Integral & differential, factors influencing heat of sorption. Conditioning of fibres, factors influencing conditioning. Types of swelling.

Humidity: The absolute humidity h of an atmosphere is defined as the mass of water in unit volume of air.

Relative Humidity: It is the ratio of mass of water in unit volume of air to the mass of water in unit volume of saturated air. $H = [h / h_s] \times 100$

where h_s is the absolute humidity of saturated air at the same temperature.

Moisture Regain:

$$\text{Regain (R)} = \left[\frac{\text{Mass of absorbed water in specimen}}{\text{Mass of dry specimen}} \times 100 \right]$$

Moisture Content:

$$\text{Moisture content (M)} = \left[\frac{\text{Mass of absorbed water in specimen}}{\text{Mass of untried specimen}} \times 100 \right]$$

Moisture hysteresis:

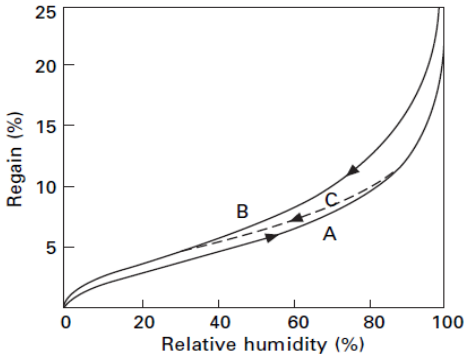

The first curve A, commonly called the absorption isotherm, is a plot of equilibrium regains at successively higher humidities of a specimen initially bone-dry; the second curve B, the desorption isotherm, is a plot for a specimen initially wet, at successively lower humidities. Desorption always refers to the loss of water, but the terms sorption, absorption refers the uptake of water.

The curves usually have the sigmoidal shape shown in Fig. a rapidly increasing regain at low humidities, followed by an almost linear portion, and then a more rapid rise at high humidities. The material initially having high regain value also has high regain in any RH% an having lower regain value initially also have lower regain value in any RH %. The sigmoidal curve represents the rate of absorption with respect to RH% is not equal to rate of desorption.

Qus: Moisture absorption behaviour of natural & manmade fibres (Or)
Effect of hydrophilic groups on moisture absorption behaviour of various textile fibres

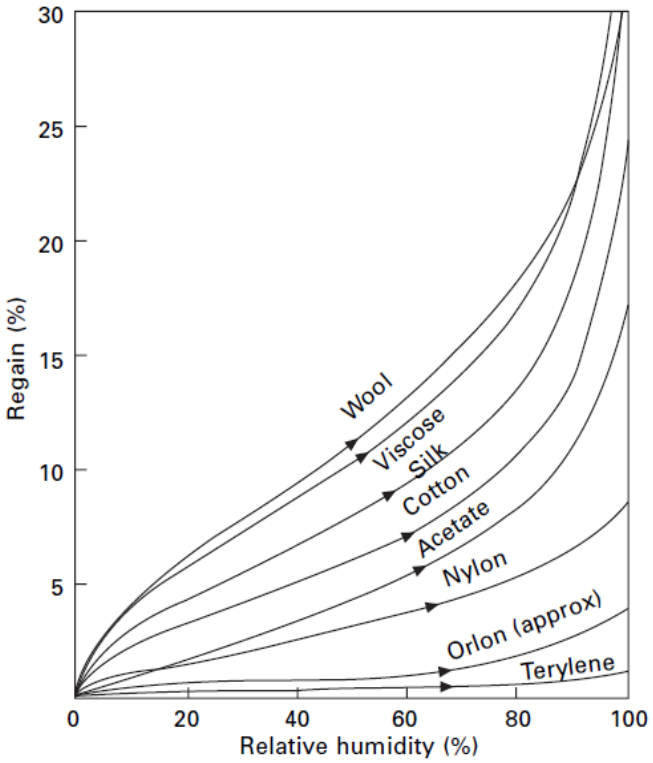

The cellulose molecule contains three hydroxyl groups for each glucose residue, and hydrogen bonds will be formed between water molecules and the hydroxyl groups. So the cotton has the regain value in the middle range(8%).

Mercerisation without tension can increase the regain at a given relative humidity to 1.5 times its previous value; mercerisation under tension does not cause such a large increase.

A sample of cotton straight from the boll of the cotton plant shows a desorption curve higher than the usual one. This is known as the primary desorption curve.

Acetate has a curve of a different shape and does not show a rapid rise of regain at low humidities. The regains are lower than those of cotton. In cellulose acetate, all or most of the hydroxyl groups have been replaced by the comparatively inert acetyl (CH3·COO—) groups. These groups do not attract water strongly, so the absorption of water by acetate is low.

The protein fibres contain amide groups (—NH—) in the main chain, to which water can be hydrogen bonded, and other water-attracting groups such as —OH, —NH_3 —COO–, —$CO{\cdot}NH_2$, in the side chains. Due to that reason its having higher regain value.
At higher humidities the regain of wool is lower. The type of wool and its processing also affect the regain values. Acid-treated wool has a lower regain value.

Wool contains many active groups in the side chains, but **silk** contains only a few. Hence, silk has a regain intermediate between cotton and wool. Silk gum has a high regain, and the degumming causes a reduction in regain. Casein fibres have regains very close to those of wool at the same humidity.

The synthetic fibres have low regains. Nylon has about half the regain of cotton. All the synthetic fibres so far produced contain few if any water-attractive groups, and this accounts for their low moisture absorption. The polyamide fibres, nylon 6.6 and 6 and aramids, contain one amide (—NH—) group for every six carbon atoms in the chain, which would give a regain of 16% if each amide group held one water molecule.

The polyester fibres, polyethylene terephthalate, are composed only of benzene rings, —CH2— groups, and —CO·O— groups, none of which attracts water strongly.

Acrylic fibres, containing —CN groups and other groups from the minor components, absorb slightly more than the other vinyl fibres, and
Polyvinyl alcohol, containing some —OH groups, absorbs still more.

Influence of humidity & temperature (or) Explain the influence of various factors on regain of textile materials.

1. Effect of Temperature:

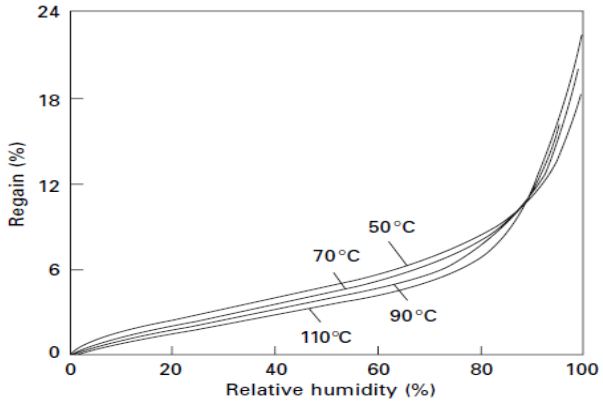

Except at, high temperatures and humidities, the regain decreases as the temperature increases. The increase above 50 °C at high humidities is due to a change in the internal structure and is associated with the irreversible hysteresis effects.

2. Effect of Stress:

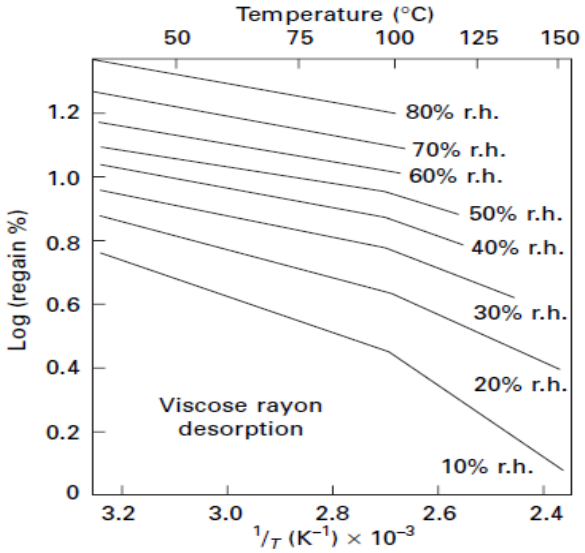

The swelling of fibres during absorption means that the application of stresses will change the regain. Table shows the increases in regain due to the application of a tension to filaments.

Isotropic cellulose		Oriented cellulose	
Stress (MPa)	Increase in regain (%)	Stress (MPa)	Increase in regain (%)
5.7	0.2	10.2	0.1
10.2	0.4	17.7	0.4
13.6	0.6	35.6	1.1
27.4	1.5		
40.5	1.1		

3. Absorption in crystalline & amorphous region

In crystalline regions, the fibre molecules are closely packed together in a regular pattern. The active groups form crosslinks between the molecules, for example by hydrogen bonding in cellulose.

In native cellulose, with the crystalline arrangement known as cellulose I, the Xray diffraction pattern is unchanged during the absorption of water by the fibre, which indicates that no water is absorbed in the crystalline regions. In regenerated cellulose, with a slightly less compact crystal structure known as cellulose II, there is a change of crystal structure on absorption. This is due to the formation of a hydrate, which probably contains one water molecule to every three glucose residues.

It would then be expected that the regain at any particular relative humidity would be proportional to the amount of this non-crystalline material. The material easily accessible to moisture will be either the non-crystalline regions.

4. Effect of RH %

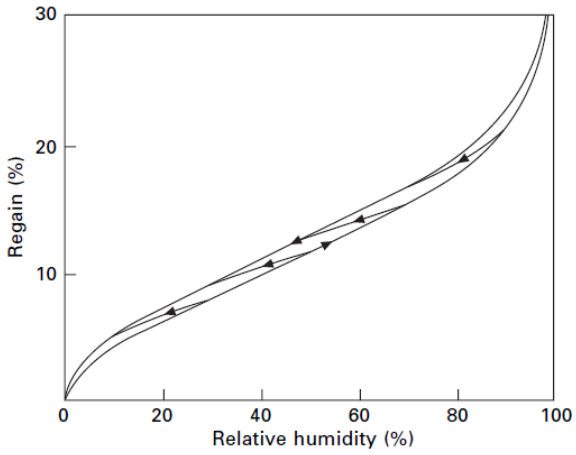

Increase in RH % will tend to increase in regain values.

Hysteresis: molecular explanation

In non-crystalline cellulose, there are some cross links, formed where molecules pass near to one another. As absorption increases, the cross links will tend to be broken and replaced by water. Thus there is the following change:

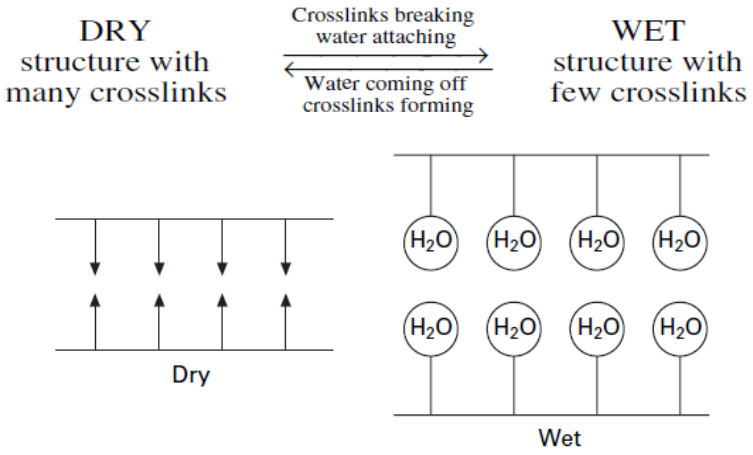

There will be a hysteresis in the breaking and re-forming of cross links in the moisture absorption. The figure shows a dry structure with cross links and a wet structure with water absorption.

Suppose that the two structures are both put in the same atmosphere, causing the continual motion of atoms takes place (breaking of cross inks or the evaporation of water).

Free active group will not remain free indefinitely, since either a water molecule will be absorbed on it or a crosslink will form.

The chance of water absorption depends on the number and velocity of the water molecules present in the atmosphere. The chance of a crosslink forming depends on the nearness of another active group.

Thus an initially dry specimen will always retain a higher number of cross links and less water absorption than an initially wet specimen in the same atmosphere.

When cellulose is first formed in the cotton plant, it is laid down in the presence of water. The resulting structure has few cross links, giving rise to the high primary desorption curve. it has been dried below a certain humidity, cross links will form. Some of these will remain permanently and prevent such high regains from being obtained again.

Integral & differential Heat of sorption

The **differential heat of sorption** *Q* (sometimes called the heat of absorption) is the heat evolved when 1 g of water is absorbed by an infinite mass of the material at a given moisture regain. It is expressed in joules per gram.

The **integral heat of sorption** *W* (sometimes called the *heat of wetting*) is the heat evolved when a specimen of the material at a given regain, whose dry mass is 1 g, is completely wetted.

Measurement: Heats of wetting may be measured calorimetrically. A known mass of the material at the required regain is placed in a calorimeter, and an excess of water is added. From the rise in temperature and the thermal capacity of the system, the heat evolved from the specimen can be calculated and the heat of wetting to be determined. The temperature rise will be small, and careful experimental technique and sensitive temperature measurement are necessary to find heat of wetting.

Factors influencing heat of sorption

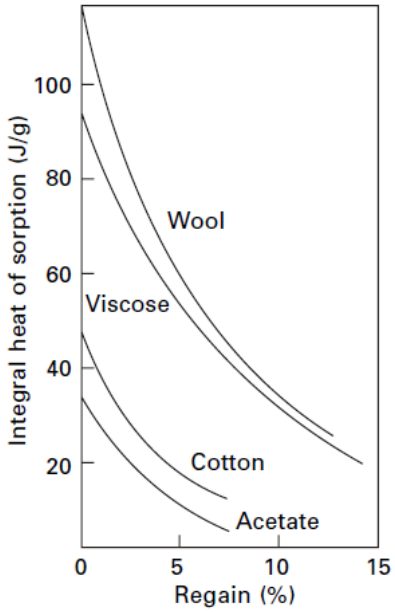

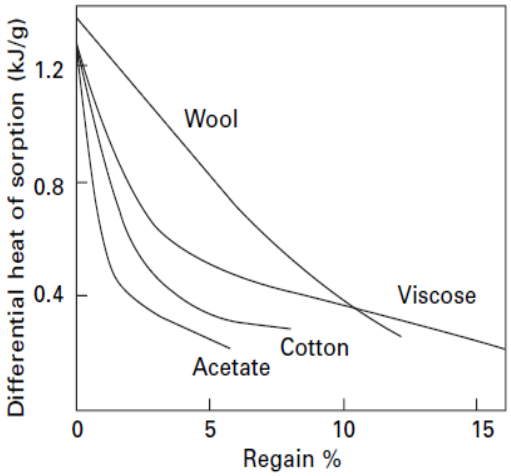

1. Regain:

The heat of wetting is greatest for the most highly absorbing fibres and is very small in the non-hygroscopic fibres. Figure 1 shows that the heat evolved in going from 0% to 65% r.h. is proportional to the regain of the fibre at 65% r.h.

Figure 2 shows the decrease in the differential heat of sorption as the regain increases. At zero regain, the differential heat of sorption of the cellulosic fibres is of the order of 1250 J/g.

Wool and nylon have values that are close together, which indicates absorption on similar sites.

Conditioning of fibres:

During the conditioning of a mass of fibres, diffusion must take place in three stages.

First, there will be diffusion (or convection) in the air from the source of water vapour to the surface of the mass of fibres.

Secondly, there will be diffusion in the air in the interstices between fibres, from the surface of the mass to the surface of a fibre.

Thirdly, there will be diffusion from the surface of a fibre to its interior.

Suppose we have 100 g of dry cotton in a package 10 cm long and 2 cm in radius, placed in a close container, 10 cm from a solution giving a relative humidity of 65% at its surface, that is, a

concentration of water vapour of 10^{-5} g/cm^3 at 20 $^{-}$C. The mass of water to be absorbed for equilibrium is about 7 g.

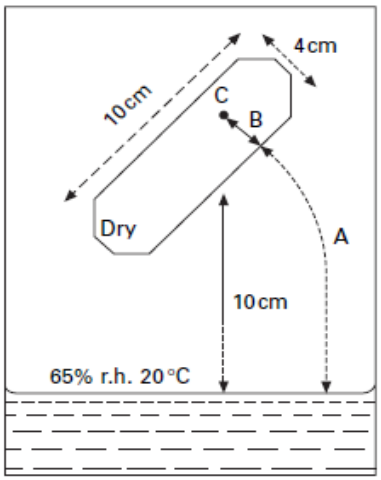

Time taken for conditioning with in the fibre is:

$t = r^2/2D$

t -conditioning time.

r -fibre radius

D-diffusion coefficient

For example A value of 10^{-7} cm^2/s may be taken for the diffusion coefficient within a hygroscopic fibre at medium humidities and, with a fibre radius of 10^{-3} cm, the conditioning time will be

$t = (10^{-3})^2 / (2 \times 10^{-7}) = 5$ seconds.

The time taken for diffusion in the air, whether inside or outside the specimen, will depend on the size, shape and density of the specimen; that for the diffusion outside will also depend on the ease of access to a source of moisture.

Diffusion in the air will be given by the following equation:

$t = Ml / (D (C_0 - C_1) A)$

M : Mass of water to be absorbed for equilibrium

C0 : Initial concentration at surface of absorbent

C1 : Concentration at surface of conditioning solution

A : area across which diffusion occur

D : Diffusion coefficient

The times for diffusion in the air are much greater than the time for diffusion in a fibre.

Conditioning process:

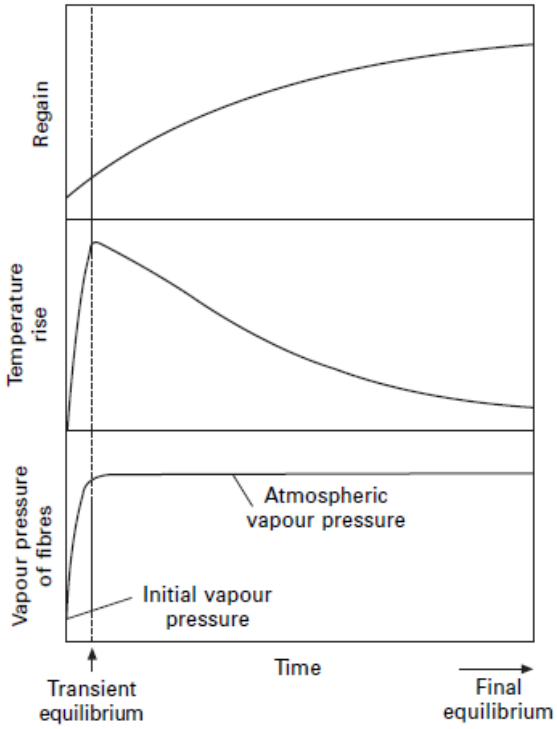

When textile fibres absorb moisture, they generate heat, The evolution of heat raises the temperature of the fibres and increases their water vapour pressure, consequently slowing down the rate of absorption. The higher vapour pressure in the atmosphere at the start of the process, gives an increase in regain, generation of heat and a rise in temperature.

The vapour pressure of the fibres will therefore increase, this process will continue until the vapour pressure of the fibres has become almost equal to that outside. This is a state of transient equilibrium in which further absorption is impossible until heat has been lost by the specimen.

As heat is lost to the surrounding atmosphere, the temperature decreases, which allows a further increase in regain to occur and maintains the vapour pressure close to that of the atmosphere. This continues until final equilibrium is reached. In this cooling process, the absorption that occurs is generating heat which must also be lost to the surroundings.

FACTORS INFLUENCING THE RATE OF CONDITIONING:

Size and shape of package:

As the size of the package increases, it will take long time to transfer the heat to its surface from center, which reduces the rate of conditioning.

Heat generated in the centre of a bale will take a long time to escape. It will escape more rapidly from a smaller package or from the same mass of material spread out in a thin layer.

The total amount of heat that has to be lost is proportional to the volume of the package. The rate of loss of heat decreases as the distance to the surface increases, and the rate of loss of heat from the surface, increases as the surface area increases. In fact, mathematical analysis shows that:

Conditioning time **α** (Volume / Surface area)^2

Bulk density:

The mass of moisture absorbed, and the amount of heat evolved, for a given regain is proportional to the density of packing of the material .

Conditioning time α density

***Material*:**

There are some variations depending on the nature of the material. The numerical values are given in Table.

***Regain*:**

The rate of conditioning is slower at the extreme values of regain, which is shown in Table.

Temperature:

Conditioning is more rapid at higher temperatures, since the heat transfer occurs more rapidly at higher temperatures. At low temperatures, conditioning is slow.

Air circulation

The ventilation around a mass of fibres is important in affecting the rate of loss of heat from the surface of the specimen and thus the rate of conditioning.

Conditioning may be speeded up by carrying it out in two stages.

The conditioning is more rapid when the specimen is first placed in an atmosphere much damper than is required, for the final state.

Another procedure that may be adopted is to place the material in a closed system containing the required total amount of water.

TYPES OF SWELLING:

AXIAL SWELLING, TRANSVERSE SWELLING, AREA SWELLING AND VOLUME SWELLING

When fibres absorb water, they change in dimensions is called swelling.The swelling may be expressed in terms of the increase in diameter, area, length or Volume.

Transverse diameter swelling = fractional increase in diameter = $S_D = \Delta D / D$

Transverse area swelling = fractional increase in area of cross-section = $S_A = \Delta A / A$

Axial swelling = fractional increase in length = $S_l = \Delta l / l$

Volume swelling = fractional increase in volume = $S_V = \Delta V / V$.

Relation between volume, area swelling

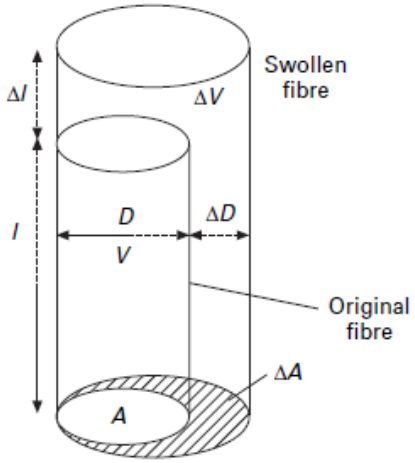

$V = A\ l$

$V + \Delta V = (A + \Delta A) (l + \Delta l)$

$S_V = \Delta V / V = ((A + \Delta Al) / Al) = \Delta l / l + \Delta A / A + \Delta l . \Delta A / Al = S_l + S_A + S_A S_l$

Measurement of swelling:

1. Axial swelling measurement

The axial swelling of a continuous filament may be found by hanging up a length under a low tension and measuring the change in length with a cathetometer or extension gauge. The change in length of short fibres may be made with a traveling microscope.

2. Volume swelling measurement

$V = 1 / \rho_0$

$V + \Delta V = (1 + m) / \rho_s = (1+ r(/ 100)) / \rho_s$

where ρ_0 = density when dry, ρs = density when swollen, m = mass of water absorbed and r = regain percentage.

$S_V = \Delta V / V =$ $\dfrac{\rho_0}{\rho_s} \Big/ \left(\dfrac{1 + r}{100}\right) - 1$

3. Transverse swelling measurement

Microscopy methods are used, for examining the fibre diameter or for examining sections and measuring the area of cross-section.

THE SWELLING OF FIBRES IN WATER

Most moisture-absorbing fibres show a large transverse swelling, with a smaller axial swellling. Nylon is exceptional in having a value of the anisotropy that is close to or less than unity. It

has been suggested that the nylon fibre is surrounded by a skin or sheath, which restricts the transverse

The swelling of amorphous regions between crystallites in the quasi-fibrils will have a larger effect than the swelling between the fibrils.

UNIT : III

MECHANICAL PROPERTIES OF FIBERS

MECHANICAL PROPERTIES OF FIBRES

Definitions

Load:

It is the force applied to a fibre to deform it. If the load is applied along the axis of the fibre, then it is known as “Tensile Load”. The tensile load for fibres is expressed in milli-newton (mN), centi-newton (cN), Newton (N), or gram force (g).

Breaking Load:

The tensile load at which the fibre breaks is known as “Breaking Load” or “Breaking strength” of the fibre.

Elongation:

It is an increase in the initial length of the fibre due to application of a tensile load. The unit of elongation is millimeter (mm) or centimeter (cm).

Breaking Elongation

The elongation at which the fibre breaks is known as “Breaking Elongation” or “Elongation at-break”.

Stress

The stress is expressed as the ratio of load applied to area of cross-section of a specimen. Since the textile structures are flexible, it is difficult to measure their area of cross-section accurately. Hence a quantity, which can be easily measured and related to the area of cross-section, known as the linear density has been used for fibres to determine the stress. The stress so calculated is known as “Mass Stress” or “Specific Stress”. Therefore, the Specific Stress is given by:

Specific Stress = [Load / Linear density (mass per unit length)]

The unit of specific stress for fibre is mN/tex, cN/tex, g/tex or g/den.

Tenacity

The specific stress at break is known as “Tenacity” or “Specific Strength” of the fibre. As the tenacity of a fibre is normalized with its linear density. The fibre with higher tenacity is obviously regarded as stronger than the fibre with lower tenacity.

Tensile Strain

The tensile strain or simply strain represents a fractional increase in the initial length of the fibre. It is given by the ratio of elongation to initial length of the fibre as shown below:

Strain = (Elongation / Initial length of specimen)

The strain at beak is termed as “Breaking Strain”.

Breaking Extension

The breaking strain expressed as a percentage is known as “Breaking Extension” or “Extension-at-break”, and is given by:

Breaking Extension = (Elongation / Initial length of specimen) x 100%

Work of Rupture

It is defined as the energy required to rupture (break) the fibre. It is a measure of toughness of the fibre. The unit of work of rupture is Joule.

The work of rupture is a useful measure in assessing the performance of ropes, parachutes, and the yarn breakage during high-speed weaving or knitting operation. As the work of rupture is the work done to break the fibre, it can be represented as:

Work done = Force (F) x Displacement (dl) = Load x Elongation.

Initial Young’s Modulus

The Young’s modulus represents resistance to extension. The initial young’s modulus or simply initial modulus of a fibre is a measure of its “initial resistance to extension”. It is given by the slope to the initial linear portion of the load-elongation curve or stress-strain curve. It is also represented by

$$\text{Initial modulus} = \tan\theta.$$

The reciprocal of modulus is known as “Compliance”.

Yield Point

When a tensile load is applied to a fibre, initially the fibre resists extension due to its initial modulus. With increase in load, the molecular chains in the fibre and the cross links between the molecular chains will be extended resulting in small extension and the stress strain curve is linear. If the load is removed at this instant and the fibre is allowed to recover its original dimensions (elastic nature). This initial region of the stress-strain curve is known as “Hookean region” where the stress is proportional to strain.

A further increase in stress causes the fibre to yield due to breaking of cross links and sliding of molecular chains resulting in higher extension. Now the fibre follows a plastic deformation.

After an initial period with a steep slope, extension suddenly becomes much easier. It is in this region that the yield point occurs. In order to locate a precise position of yield point, draw the

tangent to the curve which is parallel to the line joining the origin to the breaking point. This point is then characterized by its stress and strain as the yield stress and yield strain.

The point on the stress-strain curve at which the fibre yields to the applied stress is known as “Yield Point”. The stress at yield point is known as “Yield Stress” and the strain at yield point is termed as “Yield Strain”.

Significance of Stress-Strain Curves.

The stress-strain curves of fibres help to:

Determine the Load at various levels of extensions, Breaking load, Tenacity, Breaking extension, Initial modulus, yield stress, yield strain, and work of rupture.

Enable to compare the tensile properties of different fibres.

To predict the end uses of different fibres and their selection for different applications.

Influence of various factors on Tensile Properties of Fibres.

1. Effect of Moisture

The increase in the moisture (due to increased regain or relative humidity) of most hygroscopic fibres decreases the strength but increases the extension. The absorbed water breaks the cross links and makes the molecular chains, which are relatively shorter, to slide. Thus the fibre structure becomes flexible with the strength and modulus decreased. (Except cotton)

Cotton shows an exception in this regard as its strength increases with increase in moisture regain. In dry state the fibre has many cross links. If a tensile load is applied to the dry fibre, the load is not uniformly borne by the molecular chains, which are not perfectly straight and parallel. The straight portion in a chain may break earlier than the spiraled portion in the neighboring chain, resulting in lower strength of the fibre.

In wet state the absorbed water breaks some cross links rendering the spirally configured portions of molecular chains to become straight and parallel for some length. If the load is now applied to the fibre, the straight and parallel molecular chains bear the load and it contributes to higher strength of the fibre.

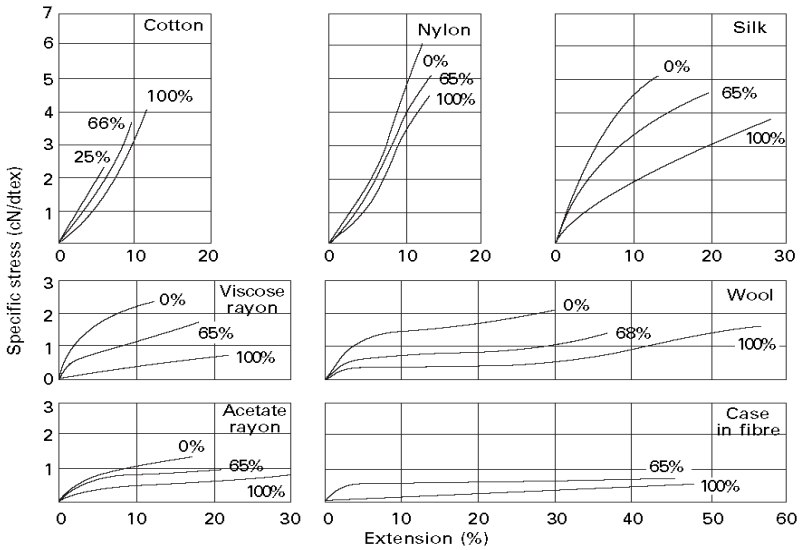

2. Effect of Temperature

The increase in temperature, decreases the strength of most textile fibres. The increase in temperature from room temperature to glass transition temperature causes the molecular chains to become flexible, which decreases the fibre strength, modulus, but increases its extension. A further increase in temperature nearer to melting leadis highly reduced strength.

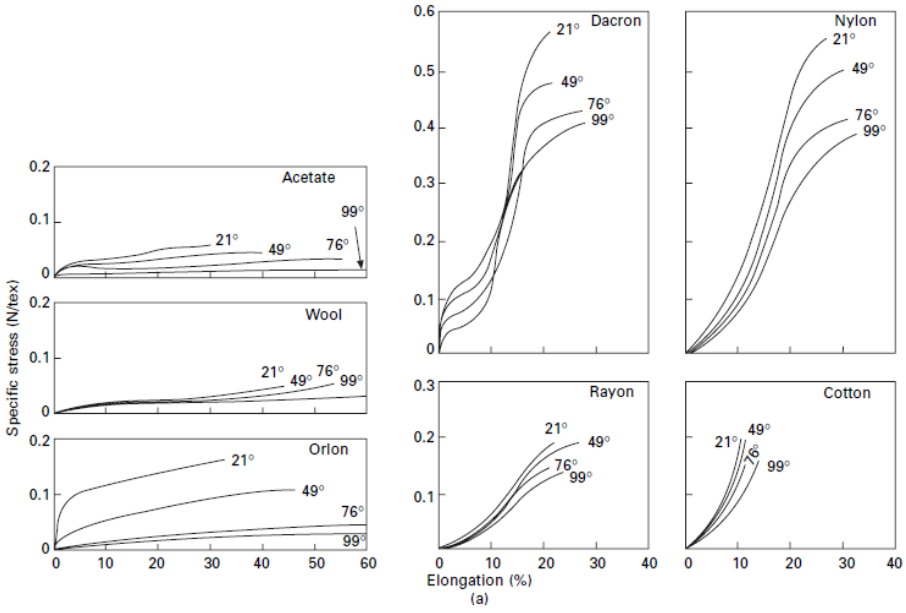

3. Effect of Light

A prolonged exposure to light reduces the strength and extension of fibres due to structural deterioration.

4. Effect of Chemicals

The tensile characteristics of fibres change when subjected to the action of chemicals, like acids, alkalis, etc. the strength generally decreases depending upon the nature and duration of chemical treatment.

5. Molecular Orientation

Increase in orientation of the molecules in the fibre increases the strength of the man made fibres.

Differentiate Constant rate of loading & constant rate of extension

CRE : Extending the specimen at a constant rate throughout the test.

CRL : Loading the specimen at a constant rate. Example: Inclined plane tester, Stelometer.

STRESS-STRAIN CHARACTERISTICS OF VARIOUS TEXTILE FIBRES.

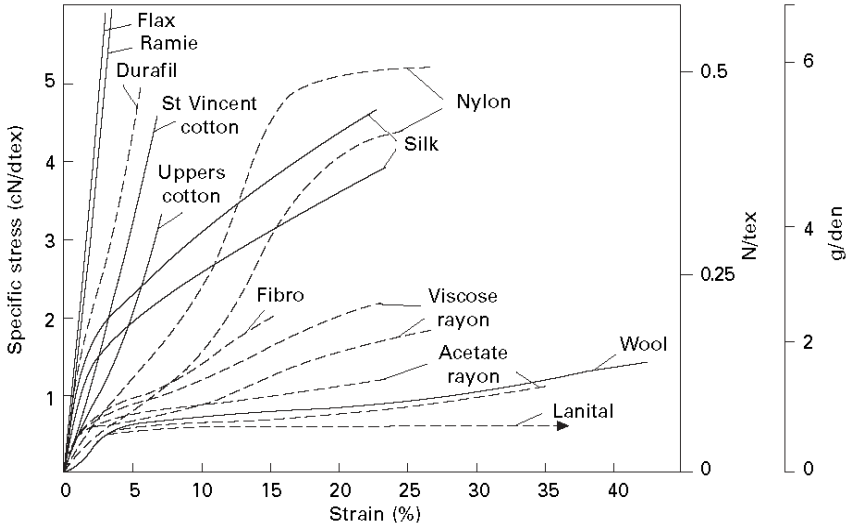

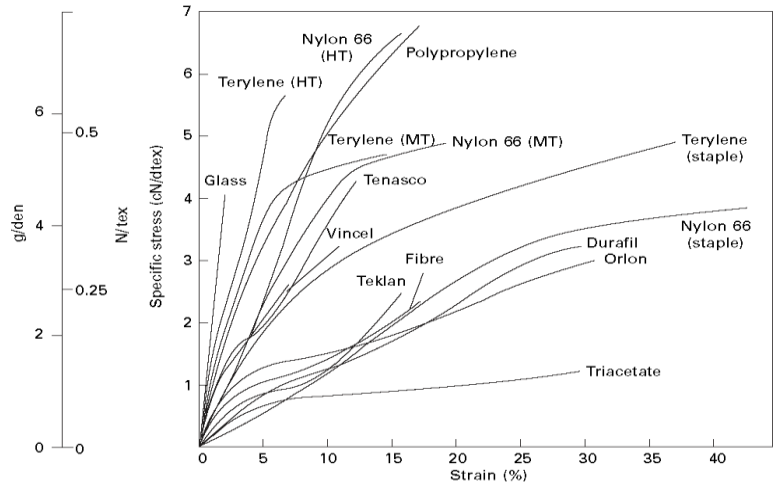

Cotton and the other natural cellulose fibres

The stress–strain curve for cotton is slightly concave to the Y axis, and there is no obvious yield point. The finer cottons shows a higher tenacity and a higher initial modulus than the coarser cotton.

There was a better correlation between tenacity and molecular orientation. The orientation increases as the Tenacity of cotton also increases.

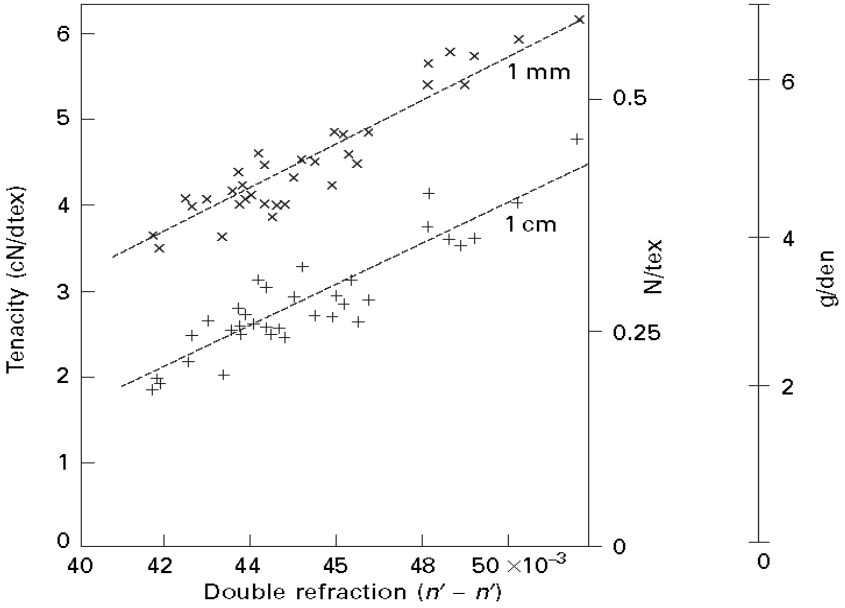

Above fig shows the correlation between tenacity and the birefringence for different samples of cotton.

Hessler investigated the effect of the length of chain molecules in the cotton and found there is a good correlation with the tenacity. It is the effective factor in determining the tenacity of different varieties of cotton.

Morlie,. Found, in most cases, the tenacity and breaking extension increased with increasing length of fibre. An example of their results is given in fig.

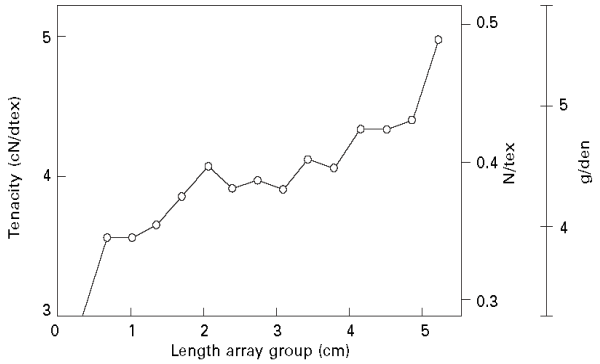

The bast fibres, in which the molecules are very nearly parallel to the fibre axis, show a greater tenacity, a higher modulus, a lower breaking extension and a lower work of rupture.

Regenerated cellulose and related fibres

The stress–strain curves of rayon and acetate fibres show an initial rapid rise with a marked yield point, followed by a nearly flat portion and a rise again near breakage.

A highly stretched fibre, such as, high molecular orientation, which gives high strength and low extensibility, similar to the bast fibres.

The effect of orientation is clearly shown in Fig, for acetate of varying degrees of orientation. If orientation is increased the tenacity of the yarn is higher. If cellulose yarns are regenerated from the acetate, the locus of strengths is somewhat higher.

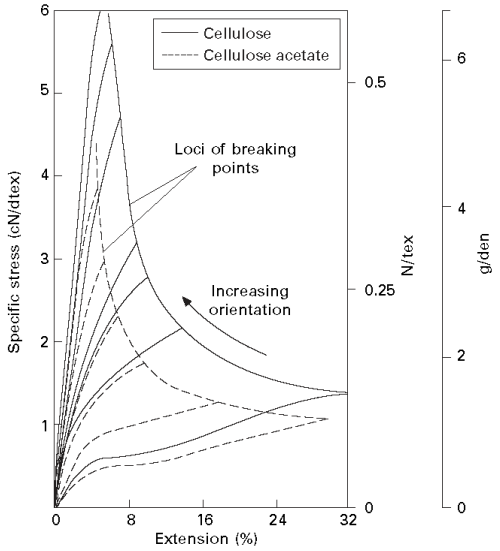

Fig. Stress—strain curves of filaments of varying degrees of orientation. The dotted curves are secondary cellulose acetate and the full curves are cellulose fibres regenerated from acetate. The lowest curve in each set is for unoriented material.

There are also important differences in the tensile properties of viscose rayon, depending on their fine structure. An improvement in structure will cause the whole locus of breaking points to be moved farther from the origin, so that strength is increased without the loss of extensibility when orientation is increased. This is illustrated in fig.

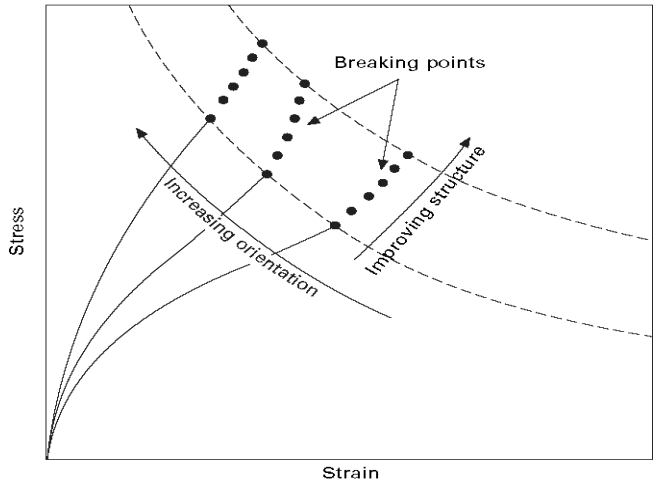

Fig. Load—extension curves for viscose rayon, showing changes produced by increasing orientation and improving structure.

Chamberlain and Khera investigated the variation in the properties as the outer layers of viscose and cuprammonium rayon filaments are removed chemically. It appears from these results that the outermost layers are less extensible than the layers below the surface, the stress would concentrate in the least extensible parts of the fibre.

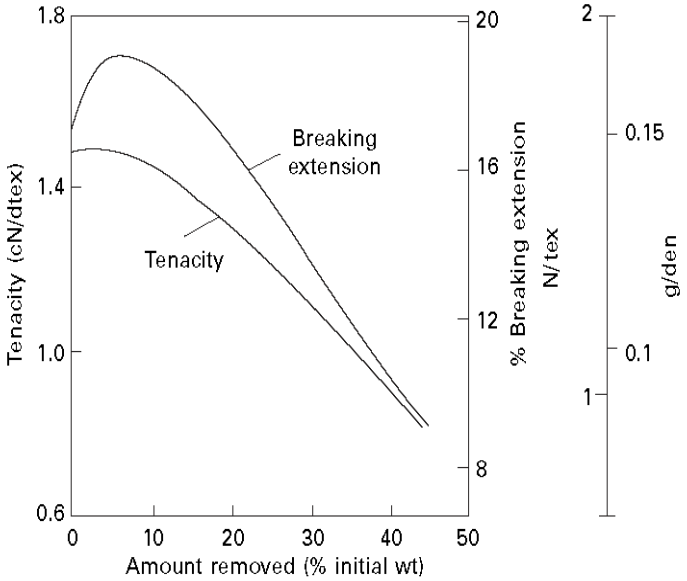

Fig. Change of tenacity and braking extension of viscose rayon as outer layers are removed.

Protein fibres

Silk, is characterized by fairly high strength and breaking extension, which combine to give a work of rupture very much greater than that of the other fibres.

Wool and other hair fibres are characterized by low strength but great extensibility. Different types of wool give slightly different curves, but these are always characterized by an initial linear Hookean region up to 2% extension, a yield region of very low slope from 2 to 30% extension, and finally a post-yield region of greater slope, up to a breaking extension around 45%.

The tenacity of wool fibres increased with the fibre diameter. There was a slight positive correlation between breaking extension and fibre diameter.

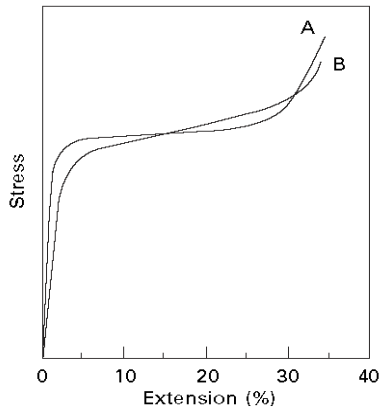

Fig. Stress—strain curves of wool fibres: A, with good uniformity; B, more irregular fibre.

Synthetic fibres

The tensile properties of synthetic fibres depend to a considerable extent on the molecular weight of the polymer and on the conditions of spinning and drawing. A good example of this is polyester fibre, which can have a variety of stress–strain curves, as shown in Fig.

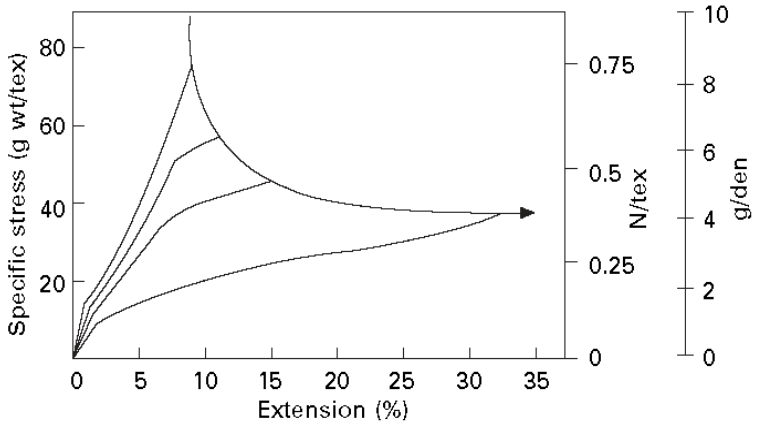

Fig. Stress—strain curves of polyester fibre (Terylene) at varying orientations.

As the degree of orientation is increase, the strength and stiffness of fibre increases and but reduces its breaking extension.

If the molecular weight increases, the locus of breaking points moves upwards, which increases its tenacity.

The spinning at higher speed, c. 3000 m/min, gave partially oriented yarns (POY), and spun at around 6000 m/min are sometimes referred to as fully oriented fibres (FOY), it gives higher tensile strength. Its shown in the following diagram.

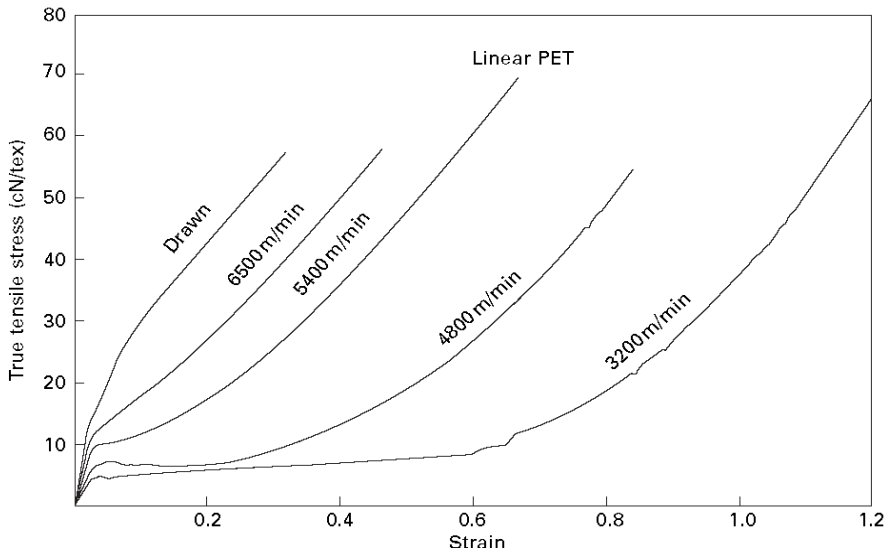

The effect of draw ratio and spinning speed has significant effect on the tensile strength of nylon. Following figure shows stress–strain curves for nylon 66 fibres spun at different speeds.

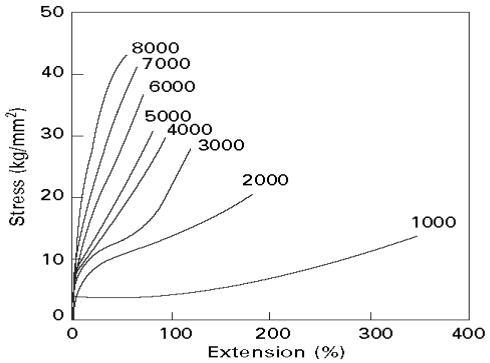

Fig. Stress—strain curves of nylon 66 fibres spun at different speeds.

The shape of the stress–strain curve of both nylon and polyester fibres can be considerably altered by heat treatments under tension.

As in all acrylic fibres, there is a yield point at around 2% extension. Although treatments can give higher strength and lower breaking extension, commercial acrylic fibres are usually at the lower strength. Acrylic fibres are not quite as tough as nylon, polyester or polypropylene fibres.

Elastic Property

Elastic Recovery: The material recover its original dimension after releasing the load is called as elastic recovery.

Elastic recovery = Elastic extension / Total extension.

Elastic deformation is due to a stretching of inter-atomic and intermolecular bonds,

Non-recoverable or plastic deformations result from a breaking of bonds and their re-forming in new positions.

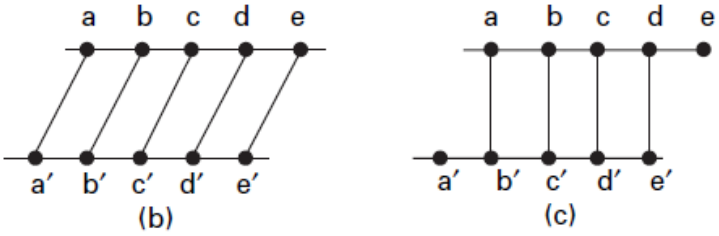

b. Elastic deformation c. Plastic deformation

Work Recovery: It is the ratio of work returned during recovery to the total work done during extension.

Work recovery = Work returned during recovery / Total work done during extension

ELASTIC RECOVERY PROPERTY OF VARIOUS FIBRES

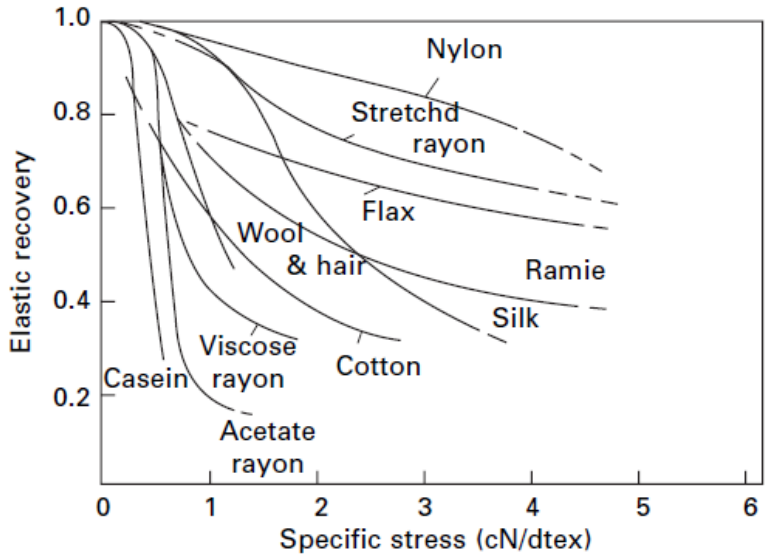

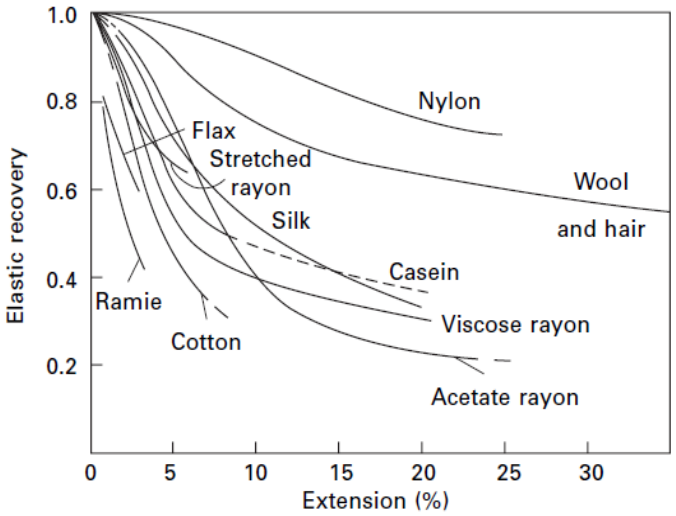

Cotton shows no yield point (or it may be more correct to say that the yield point is at zero stress and zero strain). The elastic recovery falls steadily to about 0.3. Compared with that of other fibres, the recovery of cotton is only moderate.

The bast fibres show poor recovery from strain but can withstand large stress without great permanent damage.

Viscose rayon and acetate show a marked yield point. Below this point, the recovery is good, but above it the curve drops rapidly, and the recovery is poor. The stretched rayon can stand higher stresses without suffering permanent deformation.

Wool and hair also show a yield point, but the drop in the curve is less rapid, and even near break there is still considerable recovery. These fibres are not good under high stresses but can recover from large strains. Thus they show 60% recovery from an extension of 35%. Wet wool fibres show complete recovery up to the end of the yield region (30% extension) and very good recovery from higher strains. However, the path of the recovery curve is different from that of the extension curve.

Silk shows fairly good elastic recovery from both stress and strain.

Nylon shows the best elastic recovery, whether considered on the basis of stress or on that of strain. Even near break, its recovery falls only to 0.7. The strength and extension at break, nylon is surpassed by some other fibres. In case of work recovery, (at large strains) the energy dissipated by nylon is considerably less than that by other fibres.

Material	Elastic recovery (%) from:					
	1% extension		5% extension		10% extension	
	60% r.h.	90% r.h.	60% r.h.	90% r.h.	60% r.h.	90% r.h.
Cotton	91	83	52	59	–	–
Viscose rayon	67	60	32	28	23	27
Acetate	96	75	46	37	24	22
Wool	99	94	69	82	51	56
Silk	84	78	52	58	34	45
Nylon	90	92	89	90	89	–
Polyethylene terephthalate (Dacron)	98	92	65	60	51	47
Polyacrylonitrile (Orlon)	92	90	50	48	43	39
Casein	90	76	47	43	30	25

In the above table shows, Nylon has best elastic recovery than any other fibres.

MECHANICAL CONDITIONING

When the fibre is first strained, the stress–strain curve OA is followed, but, on removal of the load, recovery takes place along AB, the permanent extension OB being left. If the fibre is again stressed, the curve BAC is followed. Re-plotting this as a new stress–strain curve (Fig (b)).

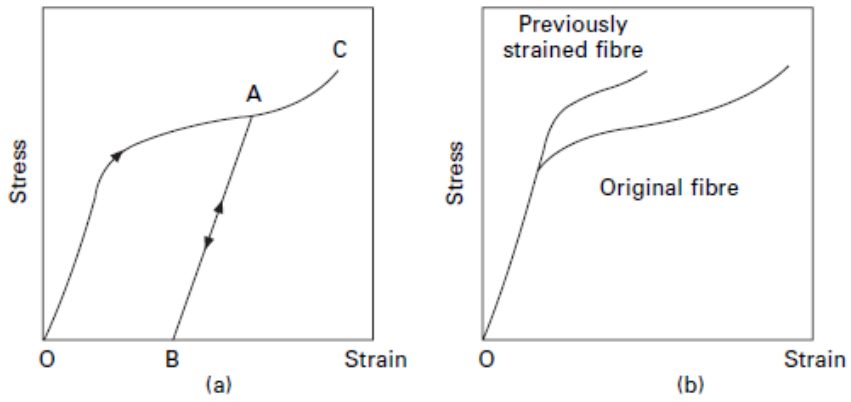

The effect of the first straining has been to raise the yield stress and reduce the breaking extension. The rise in the yield stress means that the application of a given stress to a fibre for some time usually results in almost perfect recovery from subsequent stresses below this value. This treatment is known as mechanical conditioning.

Material	Elastic recovery % near breaking point	
	Before mechanical Conditioning	After mechanical conditioning
Cotton yarn	56	80
Fortisan (stretched cellulose)	72	94
Acetate	30	92
Silk	36	93
Viscose rayon	39	74
Dacron polyester fibre	55	92
Orlon acrylic fibre	58	92
Vicara (zein protein)	43	97
Casein	39	80
Nylon	72	92
Wool	59	88

Table. Effect of elastic recovery on mechanical conditioning

In the above table, the process of mechanical conditioning improves the elastic recovery property of fibres.

UNIT : IV

OPTICAL AND FRICTIONAL PROPERTIES OF FIBERS

Unit – IV OPTICAL & FRICTIONAL PROPERTIES

Refractive index: Measurement, Birefringence. Factors influencing birefringence. Absorption & dichroism. Reflection and luster.

Friction: General theory, various influencing factors: Load, area of contact, speed, state of surface & moisture. Directional frictional effect of wool.

REFRACTIVE INDEX

In isotropic materials, refractive index *n* , is the ratio of the velocity of light in a vacuum to the velocity of light in the material.

Or

The direction of travel of light is refracted or bent on passing from one medium to another. This leads to an alternative definition:

refractive index *n* = sine of angle of incidence/sine of angle of refraction.

In anisotropic materials, such as textile fibres, the molecules are lined up in certain preferred directions, and the refractive index will therefore vary with the direction of the electric field.

MEASUREMENT

The refractive index of a material varies with the temperature and wavelength of the light being transmitted. The standard conditions of measurement involve the use of monochromatic sodium light, with a wavelength of 589 nm, at 20 °C.

1. If a fibre is immersed in a liquid of the same refractive index as itself, then its boundary not to be visible. If the refractive indices of the fibre and the liquid are different, a bright line (the Becke line) can be seen at the boundary between them. By trial and error with a series of liquid mixtures of varying composition, may be used to measure the refractive index of the fibre.

2. A circular fibre acts like a convex lens and will focus a beam of light.

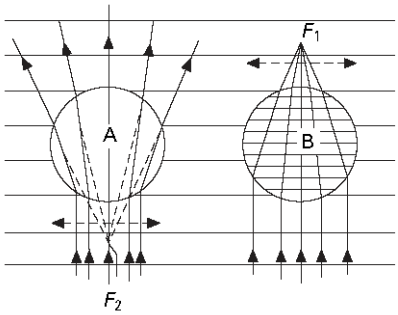

If parallel light comes from below, and the fibre has a higher refractive index than the immersion liquid, an image will form above the fibre. This may be observed as a bright band in the centre of the fibre when the microscope is focused above it.
Conversely, if the refractive index of the fibre is less than that of the liquid, a virtual image will be formed below the fibre. The bright band will then be observed on lowering the microscope below the position where the fibre itself is in focus.

3. Frey-Wyssling has adopted the technique of varying the wavelength of the light with which the fibre is observed in the liquid until the fibre outline disappears.

4. Preston and Freeman technique, a glass plate carrying the fibre is immersed in an appropriate liquid, which is placed in the path of the light dispersed by the prism. At the wavelength for which the refractive indices of liquid and fibres are equal, the light passes straight through and appears brightly on the screen. For other wavelengths it is scattered on the screen.

5. In Vries technique, If several ends of yarn, wound parallel to one another on a frame, are immersed in a liquid, they will act as a phase-grating and give a diffraction pattern if the refractive indices of fibre and liquid are different. If the refractive indices are the same, diffraction will not occur.

Variations in refractive index across a fibre are better investigated by interference techniques. In the interference microscope, differences in refractive index are transformed into dark and light fringes with monochromatic light.
Both double-beam and multiple-beam interference techniques have been used by Faust. In the first method, the light is split into two beams, one of which passes through the specimen, while the other bypasses it. The two are then combined and give an interference pattern.
In the second method, the specimen is placed between two partly silvered mirrors. A series of beams, which have passed through the specimen for a differing number of times, depending on the number of reflections, are transmitted by the system and combine to give the interference pattern.

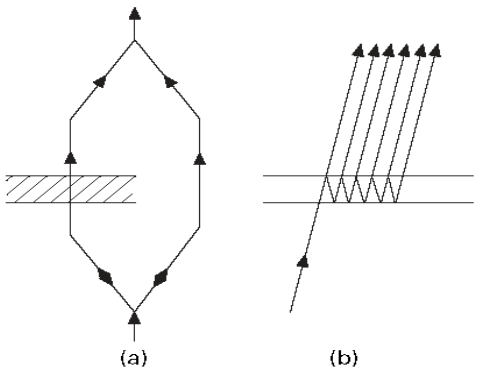

BIREFRINGENCE

The difference ($n_{\parallel} - n_{\perp}$) between the principal refractive indices is known as the birefringence of the fibre.

The refractive index of an isotropic fibre n_{iso}, is given by the mean of the refractive indices of an oriented fibre in the three principal directions. That is $n_{iso} = 1/3 \times [(n_{\parallel} + 2 n_{\perp})]$

BIREFRINGENCE MEASUREMENT TECHNIQUES

1. The birefringence of a fibre is often determined by measuring the two principal refractive indices and subtracting one from the other.

2. It can also be measured directly, by determining the retardation, or difference in optical path length, of the one principal ray relative to the other. Since the optical path length equals the product of the refractive index and the thickness of the specimen through which the light passes.

retardation = (N + N) = ($n_{\parallel} - n_{\perp}$)t, where N + N is the number of wavelengths, and *t* is the thickness.

3. Compensators are used to measure retardation. If the retardation introduced by the compensator is equal and opposite to that introduced by the specimen. If neither compensator nor specimen was present the field appears dark. The compensator can be adjusted until this condition is satisfied in order to determine the retardation at any point in the fibre, either by the use of white light or, by the use of monochromatic light.

EFFECT OF FACTORS LIKE FIBRE ORIENTATION, DENSITY AND REGAIN

Effect of Density

The refractive index will increase as the number of molecules present increases, i.e. as the density increases. The relation between the two is given by Gladstone and Dale's law,

$(n - 1)/p$ = constant, where p = density.

Effect of Regain

The two components cellulose and water were present, and the refractive index of water taken as 1.333, this expression is:

$$v_r (n_r - 1) = v_0(n_0 - 1) + 0.333r \quad \text{---------- > 1}$$

where v_0 is the volume of 1 gram of dry cellulose, v_r is the volume of the same specimen at a fractional regain r, and n_0 and n_r are the refractive indices of the dry and swollen cellulose, respectively.

The rise in the curve at low regains corresponds to the increase in density that occurs as empty space is filled up.

$$v_r (n_{\parallel} - n_{\perp}) r = v_0 (n_{\parallel} - n_{\perp}) \text{ ---------- } > 2$$

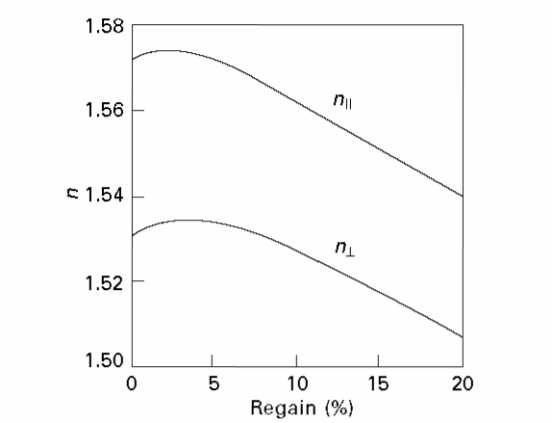

The above equation fits in with the experimental results up to regains of about 15%, and it indicates that the absorbed water is not preferentially oriented. Above 15% regain, the birefringence gradually becomes greater.

An increasing amount of birefringence, arising from the arrangement of the crystalline regions within the non-crystalline regions. At low moisture contents, the differences in the refractive indices of the two regions are so small that the form birefringence would be negligible. At high moisture contents, the moisture absorption takes place almost entirely in the non-crystalline regions, the differences are greater and may have an appreciable effect.

OPTICAL ORIENTATION FACTOR, ITS RELATION WITH BIREFRINGENCE

Optical Orientation Factor

The difference in the refractive indices depends on the direction of alignment of the molecular chain. It is therefore to be expected that the birefringence will be greatest when the molecules are all lined up parallel to the fibre axis and that it will be zero when they are randomly directed.

An **optical orientation factor *f*** as the ratio of the birefringence of the fibre to that of an ideal fibre in which the molecules are perfectly oriented parallel to the fibre axis.

$$\text{Optical orientation factor (f)} = \left(\frac{n_{\parallel} - n_{\perp}}{n'_{\parallel} - n'_{\perp}} \right)$$

$n'_{\parallel} - n'_{\perp}$ refer to the ideally oriented fibre

Hermans has used the average angle of inclination of the molecules φ

$$f = 1 - (3/2 \sin^2 \varphi)$$

In a perfectly oriented fibre, $f = 1$ and $\varphi = 0$. In an isotropic fibre, in which there is no birefringence, $f = 0$, so that $\sin 2\varphi = 2/3$ and φ is approximately 55°.

Refractive Index / Birefringence in relation with Orientation

The refractive indices vary with orientation is shown below.

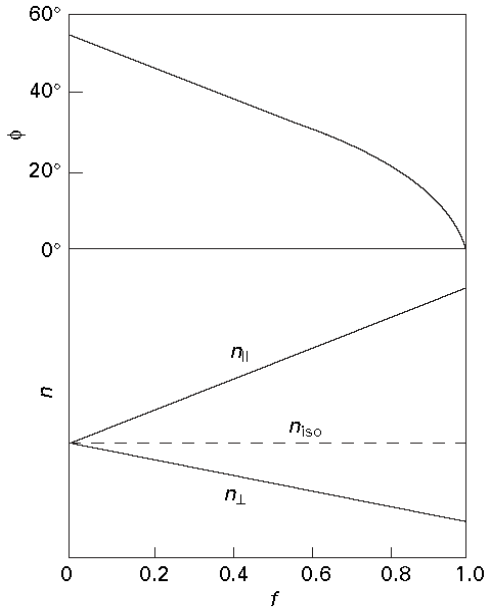

From the above fig, the difference in refractive index value increases as birefringence increases, but helix angle decreases with increase in birefringence.

The birefringence value of cotton and other natural cellulose fibres (in Table) are reduced, due to the helix arrangement of molecules around the fibre axis. The longer cottons have higher values of $n_{||}$ and birefringence and a smaller helix angle.

Fibre	$n_{\|\|}$	$n_{\perp}$	$(n_{\|\|} - n_{\perp})$	f	ϕ	n_{iso}
Ramie	1.588	1.519	0.069	0.97	8°	1.542
Viscose rayon						
10% stretch	1.560	1.533	0.027	0.53	34°	1.542
80% stretch	1.568	1.531	0.037	0.74	25°	1.543
120% stretch	1.573	1.528	0.045	0.88	16°	1.542
Model filaments						
oriented	1.572	1.531	0.041	0.82	20°	1.544
isotropic	–	–	0	0	55°	1.544

Above Table shows values of the refractive indices of various textile fibres. All the values lie within the range 1.5 to 1.6, with the exception of the values for acetate, which fall below it, and the value of $n_{||}$ for Terylene polyester fibre, which is 1.725.

Fibre	$n_{||}$	$n_{\perp}$	$(n_{||} - n_{\perp})$
Cotton	1.578	1.532	0.046
Ramie and flax	1.596	1.528	0.068
Viscose rayon	1.539	1.519	0.020
Secondary acetate	1.476	1.470	0.006
Triacetate	1.474	1.479	–0.005
Wool	1.553	1.542	0.010
Silk	1.591	1.538	0.053
Casein	1.542	1.542	0.000
Vicara (zein)	1.536	1.536	0.000
Nylon	1.582	1.519	0.063
Terylene polyester fibre	1.725	1.537	0.188
Orlon acrylic fibre	1.500	1.500	0.000
Acrilan acrylic fibre	1.520	1.524	–0.004
Polyethylene	1.556	1.512	0.044
Glass	1.547	1.547	0.000

The magnitude of the birefringence, which ranges from –0.005 for triacetate to 0.188 for polyester, depends on two factors: the degree of orientation of the molecules, and the degree of asymmetry of the molecules themselves.

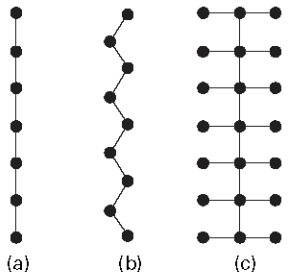

(a) Straight chain. (b) Zigzag chain. (c) Chain with side groups.

If all the atoms in a molecule are arranged in a straight chain Fig. (a), the bond polarisabilities are greatest along the line joining the atoms, then, for the reasons, a high birefringence will be expected.

However, the actual molecules in fibres do not have this form and their birefringence will be reduced for two reasons.

Firstly, most main chains have a zigzag form Fig.(b) but, that the bonds diverge from the main axis by less than about 55°, this still gives a positive birefringence. The coiling of the keratin molecule will have a similar effect in wool.

Secondly, there will be side groups attached to the main chain, as in (c), This will increase the value of $n_{\perp}$ and reduce the birefringence. In triacetate and acrylic fibres, the side groups have a greater effect than the main chain, and the birefringence is negative.

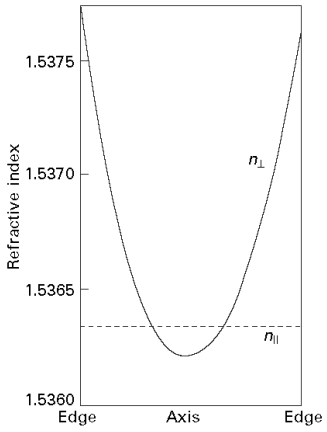

The refractive index may also vary through a fibre cross-section. For example, above fig shows the variation of refractive index across the fibre in un stretched viscose rayon filament. The value of $n_{\parallel}$ is almost constant, but $n_{\perp}$ is a minimum at the centre.

The birefringence of wool, decreases with moisture regain and increases with stretching. In polyester, the presence of a benzene ring in the main chain causes a great increase in the birefringence.

LUSTRE, FACTORS INFLUENCING LUSTRE: (Reflection of light – specular and diffused reflection)

If a beam of light falls on a surface, it may be reflected specularly, along the angle of reflection as in Fig. (a); diffusely, in varying intensity over a hemisphere as in Fig. (b); or in a combination of both. The reflection may vary with the angle of incidence. The total visual appearance resulting from these flections determines the lustre of the material.

If a fibre behaved as a perfectly reflecting circular cylinder, it would reflect light as shown in Fig a. If the light falls across the fibre, it is reflected at various angles, whereas if it falls along the fibre it is predominantly reflected at a constant angle. This shows the importance of fibres to lie parallel to one another in a lustrous yarn or fabric.

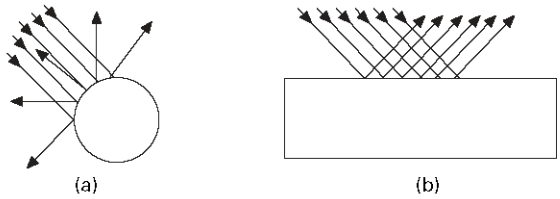

Reflection of light from a circular cylinder (a) axis normal to incident plane; (b) axis in incident plane.

Influencing factors

Finer fibres have a lustre which differs from that shown by coarse fibres. Irregularities on the surface of the fibre and in its cross-sectional shape will cause light to be reflected in various directions and will reduce the lustre. For this reason, lustre is greatest in regular filaments, such as those of silk and the manufactured fibres.

Fibre shape is itself an important factor. The particular types of lustre associated with nylon, rayon and silk must be due partly to the influence on the pattern of light reflection of their respective circular, serrated and triangular shapes.

In cotton, it shows a high degree of correlation between lustre and fibre ellipticity, as given by the ratio *a/b* between two axes taken, respectively, along the longest possible line through the fibre cross-section and perpendicular to this line at the mid-way position.

Mercerisation, which swells the fibres and makes them rounder, increases the lustre of the fibres.

Foster, found that for fibres with an elliptic cross-section, the lustre should be proportional to $[(a2/b2 + 1)/(a2/b2 - 1)] / ac$, where c is the number of convolutions per unit length. This relation gave reasonable agreement with the experimental results If there were no convolutions, the light would be more regularly reflected, and the lustre would be different.

If the fibre contains small particles (e.g. of titanium dioxide) or cavities, as these will scatter the transmitted light at varying angles and cause it to emerge as apparently diffuse reflection. This may be used to delustre manufactured fibres.

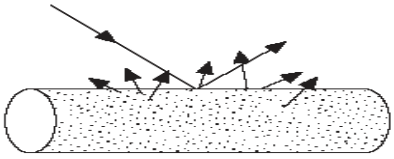

ABSORPTION OF LIGHT – DICHROISM, DICHROIC RATIO

This is the variation in the absorption by the dye with the direction of polarisation of the light, the phenomenon known as *dichroism*, which may result in differences in the depth of shade.

For this to happen, there are three requirements that must be satisfied.

Firstly, the dye molecule must be asymmetrical, so that its absorption varies with the direction of the electric field exciting the characteristic vibrations.

Secondly, the dye molecule must be absorbed into the fibre molecule in a particular direction, so that all the dye molecules make the same angle (or a limited range of angles) with the axis of the chain molecules.

Thirdly, the chain molecules must be preferentially oriented.

When the first two conditions are satisfied, the magnitude of the dichroism may be used as a measure of the orientation of the molecules in the fibre. The absorption of light in a material is given by Lambert's Law: $I = I_0 \exp(-kd)$,

where I is the intensity of light after passing for a distance d through a material with an absorption coefficient k, and I_0 is the intensity of the incident light.

This may also be written: $\log (I / I_0) = - kd (\log e)$

Material exhibiting dichroism, it is necessary to separate the light polarized parallel and perpendicular to the fibre axis, intensities $I_{\parallel}$, and $I_{\perp}$ and absorption coefficients, $k_{\parallel}$, and $k_{\perp}$.

Dichroic ratio

Dichroitic ratio or constant is defined as the ratio of the absorption coefficients parallel & perpendicular to fibre axis.

$$\frac{\log(I_{\parallel} / I_0)}{\log(I_{\perp} / I_0)} = \frac{k_{\parallel}}{k_{\perp}} = Ø$$

The quantity Ø has been called the *dichroic* or *dichroitic ratio* or *constan* & may be used as a measure of orientation in the fibre. Values of the dichroic constant vary from unity in an isotropic material to infinity in a perfectly oriented fibre.

FRICTIONAL PROPERTY

AMONTON'S LAW, BOWDEN'S ADHESION SHEARING MECHANISM.

Amonton's Law:

It states that the frictional force is independent of the area of contact between the two surfaces and is proportional to the normal force between them.

Mathematically, it is expressed as: **$F = \mu N$**

where F = frictional force acting parallel to the surface in a direction opposing relative movement.

μ = coefficient of friction and

N = Normal force between the surfaces in contact.

Types

Static friction: The force that must be overcome in order to start sliding.

Kinetic friction: The force resisting in continued sliding.

Amonton observed that kinetic friction was independent of the speed of sliding. This is sometimes called the third law of friction.

Bowden's Law

Bowden showed that an actual union, or welding, of the two surfaces occur at points of real contact, and the breaking of these junctions when sliding starts.

The surfaces of most materials are irregular, and they are bringing into contact. The contact occurs at the tips of the peaks. If a load is applied, the pressure at the few points of real contact is very great, and they squash down until the area in contact is adequate to support the load.

The nature and extent of the deformation will depend on the mechanical properties of the materials. Metals flow plastically under high loads, and the flow will continue until the pressure at the points of contact is reduced to the yield pressure, when it will support the load without further deformation. If *A* is the total area of real contact, we have:

$$p_y = N / A$$

$$A = N / p_y$$

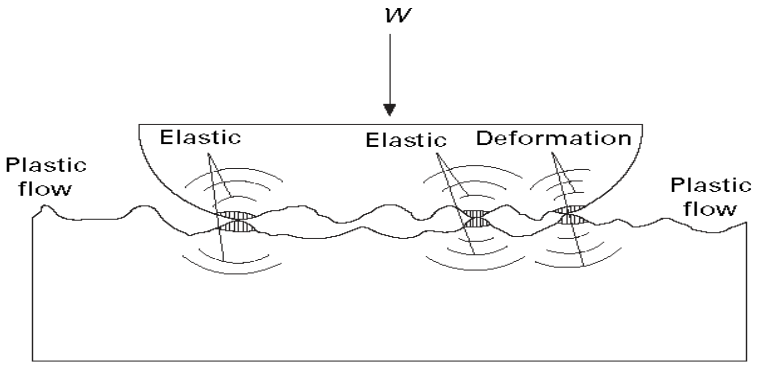

Deformation at points of real contact, showing welded junctions. After Bowden and Tabor

where N = applied load and py = yield pressure.

Thus the area of real contact is proportional to the applied load.

ADVANTAGE & DISADVANTAGE OF FRICTION

1. Friction is the force that holds the fibres together in a spun yarn and the interlacing threads in a fabric. If the friction is too low, the yarn strength will fall, and the dimensional stability of cloth will be reduced. Here high friction is an advantage, enabling a greater strength.

2. In many other places, however, fibre friction is a nuisance. If a yarn passes over a number of guides and makes the angle θ. Excessive breaks are to be avoided if frictional resistance is low.

3. In the stitching of fabrics, high friction causes trouble. The threads will not slide over one another in order to allow the needle to pass between them. This causes many more threads to be broken.

MEASUREMENT OF FRICTION – FRICTION BETWEEN SINGLE FIBRES, FRICTION BETWEEN FIBRE ASSEMBLIES

1. Pascoe and Tabor apparatus is shown in the following fig.

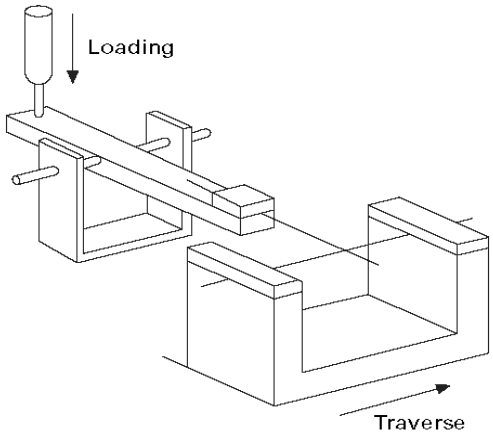

Measurement of fibre friction under very low loads

The sliding fibre is mounted at one end only. The other end rests on the second fibre, which can be traversed along in a frame. The upper fibre acts as a cantilever. Its displacement in the vertical plane gives the load, and its displacement in the horizontal plane gives the force opposing the frictional drag. The displacements are determined by microscopical observation of the free end of the fibre.

2. A loop of fibre is placed over the guide and a small load placed on one side. The load on the other side is then decreased until slippage commences.

Alternatively, a dynamic method may be used, with the yarn running continuously over the guide. A typical modern instrument will have a means of pulling yarn over a guide, with tension meters on either side.

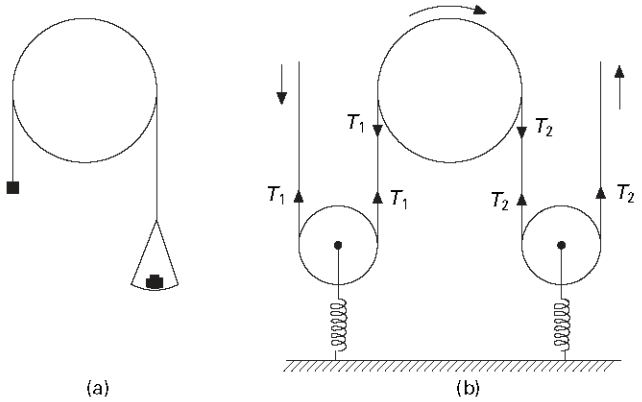

(a) Static capstan method. (b) Dynamic capstan method.

3.For the measurement of inter-fibre friction, Lindberg and Gralén introduced a method in which the two fibres are twisted together as shown in the following fig.

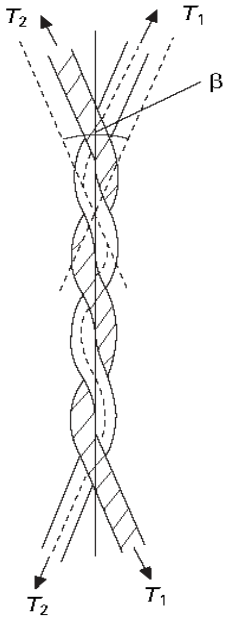

Fig. Measurement of inter-fibre friction

If the difference between the tensions applied to the opposite ends of each fibre is increased, the fibres will eventually slip over one another. It is shown that:

$$\mu = \log_e [(T_2 / T_1) / (\pi n \beta)]$$

where T2 and T1 are the tensions in the fibres, n is the number of turns of twist and β is the angle between the fibre axes and the axis of the twisted element.

4. Another technique that has been used to investigate fibre friction is the measurement of the force necessary to remove a single fibre from a mass of fibres under pressure, or to pull interlocking fringes of fibres. In latter method one fringe of fibres is pulled over. These measurements will be related to the practical behavior of fibres in drafting and in yarns.

5. A very simple means of measuring friction is the inclined plane method. Several turns of yarn are wound as a bow over a bridge and rested on a horizontal plate of the other material. This plate is gradually inclined. The coefficient of friction is equal to the tangent of the angle of inclination at which slippage starts.

FACTORS INFLUENCING FIBRE FRICTION

1. Load & area of contact
2. Speed
3. State of the surface
4. Effect of water.

Load & Area of contact

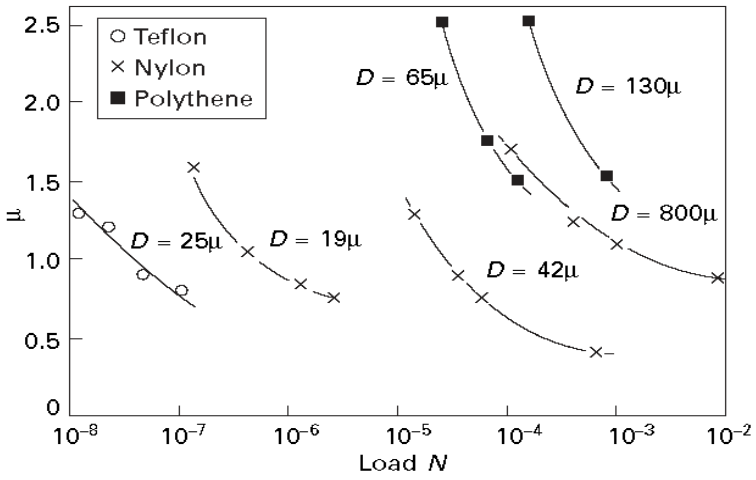

Fig. Variation of coefficient of friction with load (D = fibre diameter)

In the above fig, the ratio of frictional force F to normal load N for fibres is found to decrease as the load is increased. In other words, Amontons' law is not obeyed. Mathematical relations that have been used

to fit the experimental data as follows.

$$F = \mu_0 N + \alpha S$$

$$F / N = A - B \log N$$

$$F = aN + bN^c$$

where S = area of contact, and μ_0, α, A, B, a, b and c are constants. The most successful relation has:

$F = aN^n$ where a and n are constants.

Speed

The kinetic friction μk is usually less than the static friction μs. Any finish or lubricants on the material reduces the differences between μk and μs. At low speeds, going from 2 to 90 cm/min, the friction decreased, but at much higher speeds the friction increases. The variation of friction with speed will have a considerable influence on the behavior of fibres in drafting

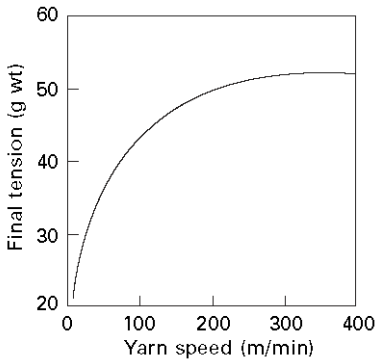

Fig. Variation of final tension after acetate yarn has passed over a guide at varying speeds.

Cotton is exceptional one, even at low speeds the coefficient of friction increases. Under medium-load conditions, the coefficient of friction was 0.23 at 3.6 cm/min, it increased to 0.25 at 200 cm/min and to 0.39 at 4500 cm/min.

State of the surface

The frictional force is changed if the surface is lubricated, either naturally by waxes or artificially in cotton.

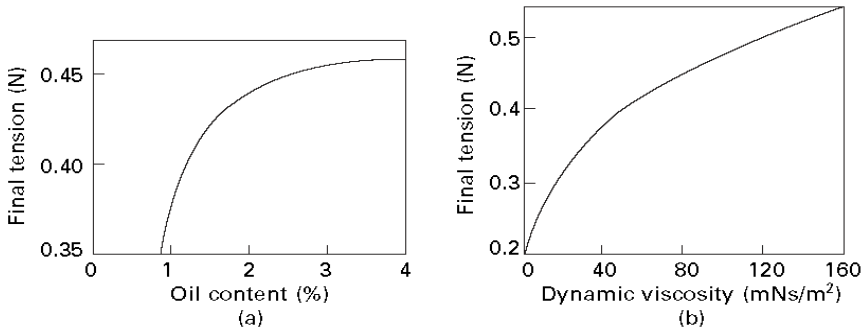

Fig. Variation of final tension after passage of acetate yarn over guide, for (a) varying amounts of oil on yarn and (b) varying viscosity of oil.

In above fig shows, the acetate yarn with more than 1% of oil applied. The frictional force increases both as the oil content is increased and as the viscosity of the oil increases.

However, fibres(cotton) from which all traces of lubricant have been removed show high values of friction; thus, in one experiment, raw cotton on steel gave $\mu = 0.25$, whereas scoured cotton on steel gave $\mu = 0.7$, and lubricated scoured cotton on steel gave values of μ ranging from 0.14 to 0.35.

Bradbury and Reicher, have found extremely high values of friction between flat continuous-filament yarns. This high value of friction was not found if the yarns were twisted, or if the glass surface was roughened by grinding: this suggests that the effect is associated with a high true area of contact.

A similar effect was observed by King, who found a reduction in the friction of wool fibres on various materials when the surface was roughened.

Table 25.4 Effect of surface roughness: Values of μ for wool rubbed on various materials [36]

Material	Polished surface		Rough surface	
	With scales	Against scales	With scales	Against scales
Casein	0.58	0.59	0.47	0.57
Ebonite	0.60	0.62	0.50	0.61
Sheep's horn	0.62	0.63	0.52	0.63
Cow's horn	0.49	0.54	0.42	0.53

Effect of water

The frictional force usually increases as the regain of the fibres is raised. The results are shown in the graph.

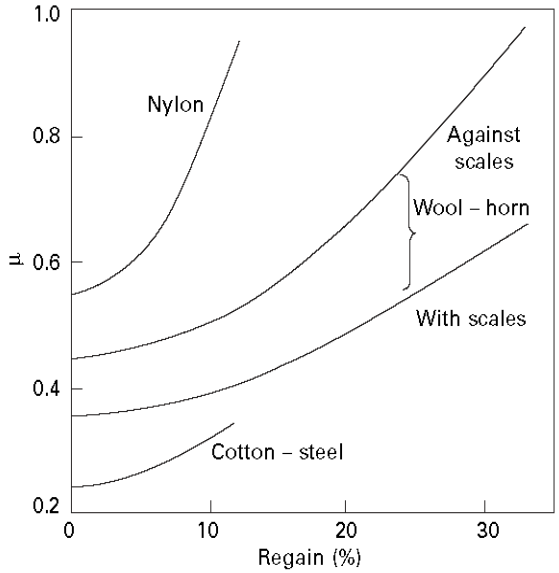

Change of coefficient of friction with regain for nylon on nylon, wool on horn, and cotton on steel.

FRICTION IN WOOL – DIRECTIONAL FRICTIONAL EFFECT

The friction of the wool fibre depends on the direction in which it is pulled. The resistance is greater when it is pulled against the scales than when it is pulled with them. This is known as the ***directional frictional effect*** **(DFE)**

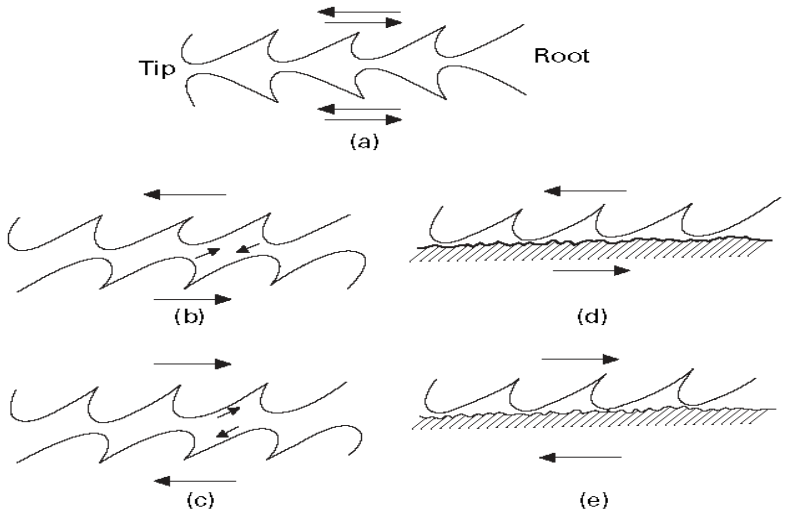

25.26 Directional friction in wool: (a) between fibres placed in same direction; (b) between fibres against scales; (c) between fibres with scales; (d) on plane surface, against scales; (e) on plane surface, with scales.

Theory of the directional frictional effect

The wool fibre acts as a ratchet, with the scales interlocking with one another or catching against asperities on another surface. Motion against the scales would be strongly resisted, since it would involve rupture or deformation of the scales.

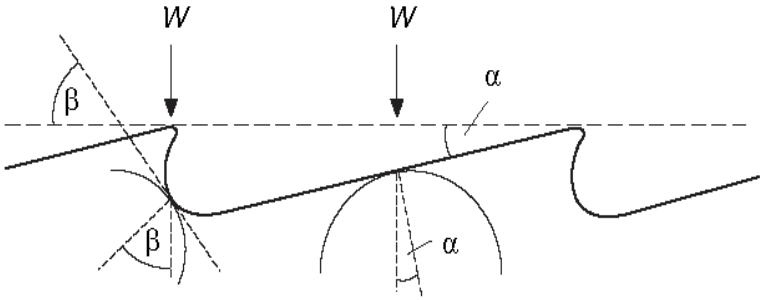

Fig. Contact between scale structure and asperities on a surface

Above fig, the scale surfaces are assumed to be inclined at an angle α, so that a tangent through the point of contact between an asperity and the scale surface makes an angle α with a line parallel to the axis of the wool fibre. Contact may also occur between an asperity and the scale edge, with the tangent at the contact making an angle β with the fibre axis. We consider the relations between the forces when contact occurs at an angle, as shown

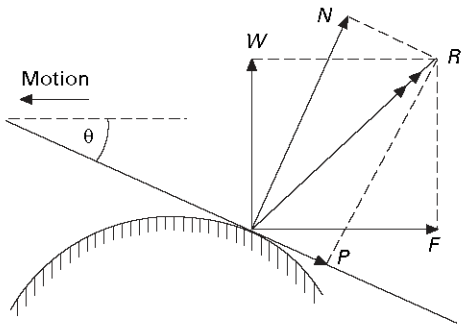

Fig. Geometry of contact.

The resultant force R acting at the contact may be resolved either into components W and F acting perpendicular and parallel to the direction of motion, or into components N and P acting perpendicular and parallel to the tangent at the contact. If the angle between these directions is θ, we must have:

$$N = W \cos \theta + F \sin \theta$$

$$P = F \cos \theta - W \sin \theta$$

For slippage to occur, the junction must be sheared. The general frictional relation $P = aN^n$.

Substituting we have $F \cos \theta - W \sin \theta = a (W \cos \theta + F \sin \theta)^{n.}$

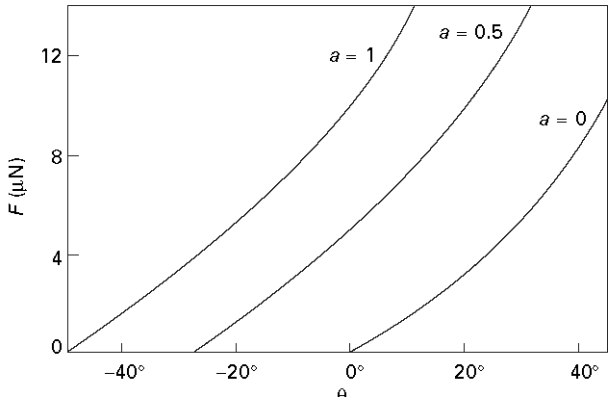

Fig. Variation of Fwith 0, with n = 2/3.

Above fig shows the values of *F* for various values of *a* and θ, when *n* = 2/3.

The resistance to motion decreases as the value of θ decreases. When θ is positive, there will be resistance to motion even if *a* = 0. It should be noted that negative values of θ correspond to motion in the reverse direction.

In wool, however, there is a regular arrangement of asperities, the scale structure for motion against the scales, the two types of contact will have values of θ equal to +β and –α, whereas for motion with the scales the values will be –β and +α. From the combination of these values, shown in Fig below, the frictional force would be greater against the scales.

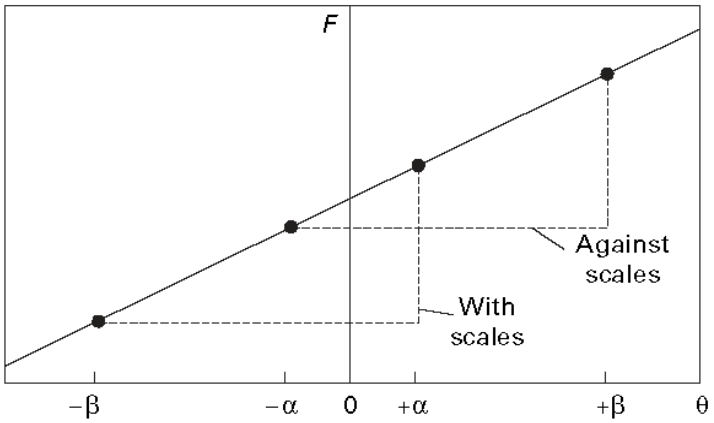

Fig. Combination of values, for motion with and against scales.

FELTING

In a mass of wool, individual fibres will show preferential movement in one direction and will continually entangle themselves with the remaining fibres: is called felting.

UNIT : 5

THERMAL AND ELECTRICAL PROPERTIES OF FIBERS

4. Thermal Properties

4 · 1 Transition Point

4 · 1 · 1 Glass Transition Point (Secondary Transition Point)

The glass transition point of polycarbonate obtained from the inflection point of refractive index is 141~149℃, as shown in Fig. 4 · 1 · 1－1. In addition, the glass transition point obtained by the measurement of expansion coefficient, specific heat, differential thermal analysis, and viscoelasticity, etc. is in the range of 130~155℃.

When the glass transition point is studied in further detail, it differs in accordance with the molecular weight, as shown in Fig. 4 · 1 · 1－2 (Tg was obtained by the differential thermal analysis).

Also, the glass transition point is known to have the pressure dependence and as for polycarbonate, it is as follows:

$$\delta T_g / \partial p = 0.044℃/atm$$

A comparison with other resins is shown in Table 4 · 1 · 1－1.

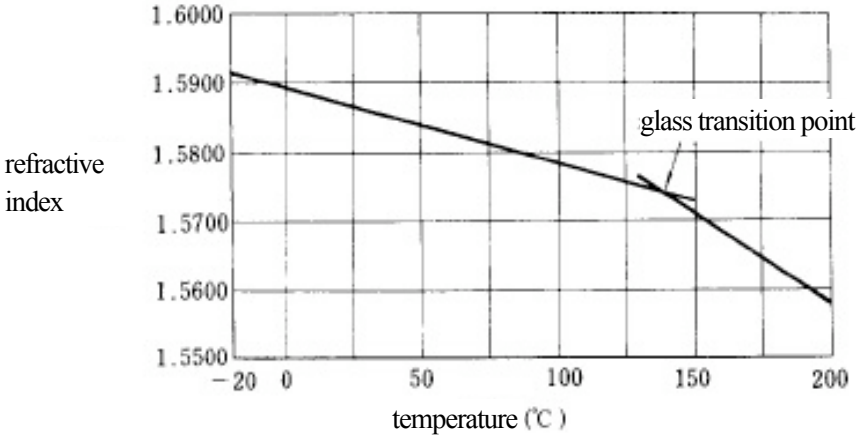

Fig. 4 · 1 · 1－1 Temperature characteristics of refractive index of polycarbonate

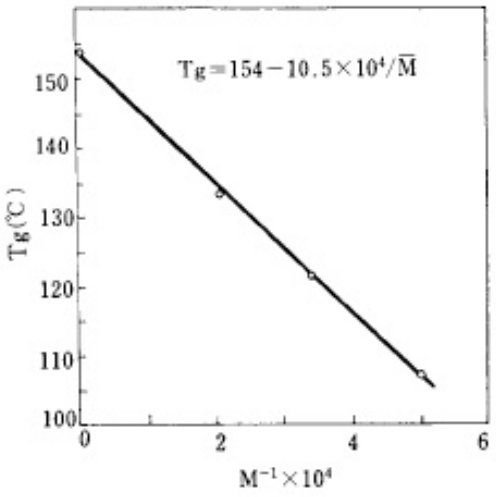

Fig. 4 · 1 · 1－2 Relation between Tg (glass transition point) and M (molecular weight)

Table 4・1・1—1 T_m, T_g and dispersion temperature of other resins

Name	T_m melting point	T_g glass transition point (℃)	Dispersion temperature				
			Crystalline dispersion	Primary dispersion	Secondary dispersion	Secondary dispersion	Secondary dispersion
Polyethylene	107—138	—53——23	60 72	—18 — 8 23	—126 —111 — 65		
Polypropylene	168—170	—35	82	— 2 22	— 83 — 40	—215 —173	
Polyvinyl chloride (PVC)	217	77		91 117 127	— 38 12		
Polyvinylidene chloride	190	—18	77	33	— 23		
Polytetrafluoroethylene	327	—73——63	127 150	—33	— 93 — 66 — 31		
Polystyrol	230	80—90		117 131 148	40	—153 — 53 87	
Polymethyl methacrylate (PMMA)		82—102		127 143 167	27 103	—115 — 69 17	—183 —143 — 53
Polyvinyl acetate		7—27		30 90	— 47	—113 —17	
Polyethylene・ terephthalate (PETP)	265	63—83		57 127	—10 7		
Polyoxymethylene	177	—40——60	127	—13 45 127	— 73 — 58 — 33		
Nylon 6	223	33—53		57 82	— 61 — 23 32	—128 —105 30	
Nylon 66	275	33—53		67 82	— 53 — 23	—125 —103	

Note: The upper, middle and lower dispersion temperatures are the measuring results at 1, 10^3 and 10^6Hz., respectively.

4・1・2 Melting Point

The melting point of Iupilon / NoVAREX pellet is 220～230℃.

The melting point of crystallized polycarbonate is about 230～260℃ (Refer to Fig. 4・5・2－2).

The melting heat of the crystalline is 134J/g (32cal/g).

The melting point of other resins is shown in Table 4・1・1－1.

4・1・3 Dispersion temperature

As for the thermoplastic resin, it is known that there are the primary dispersion zone where the macro-Brownian motion of molecular chain occurs, and the secondary dispersion zone where the local thermal motion (for example, thermal motion of methyl group of a part of main chain or side chain) occurs. Polycarbonate is not exception, too and its exixtence is recognized in many literatures.

The dispersion temperature of polycarbonate is summarized in Table 4・1・3－1.

Table 4・1・3－1 Dispersion temperature of polycarbonate

Dispersion type	Primary dispersion α	Secondary dispersion β	Secondary dispersion γ	Secondary dispersion δ
Dispersion temperature (℃)	157 (1) 175 (10^3) 195 (10^5)	0—100	−100 (1) −80 (10^3) −3 (10^6)	−200 ～ −100
Thermal motion type	Macro-Brownian motion of main chain		Free rotation motion of the C=0 group which accompanies the restricted motion of the phenyl group	Free rotation motion of the Me group (by MMR)

The results of these dispersions are shown in Fig. 4・1・3－1, 2, 3 and 4. The primary dispersion, the γ dispersion and the δ dispersion are shown in Fig. 4・1・3－1, 4・1・3－2, 4・1・3－3, respectively. As for the β dispersion, its existence is recognized in many literatures but there is not definite one. Fig. 4・1・3－4 is an example. Refer to Table 4・1・1－1 for other resins.

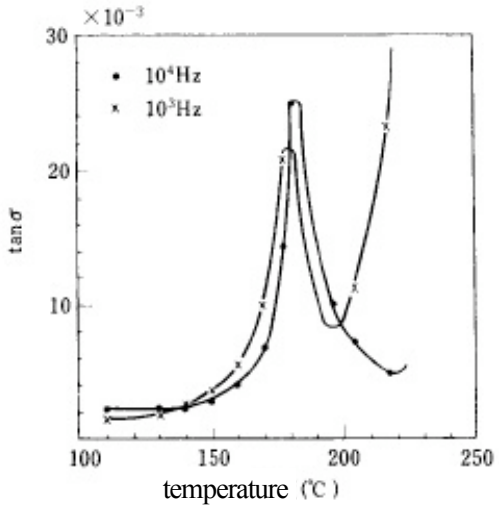

Fig. 4・1・3－1 Change in tan δ at primary dispersion zone

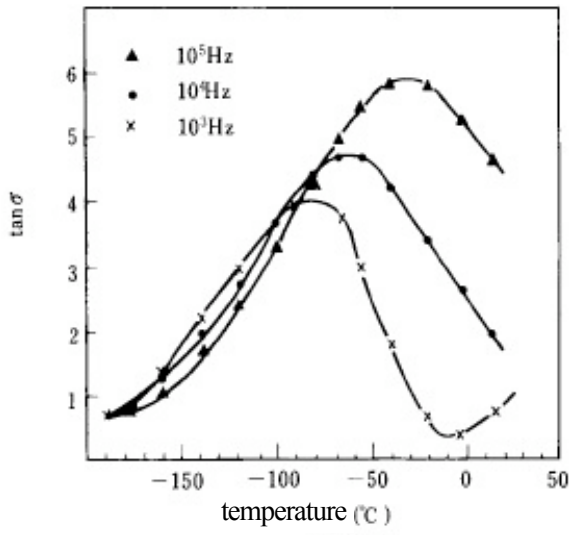

Fig. 4・1・3－2 Change in tan δ at low temperature zone

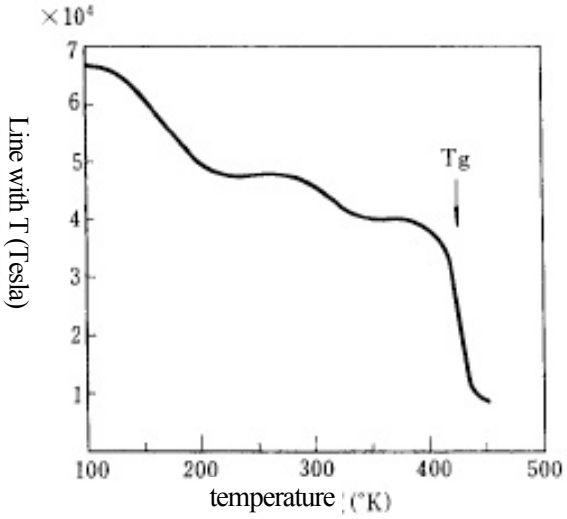

Fig. 4・1・3−3 NMR of polycarbonate Change in temperature of Line width（1Gs＝10¯4T）

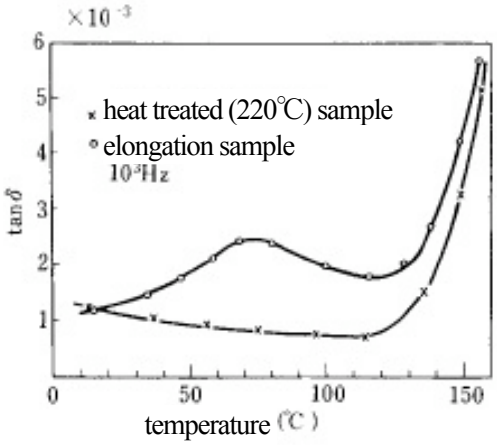

Fig. 4・1・3−4 Change in tan δ at low temperature zone

4・2 Thermal Conductivity and Specific Heat

As shown in Fig. 4・2−1, the specific heat of polycarbonate changes with temperature but it can be considered that this is 1.09～1.17J/(g.k) (0.26～0.28cal/g.℃) for the practical temperature range. This value does not differ very much from the common synthetic resins and corresponds to about 3 times of iron and copper etc.

The thermal conductivity of polycarbonate is

0.19W/(m.k)(4.6×10^{-4}cal/cm.sec℃)

This value does not differ very much from the common synthetic resins and is very small when compared with those of metals as it is 1/400 of iron, 1/1000 of aluminum and 1/2000 of copper.

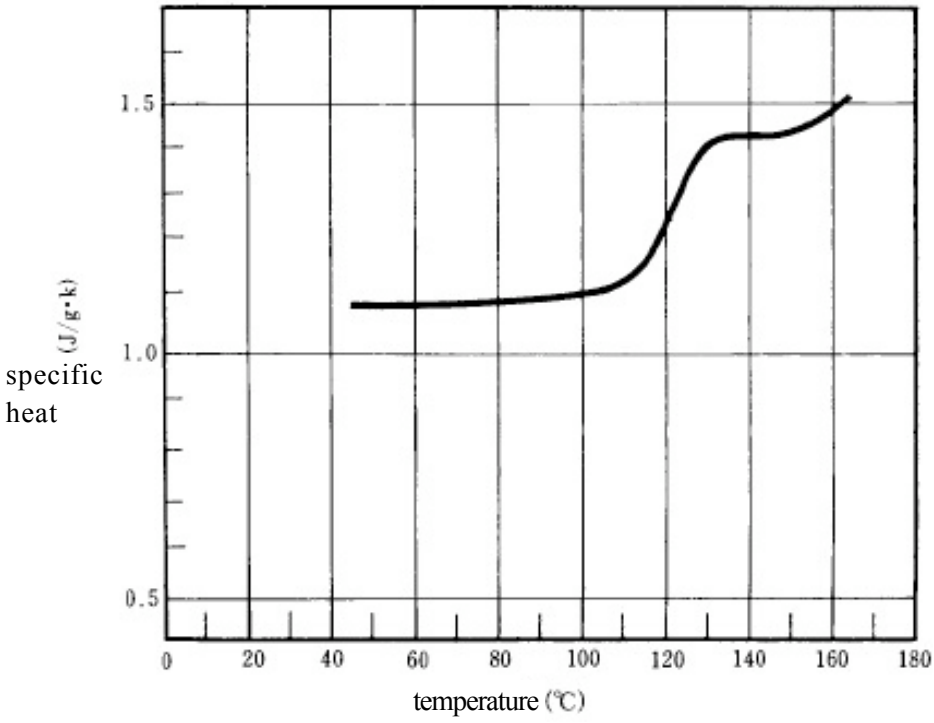

Fig. 4・2−1 Specific heat – temperature characteristic of polycarbonate

The thermal conductivity and specific heat of other resins are shown in Table 4・2－1

Table 4・2－1　Comparison of thermal properties

Name	Thermal conductivity W／（m・k）（cal/cm. sec℃）X 10^{-4}	Specific heat kJ／（kg・k）（cal／g・℃）	Linear expansion coefficient 10^{-5}・k^{-1}	Brittle temperature ℃	Deflection temperature under load（℃）	
					1820kpa（18. 6kgf／cm^2）	455kpa（4. 6kgf／cm^2）
Low density polyethylene	0. 33（8）	2. 3（0. 55）	16－18	－85－－55	32－41	38－49
High density polyethylene	0. 46－0. 52（11－12. 4）	2. 3（0. 55）	11－13	－140	43－54	60－88
Polypropylene	0. 14（3. 3）	1. 9（0. 46）	6－10	－10－－35	57－63	93－110
Acrylate（PMMA）	0. 17－0. 25（4－6）	1. 5（0. 35）	5－9	90	70－100	74－110
Polystyrene	0. 10－0. 14（2. 4－3. 3）	1. 4（0. 33）	6－8		80－90	
Polyvinyl chloride	0. 13－0. 17（3－4）	1. 0（0. 24）	5－6	81	54－79	57－82
Polyvinylidene chloride	0. 13（3）	1. 3（0. 32）	19	0－－30	55－65	
Polytetrafluoroethylene	0. 25（6）	1. 0（0. 25）	10			121
Polyvinyl acetate	0. 16（3. 8）	1. 6（0. 39）	8. 6		38	
Acryl nitrile・Styrene（AS）	0. 12（2. 9）	1. 4（0. 33）	6		88－102	
66 Nylon	0. 22－0. 24（5. 2－5. 8）	1. 7（0. 40）	10－15		66	
6 Nylon	0. 21（5. 0）	1. 6（0. 38）	8－13	－85－60	62	150
Polyethylene・terephthalate（PETP）			27			
Polyether	0. 23（5. 5）	1. 5（0. 35）	8. 2	－76－－120	110	170
Triacetyl cellulose	0. 17－0. 33（4－8）	1. 5（0. 35）	8－16		44－91	49－98
Modified PPE	0. 22（5. 2）	1. 3（0. 32）	5. 6	＜－40	117	128
Polysulfone		1. 3（0. 3）	5. 6		174	181
Polycarbonate	0. 19（4. 6）	1. 1（0. 27）	6	－135	130－136	136－142

4・3 Coefficient of Thermal Expansion

The coefficient of linear expansion of Iupilon / NOVAREX at 20~120℃ is

$6\sim7 \times 10^{-5}/K$

The coefficient of volume expansion of Iupilon / NOVAREX at 30~130℃ is

$(20\pm5) \times 10^{-5}/K$

The change in length and volume weight ratio is shown in Fig. 4・3－1 and 2, respectively. The relation between temperature and volume expansion coefficient is shown in Fig. 4・3－3. The coefficient of linear expansion has the refraction point near the room temperature and becomes small in the low temperature region.

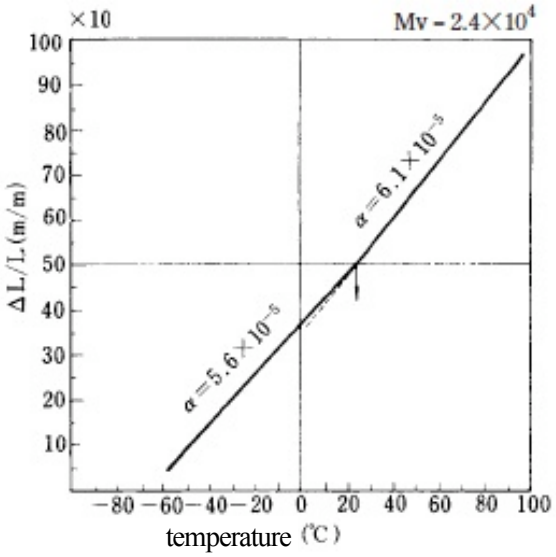

Fig. 4・3－1 Coefficient of linear expansion of Iupilon / NOVAREX

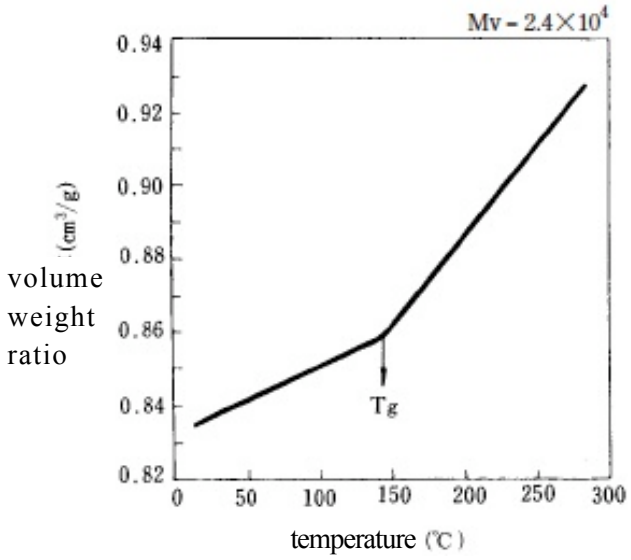

Fig. 4・3－2 Relation between temperature and volume weight ratio

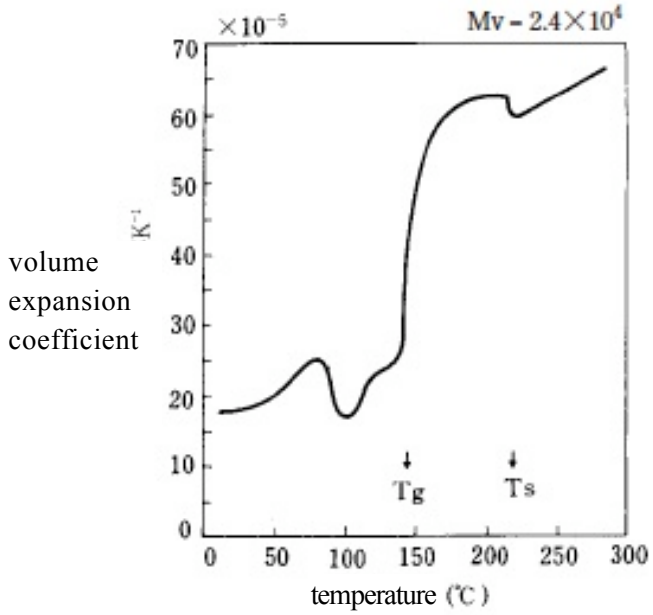

Fig. 4・3－3 Relation between temperature and volume expansion coefficient

4 . 4 Deflection Temperature

The deflection temperature（ASTM－D648－56）of Iupilon / NOVAREX is

Stress 1.82MPa (18.6kgf/cm^2)　132～138℃
Stress 0.45MPa (4.6kgf/cm^2)　138～144℃

The deflection temperature changes in accordance with the added load and is shown in Fig. 4・4－1 in case of Iupilon / NOVAREX. Also, the deflection temperature is influenced by the molecular weight in the same way as Tg (glass transition point) as shown in Fig. 4・4－2.
When Iupilon / NOVAREX is heat-treated, as indicated in other physical properties, the heat hardening is shown and the deflection temperature changes rapidly as shown in Fig. 4・4－3.
A comparison with other resins is shown in Table 4・2－1 and Fig. 4・4－4.

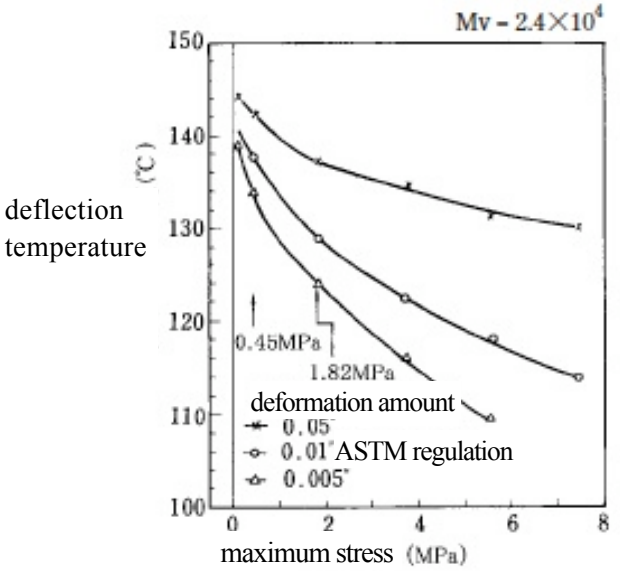

Fig. 4・4－1　Change in deflection temperature by load molecular

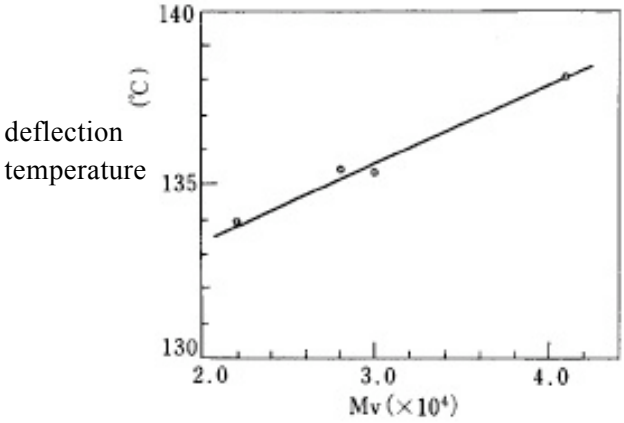

Fig. 4・4－2　Relation between weight and deflection temperature（Stress 1.82MPa）

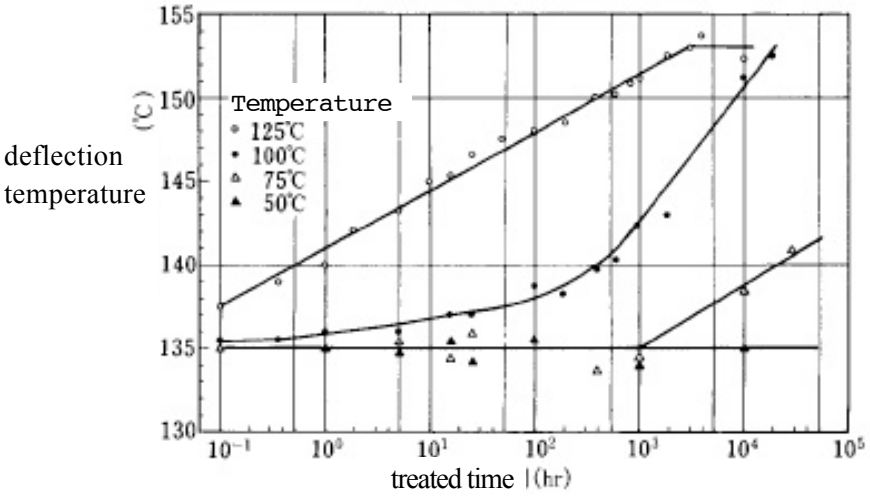

Fig. 4・4－3　Change in deflection temperature by heat-treatment (Stress 1.82MPa)
（Mv＝2. 8×10^4）

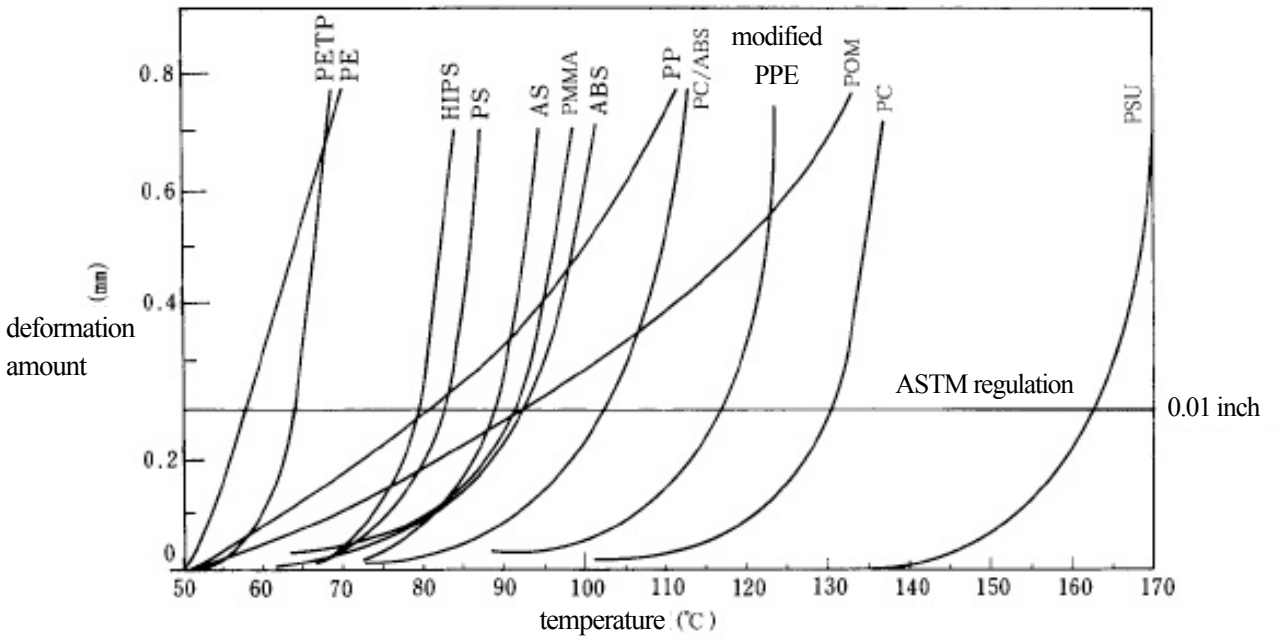

Fig. 4・4－4　Deflection temperature of other resins (Stress 1.82MPa)

4・5　Thermal Stability and Pyrolysis

It is possible to know the excellent heat resistance as shown in Fig. 4・5・2－2 where the differential thermal analysis result of Iupilon / NOVAREX is indicated. However, when examining it more in detail, the different aspect of every change in various temperature regions (practical temperature region, processing temperature region, decomposition combustion region), in the environment (in oxygen, in air, in nitrogen, in vacuum, in steam) is recognized.

4・5・1 Low temperature region

When Iupilon / NOVAREX is heat-treated at the temperature below Tg, the fact that the change in physical properties occurs due to the hardening phenomenon has already been known and there are a lot of researches to look for the cause in the change of the solid structure. However, when heating it in air at this temperature region for long time, it is observed that the chemical changes (oxidation, decomposition), discoloration, decrease in molecular weight etc. take place.

The result of arranging the yellowed degree of this temperature region is shown in Fig. 4・5・1－1. Curve (1) shows the influence of temperature on the yellowed speed, but the aspect of change is different at the up-and-down region of Tg. This might be due to the difference of the thermal effect of the molecular chain, that is, the difference of oxygen diffusion speed. Curve (2) shows the relation between temperature and treated time that the yellowed degree becomes equivalent.

Fig. 4・5・1-2 shows the CO_2 generation speed at this temperature region and the breakage of carbon bond, namely the decrease in molecular weight.

Fig. 4・5・1－3 and 4 show the comparison of the oxidation with other resins and the antioxidative property of polycarbonate.

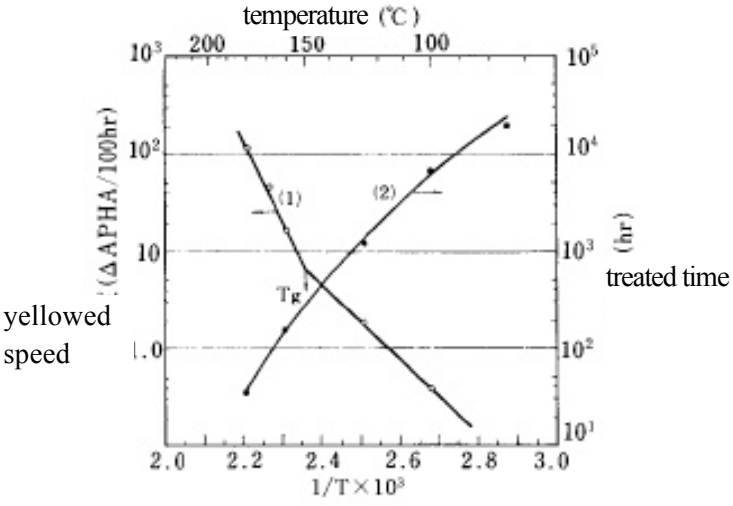

Fig, 4・5・1−1 Yellowed speed of Iupilon / NOVAREX (Mv＝2.4×10⁴)

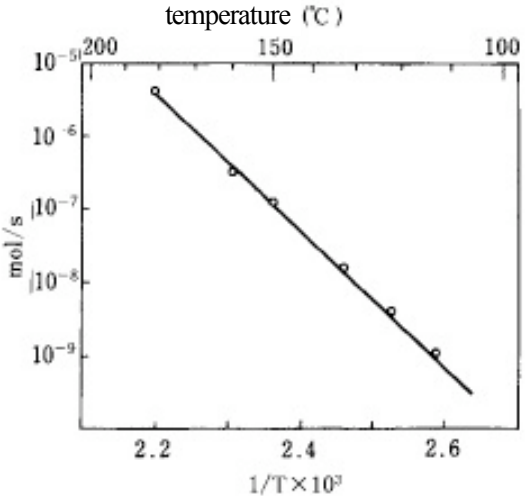

Fig. 4・5・1−2 CO_2 generation at 110~180℃ (Mv＝2.4×10⁴)

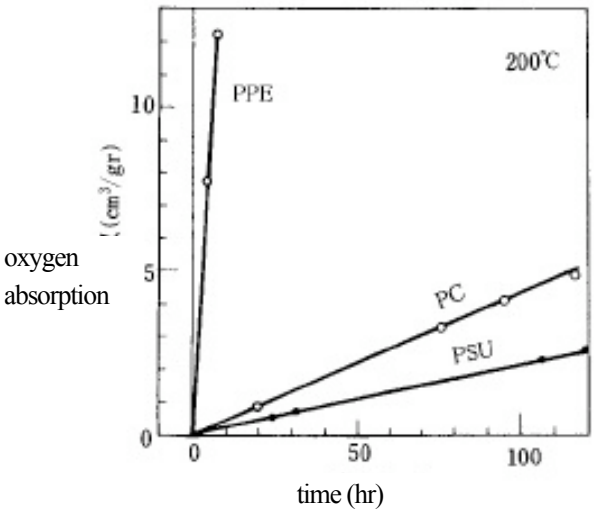

Fig. 4・5・1−3 Oxygen absorption speed at 200℃

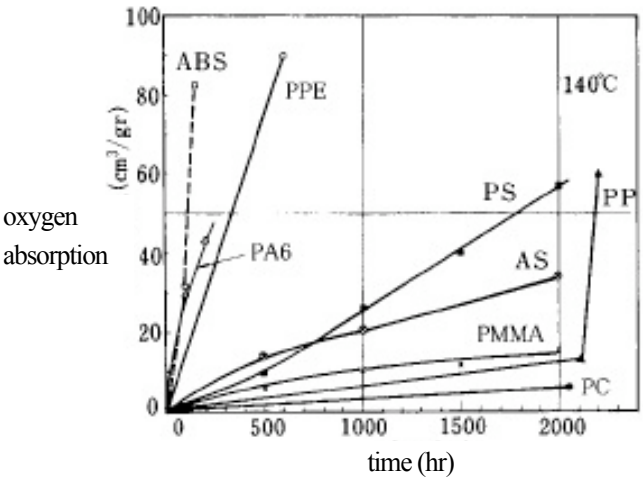

Fig. 4・5・1−4 Oxygen absorption speed of various resins

4・5・2 High temperature region

The heat stability of Iupilon / NOVAREX is excellent. As shown in Fig. 4・5・2−1, the change in heat stability is observed at the temperature above 450℃, and the influence of atmosphere, impurities, and additives is large in such a high temperature region, especially oxygen and moisture promote the heat degradation considerably.

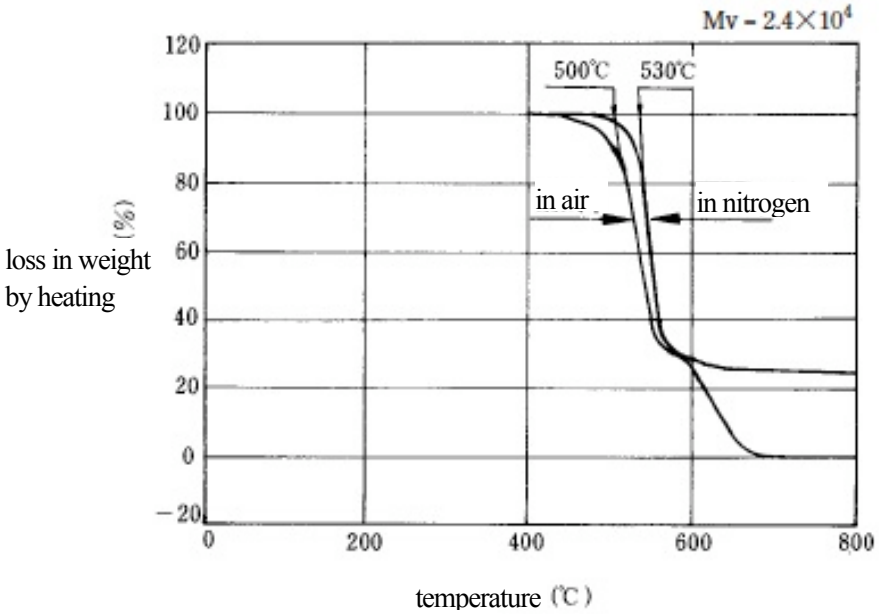

rate of temperature increase 20℃/ min
gas velocity 30cm3 / min
dried sample

Fig. 4・5・2−1 Thermobalance analysis result of Iupilon / NOVAREX

The pyrolysis of Iupilon / NOVAREX、consists of one exothermic region and two endothermic regions as shown from the result of the differential thermal analysis in Fig. 4・5・2－2. The exothermic region is the first stage of pyrolysis, the oxidation reaction is observed as an exothermic peak that starts at about 340℃and is highest at about 470℃. The first endothermic region is based on the depolymerization and peaks at 500℃. The second one is the region where the bond energy becomes equivalent to thermal energy, and dissociation of all molecular bonds takes place. The exothermic peak based on thermal oxidation and endothermic peak also decrease considerably in nitrogen and show that the influence of oxygen is remarkable.

The decomposition gases generated by pyrolysis change by atmosphere as shown in Table 4・5・2－1, but CO, CO_2 by the decomposition of carbonic acid group, CH_4 by the dissociation of methyl group, and various phenols by the decomposition of BPA (bisphenol A) are main decomposition products. The generation of CO_2, CH_4, and various phenols are shown in Fig. 4・5・2－3, 4 and 5.

The generation becomes active at around 300℃ in air, but shifts to high temperature side about 50℃in nitrogen atmosphere.

The decrease in molecular weight of Iupilon when heated for 2 hours in nitrogen and in air is shown in Fig. 4・5・2－6 and 7.

Also, the result of heating for a long time in the sealed tube in vacuum was shown in Fig. 4・5・2－8.

The relation between temperature and pyrolysis kinetics is shown in Fig. 4・5・2－9, 10, and the influence of oxygen and moisture is extremely big.

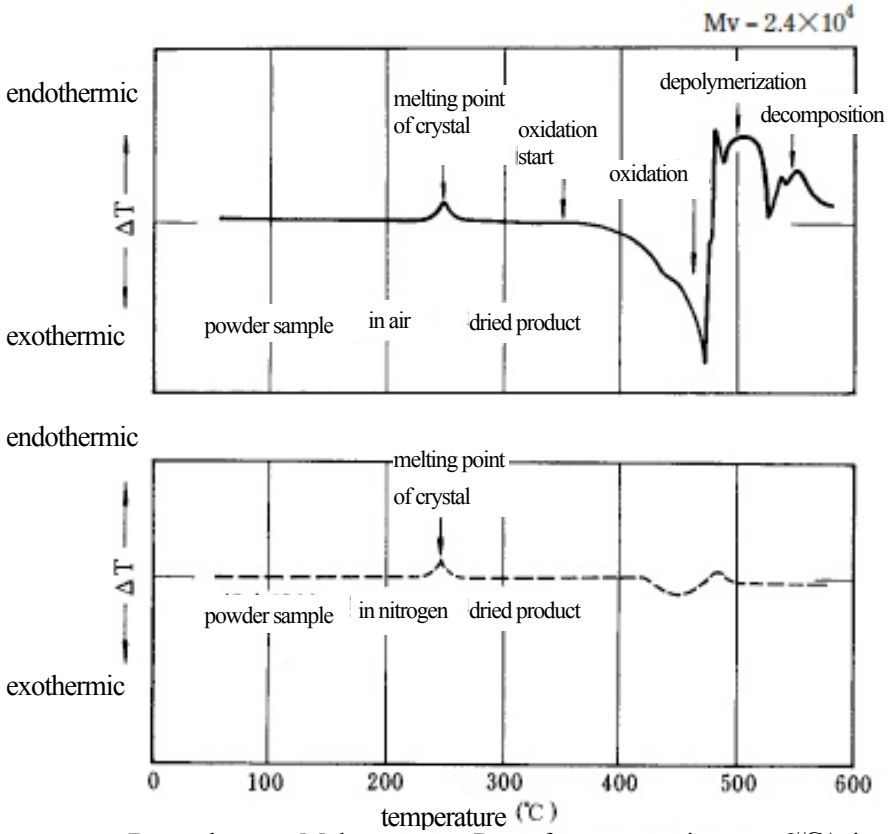

Base substance: Molten quartz　Rate of temperature increase: 8℃/min.
Packing method: Sandwitch method

Fig. 4・5・2－2　Result of differential thermal analysis of Iupilon / NOVAREX

Table 4・5・2－1　Decomposition products of polycarbonate

（＋）：generated

Decomposition products	In oxygen	In air	In vacuum sealed	In vacuum continuous	Decomposition products	In oxygen	In air	In vacuum sealed	In vacuum continuous
CO_2	＋	＋	＋	＋	Benzene	＋	＋		
CO	＋	＋	＋	＋	Toluene	＋	＋		
CH_4	＋	＋	＋	＋	Ethyl benzene	＋	＋		
H_2	＋				Phenol	＋	＋	＋	＋
H_20	＋	＋	＋		Cresol	＋	＋	＋	＋
HCHO	＋				Ethyl phenol		＋	＋	＋
CH_3CHO	＋								
Acetone		＋							
Methanol	＋				Isopropyl phenol		＋	＋	＋
Diphenyl					Isopropenyl phenol		＋	＋	＋
			＋	＋	Bisphenol A	＋	＋	＋	＋

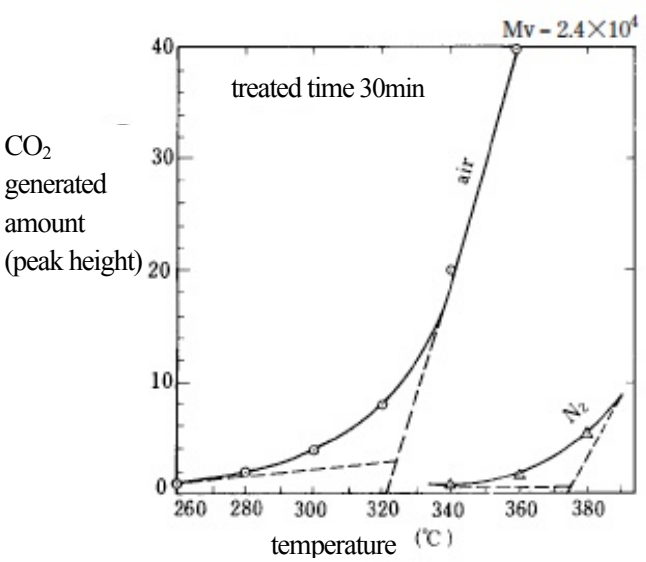

Fig. 4・5・2－3　Influence of atmosphere on CO_2 generated amount

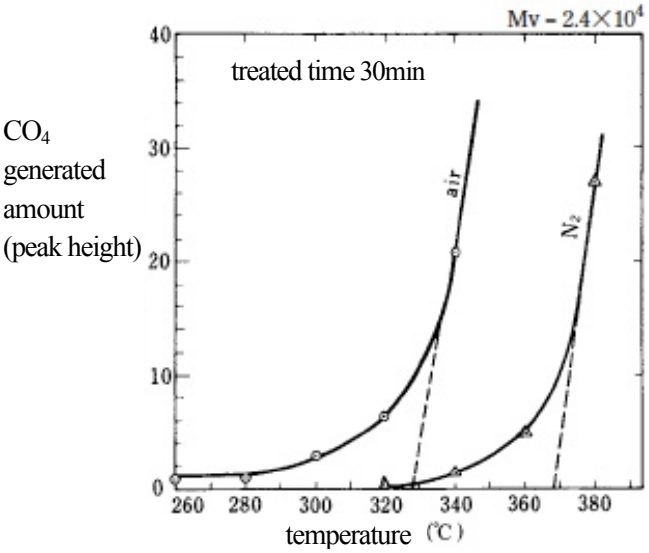

Fig. 4・5・2－4　Influence of atmosphere on CH_4 generated amount

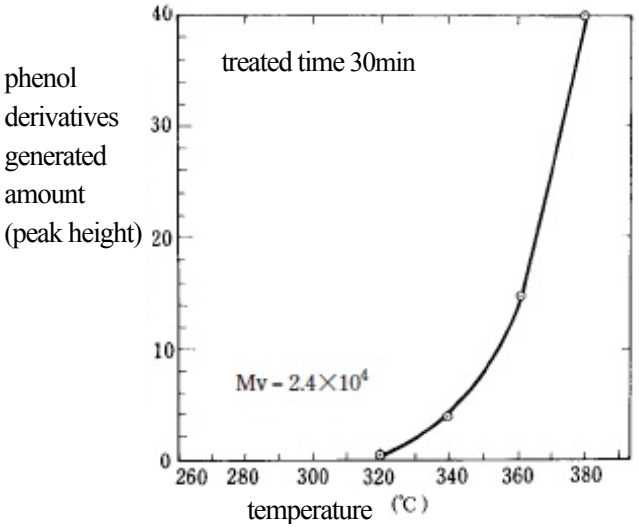

Fig. 4・5・2－5　Relation between temperature and generated amount of phenol derivatives by decomposition when heated in air

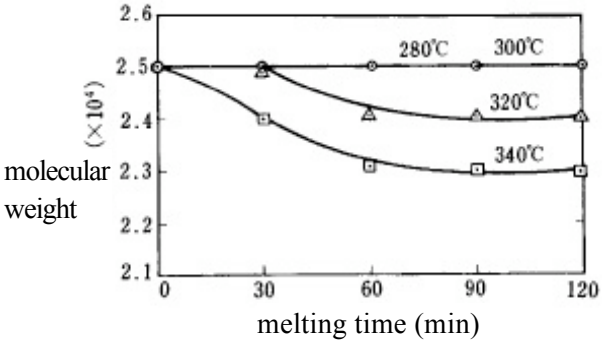

Fig. 4・5・2－6 Decrease in molecular weight of Iupilon / NOVAREX by meltin (Completely dry, melted in nitrogen stream)

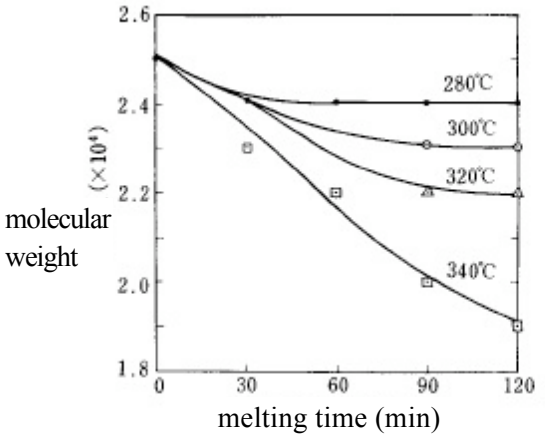

Fig. 4・5・2－7 Decrease in molecular weight of Iupilon / NOVAREX by melting (Undried, melted in air)

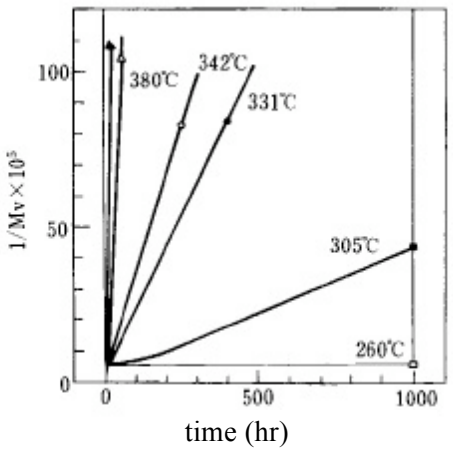

Fig. 4・5・2－8 Decrease in molecular weight (Mv) of sealed tube in vacuum

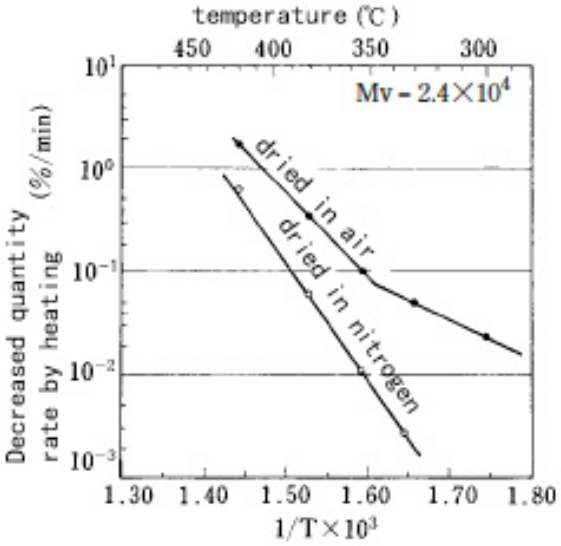

Fig. 4・5・2－9 Decreased quantity rate of Iupilon / NOVAREX by heating

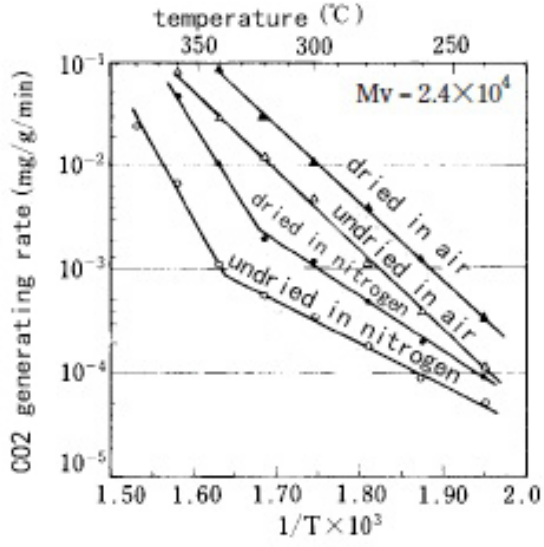

Fig. 4・5・2－10 CO_2 generating rate of Iupilon / NOVAREX

When the inorganic filling agent is added to Iupilon / NOVAREX, the influence on the pyrolysis is big. For ezample, decreased quantity rate in case of adding an iorganic filling agent in Fig. 4・5・2－11 and CO_2 generated amount in Fig. 4・5・2－12 indicate the value which is bigger than the material in any case. Also, the influence of metal salts is shown in Table 4・5・2－2. The influence of carbonates is extremely big, and the others also have influence to some degree.

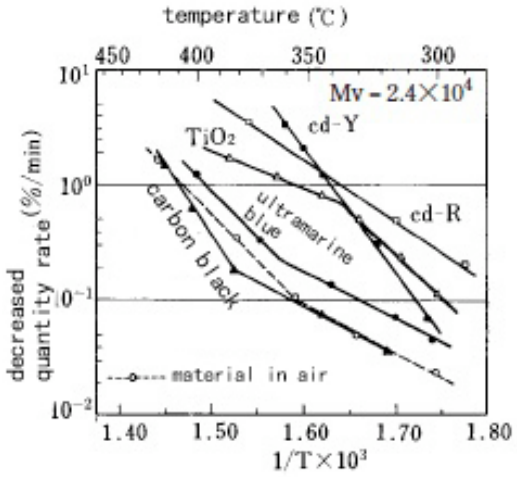

Fig. 4・5・2－11 Influence on decreased quantity rate of the pigment (pigment additive amount: 1.0%)

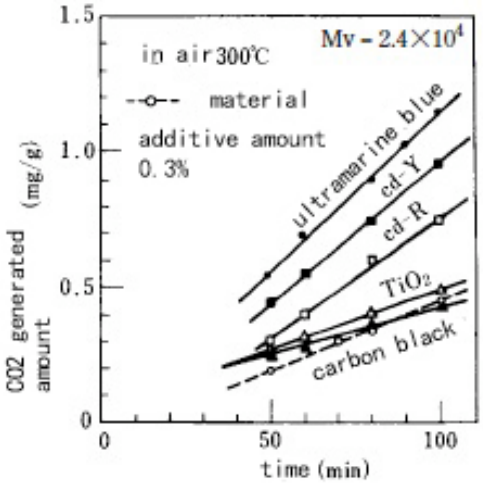

Fig. 4・5・2－12 Influence on CO2 generation of the pigment

Table 4・5・2－2　Influence of metal oxides on heat stability of Iupilon / NOVAREX

Metal oxides	Chemical Composition	pH	Molecular weight Mv x 10^4		Start temperature of decreased quantity (℃)
			0%	1%	
Stannic oxide	SnO_2	4. 2	2. 8	2. 4	340
Lead sulfate	$PbSO_4$	4. 5	2. 8	2. 6	320
Lead chromate	$PbCr_20_3$	5. 4	2. 8	2. 4	306
Lead oxide	Pb_30_4	7. 8	2. 8	2. 2	210
Lead monoxide	PbO	10. 2	2. 8	2. 5	363
Zinc sulfide	ZnS	2. 4	2. 8	2. 4	250
Zinc oxide	ZnO	7. 2	2. 8	2. 7	352
Zinc carbonate	$ZnCO_3$	7. 1	2. 8	1. 9	315
Cadmium sulfate	$CdSO_4$	6. 3	2. 8	2. 7	335
Cadmium sulfite	CdS	6. 3	2. 8	2. 4	340
Cadmium oxide	CdO	9. 4	2. 8	2. 6	315
Cadmium carbonate	$CdCO_3$	7. 0	2. 8	2. 0	280
Aluminum oxide	$A1_2CO_3$	9. 0	2. 8	2. 7	320
Cobalt oxide	CoO	8. 2	2. 8	2. 7	330
Barium sulfate	$BaSO_4$	7. 2	2. 8	2. 7	340
Titanic oxide	TiO_2	6. 8	2. 8	2. 7	343
Copper oxide	CuO	6. 9	2. 8	2. 5	340
Manganese dioxide	MnO_2	6. 6	2. 8	2. 6	350
Ferric oxide	Fe_20_3	6. 4	2. 8	2. 7	320
Chromic oxide	Cr_20_3	5. 5	2. 8	2. 7	358
Cadmium selenide	CdSe	6. 0	2. 8	2. 8	345

As for the molecular weight, the sample melted in nitrogen for 1 hour is used for measurement
As for the start temperature of decreased quantity, the sample added with 1% of the pigment is used for measurement in air.

When adding an organic additive (for example, ultraviolet absorber, stabilizer, antistatic agent, blowing agent, and plasticizer, etc.) to Iupilon / NOVAREX, the one that causes the chemical reaction with polycarbonate can not be used. Also, it is necessary to consider sufficiently not only the reactivity but also the heat stability of the additive to be used because the processing temperature of polycarbonate is high, close to the decomposition temperature of the organic substances at the temperature range above 300℃.

When polycarbonate is heated in vacuum system, it is known that if the decomposition product is removed continuously, the peculiar phenomenon to cause rapidly the gel generation is observed.

The state of gel generation, and the change of soluble part 〔η〕 of methyl chloride are shown in Fig. 4・5・2－13 and Fig. 4・5・2－14, respectively. The generation rate of the decomposition product in this system is indicated in Fig. 4・5・2－15.

It is known that this gel phenomenon is recognized not only in polycarbonate but also in polysulfone, PPE (polyphenylene ether) etc. as shown in Fig. 4・5・2－16.

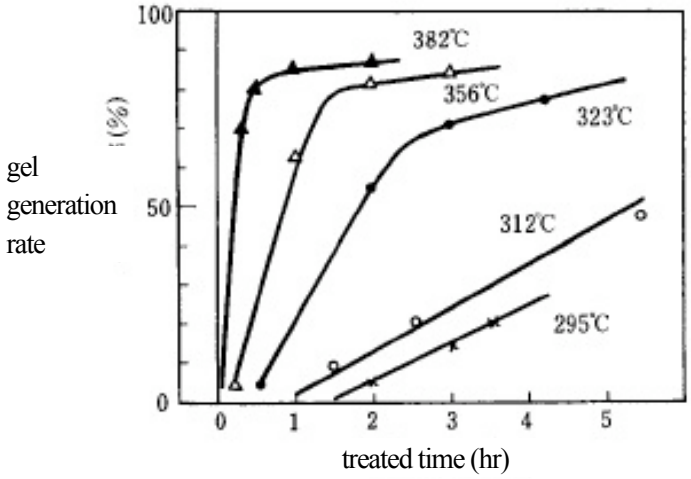

Fig. 4・5・2－13 Gel generation by heating in continuous vacuum system

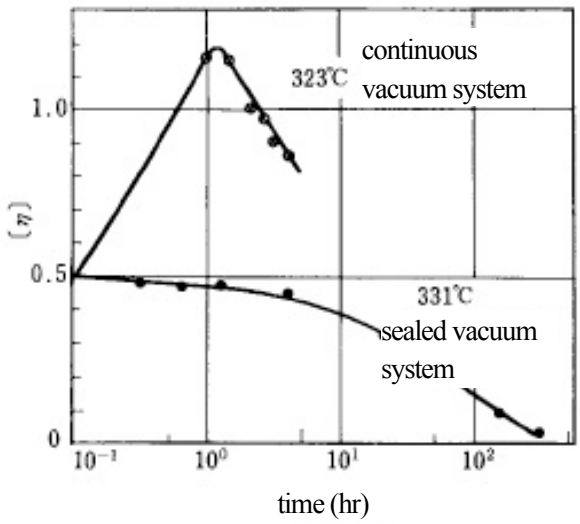

Fig. 4・5・2－14 Change in 〔η〕 by heating in vacuum system

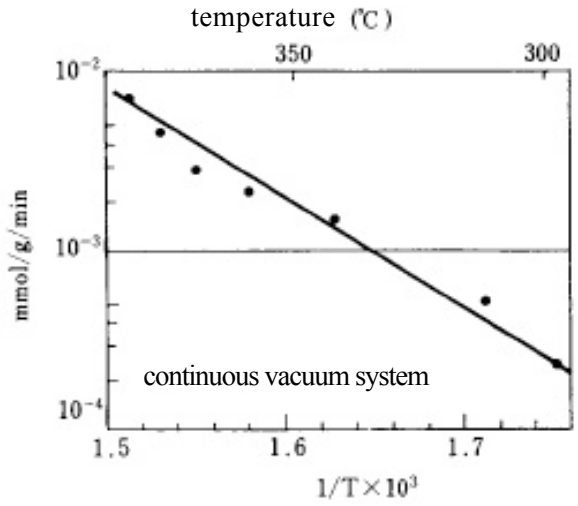

Fig. 4・5・2－15 Generation rate of decomposed gas in continuous vacuum system

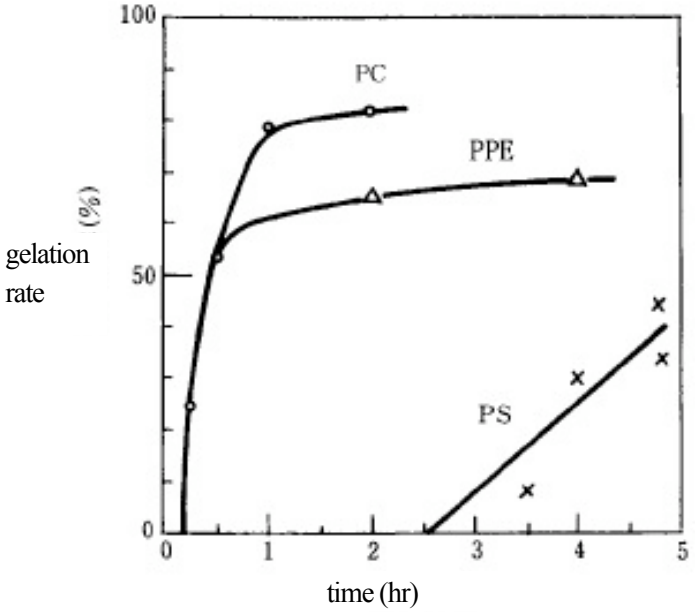

Fig. 4・5・2－16 Gel generation of other resins

The generation of decomposed gas when heating polycarbonate at 700-1200℃ is shown in Fig. 4・5・2－17. CO_2 and CH_4 generation show a constant value regardless of temperature.

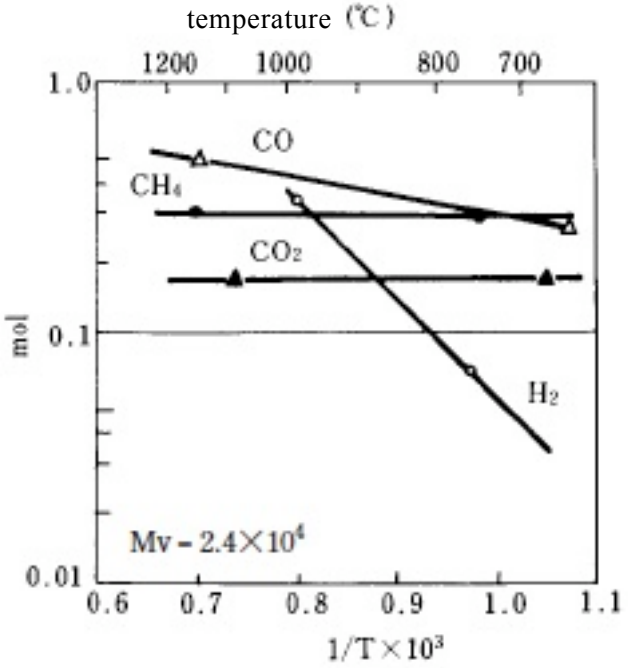

Fig. 4・5・2－17 Generation of decomposed gas at high temperature

4・6　Hot Water Resisting Property

As the bond of the main chain of Iupilon / NOVAREX is an ester bond, hydrolysis takes place gradually and molecular weight decreases when it comes in contact with hot water and steam. At the same time, cracks form with the decrease in mechanical strength after a long time.

The decrease in molecular weight of Iupilon / NOVAREX by treating with hot water is shown in Fig. 4・6－1. The decrease in molecular weight occurs rapidly by treating at high temperature. Also, the decrease in case of only one surface of the molding contacts with hot water is gentle than the case of the immersion, for example, at 75℃, the treated time when the molecular weight becomes 2.0×10^4 is 3~4 times.

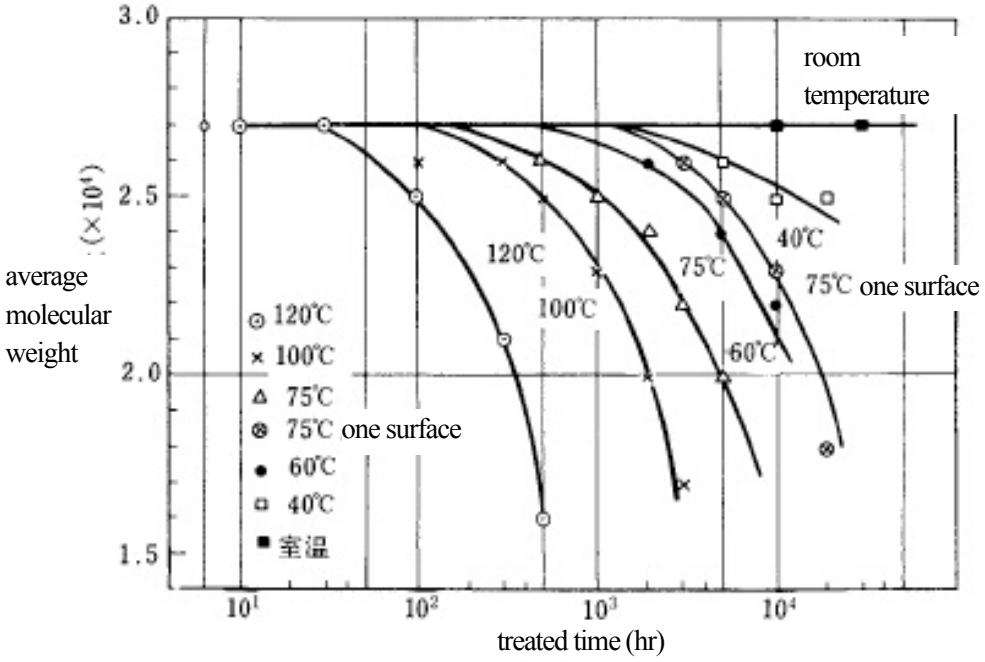

Fig. 4・6－1　Decrease in molecular weight by treating with hot water

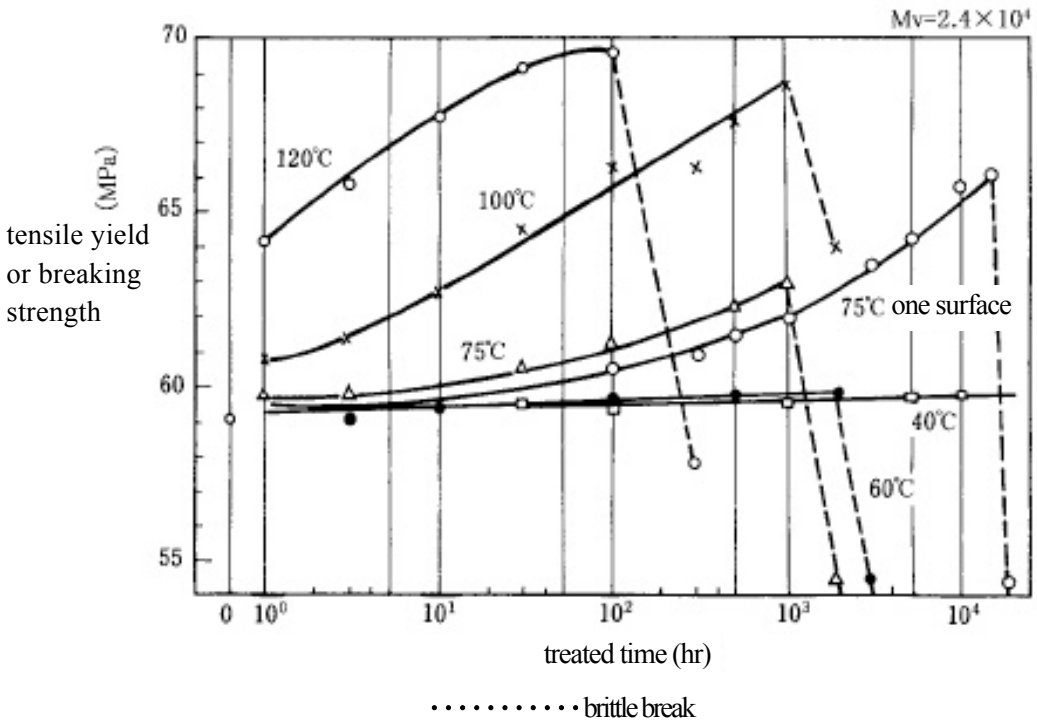

Fig. 4・6－2　Change in tensile yield or breaking strength by treating with hot water

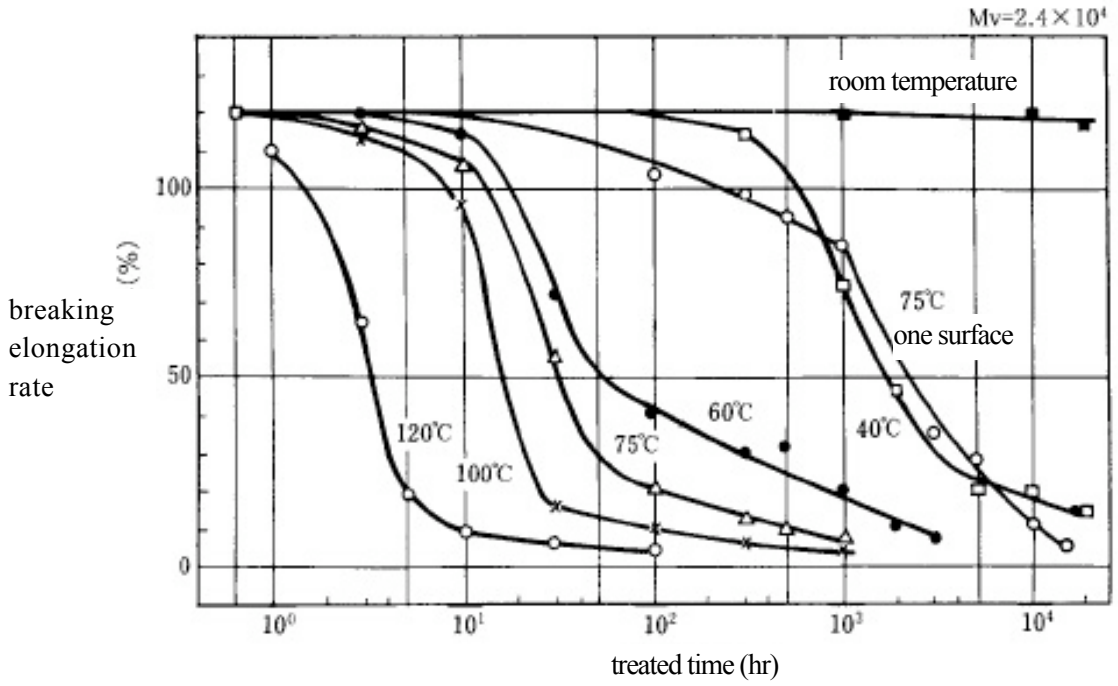

Fig. 4・6－3　Tensile breaking elongation rate by treating with hot water

The tensile properties of Iupilon / NOVAREX treated with hot water show the deterioration by crack generation with decrease in molecular weight as indicated in Fig. 4・6－2 and 3.

The time when ductile breaking moves to brittle breaking is as follows : 100~200 hours at 120℃ (in steam of 98kPa , 1kgf/cm^2), 1000~2000 hours at 100℃ and 75℃, 2000~3000 hours at 60℃, 20000 hours at 75℃ one surface, above 20000 hours at 40℃. Although the decrease in molecular weight at 75℃ and 60℃ is small but the tensile property is deteriorated. This is due to crack generation.

The deterioration of Izod impact strength is shown in Fig. 4・6－4. The deterioration rate becomes fast compared with the case of dry-heat treatment. For example, as for dry-heat treatment at 100℃, 1000 hours is needed, but only 30~50 hours in case of treating with hot water.

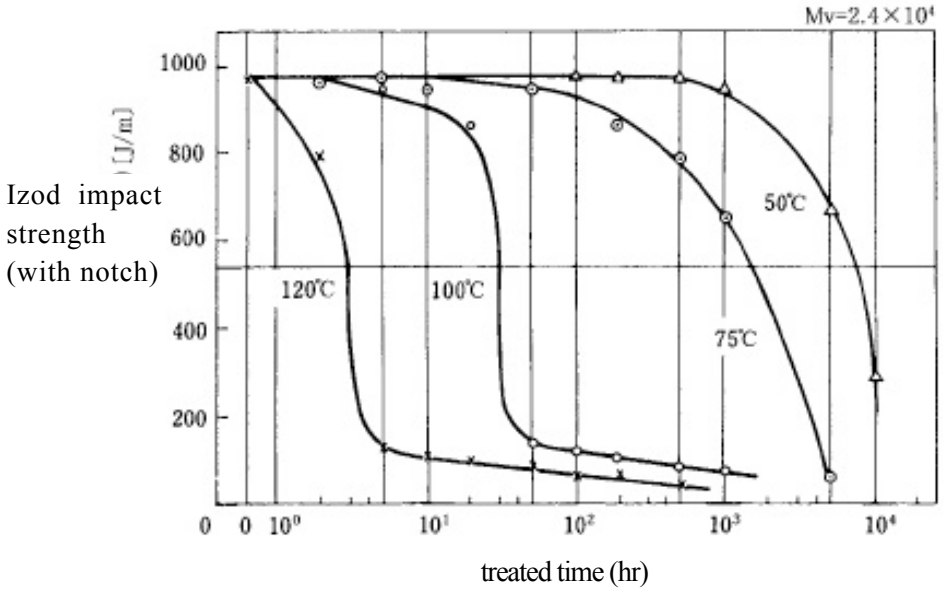

Fig. 4・6－4 Change in Izod impact strength by treating with hot water

4・7 Flammability

A comparison with other resins is shown in Table 4・7－1.

Table 4・7－1 Comparison of flammability with other resins

Polymers	Combustion heat kJ／g (cal／g)	Heat value kJ／g (cal／g)	Generated moisture wt%	Flammability cm／min (in／min)	Oxygen index (%)
Polyethylene	45. 9 (10965)	42. 8 (10225)	126. 6	2. 5 (1. 0)	17. 4
Polypropylene	44. 0 (10506)	41. 1 (9828)	115. 9	2. 5 (1. 0)	17. 4
Polyvinyl chloride	18. 1 (4315)	16. 8 (4015)	51. 3	self-extinguishing	47. 0
Tetrafluoro ethylene	4. 2 (1004)			nonflammable	95. 0
Polymethylmethacrylate (PMMA)	26. 2 (6265)	24. 6 (5869)	67. 8	2. 8 (1. 1)	17. 3
Polystyrene	40. 2 (9604)	38. 4 (9182)	72. 1	2. 5—5. 1 (1. 0—2. 0)	18. 3
Acrylnitryl・stylene (AS)				2. 5 (1. 0)	18.1
ABS	35. 3 (8424)	33. 8 (8066)	61. 2	3. 3 (1. 3)	
Polyether	16. 9 (4046)	15. 9 (3790)	43. 7	2. 8 (1. 1)	16. 2
Ethylcellulose	23. 7 (5659)			2. 0—3. 6 (0. 8—1. 4)	
Polyamide (nylon)	30. 9 (7371)	28. 7 (6863)	86. 8	self-extinguishing	28. 0
Polyphenylether (PPE)				self-extinguishing	30.2
Polysulphone				self-extinguishing	30.4
Polycarbonate	30. 5 (7294)	29. 4 (7020)	46. 8	self-extinguishing	25.0
Copolymerization Polycarbonate (Iupilon N—3)					31.0

The problem should be considered when making plastic flame-resistant does not include only the improvement of its flammability but also the composition, quantity and fuming property of generated gas. In case of Iupilon / NOVAREX, because the composition element is C・H・O, the generation of toxic gas such as HCI (PVC, Polyvinylidene chloride etc.), NH_3, cyanide (polyamide, ABS, AS etc.), SO_2 (polysulfone etc.) does not occur (Refer to Fig. 4・5・2−17). Also, as for the fuming property, results of various resins are shown in Table 4・7−2. Polycarbonate has a moderate fuming property in case of ignition combustion, but shows a characteristic with extremely low fuming property in case of burning combustion.

Table 4・7−2 Fuming property of plastics

Plastics	Thickness mm	Ignition combustion			Burning combustion		
		Dm	Rm	T16 (min)	Dm	Rm	T16 (min)
Polyvinyl chloride	6.4	660	134	0.8	300	12	3.9
Polyvinylidene chloride	2.8	125					
Polydifluoride vinyl chloride	0.04	0					
Polyfluoro vinyl	0.05	4					
Polystyrol	6.4	660	243	1.3	322	24	7.3
ABS	1.2	660	400	0.6	71	4	4.8
Polymethyl methacrylate (PMMA)	5.6	660	23	2.6	156	60	9.2
Cellulose acetate butyrate	6.4	49	12	5.0	434	45	2.7
Polycarbonate	3.2	174	43	2.1	12	1	
Polyphenylene ether (PPE)	2.0	183					
Polysulphone	1.5	40					
Nylon fiber	7.6	269	105	1.8	320	45	2.8
Acryl fiber	7.6	159	29	0.6	319	49	1.5
Polypropylene fiber	4.6	110	50	1.7	456	60	2.3
Oak	6.4	155	18	3.9	350	34	4.8

Dm : fuming quantity per unit area

Rm : fuming rate

T_{16} : time when Dm becomes 16

4・8　Other Thermal Properties

4・8・1 Brittleness Temperature

The brittleness temperature of Iupilon / NOVAREX is -135℃.

A comparison with other resins is shown in Table 4・2－1. The low temperature resisting property of Iupilon / NOVAREX is the best among plastics.

4・8・2　Heat Schrinkage

The change of heat schrinkage of Iupilon / NOVAREX when treated in hot air atmosphere is shown in Fig. 4・8・2－1. The heat schrinkage takes place even at low temperature and shows a 0.1~0.2% change. However, such a heat schrinkage also changes in accordance with the molding conditions etc. (Refer to Fig. 4・8・2－2).

The frozen orientation strain is released by macro-Brownian motion of the molecular chain in an atmosphere over 150℃and the schrinkage becomes 5~10%.

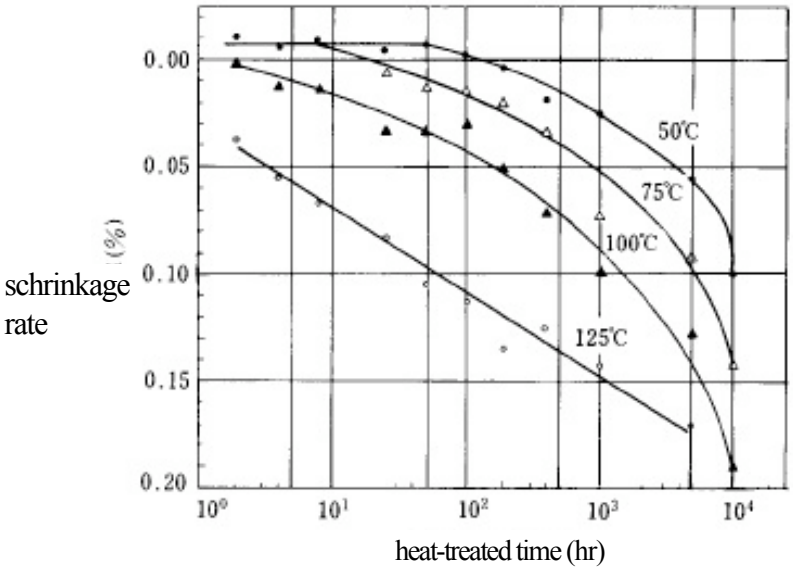

（Sample dimension　6. 4×12. 7×152mm,　Mv＝2. 2×10^4）

Fig. 4・8・2－1　Change in dimension by heat treating

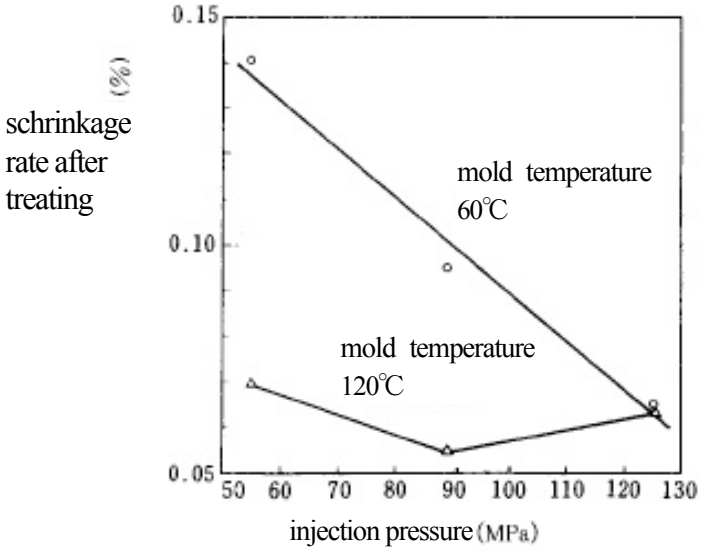

Fig. 4・8・2－2　Relation between injection molding conditions and heat schrinkage

21.1 General introduction

The electrical properties of fibres are of less obvious technical importance than, for example, the mechanical properties. Apart from their intrinsic interest, the first stimulus for their investigation came from the use of fibres as insulating materials, and much important work was done in the Bell Telephone Laboratories. Later, the use of resistance and capacity methods for measuring the moisture condition of textile materials, and of capacity methods for measuring irregularity, increased the interest in electrical properties. With the introduction of synthetic fibres, the troubles due to static charges, both in processing and in use, became more frequent and more severe. The electrical properties are interrelated. The liability of materials to static charges is determined by their electrical resistance. The electrical resistance is, on what seems to be the most likely theory, mainly determined by the permittivity of the material. It is, therefore, most appropriate to consider first the dielectric properties, then the electrical resistance, and finally static.

21.2 Definitions of dielectric properties

The *permittivity*, ε, of a material may be defined either in terms of the capacitance, C, of a condenser with the material between parallel plates of area A and separation d, or in terms of the force F between two charges Q_1 and Q_2 at a distance r in the material. Expressed in SI units as $kg^{-1}\ m^{-3}\ s^4\ A^2$ (A = ampere) or F/m (F = farad), the relations contain no arbitrary numerical factors and are:

$$C = \frac{\varepsilon A}{d} \tag{21.1}$$

$$F = \frac{Q_1 Q_2}{4\pi\varepsilon r^2} \tag{21.2}$$

This does, however, mean that *in vacuo* the equations become:

$$C = \frac{\varepsilon_0 A}{d} \tag{21.3}$$

$$F = \frac{Q_1 Q_2}{4\pi\varepsilon_0 r^2} \tag{21.4}$$

where ε_0 is the permittivity of a vacuum, which is a fundamental physical quantity with the value $8{\cdot}854 \times 10^{-12}$ F/m. For many purposes, it is more convenient to use the *relative permittivity*, $\varepsilon_r = \varepsilon/\varepsilon_0$; which is also called the *dielectric constant*.

Physically, dielectric effects are due to polarisation in the medium (Fig. 21.1). This gives rise to a reverse field, which reduces the force between two charges and reduces the potential difference between the charged plates of a condenser, which thus increases its capacitance (given by charge/potential difference). The polarisation may be due either to the alignment of permanent dipoles, such as the water molecule (Fig. 21.2), or to the separation of charge, which forms induced dipoles (Fig. 21.3). Because of its influence on capacitance, the relative permittivity is important in alternating current electricity. For a pure capacitance, current is proportional to rate of change of voltage and is therefore, with a sinusoidal applied voltage, 90° out of phase with voltage. By contrast, in a pure resistance, current is in phase with voltage. In actual practice, dielectrics are imperfect, and a real condenser (Fig. 21.4(a)) acts as a combination of capacitance and resistance. The current through the condenser due to an applied voltage of frequency f Hz is made up of a current proportional to $1/R_p$ in phase with the applied voltage and a current proportional to $2\pi f C_p$ at 90° to the applied voltage, where R_p and C_p are the equivalent parallel resistance and capacitance, respectively (Fig. 21.4(b)). The current vector diagram is shown in Fig. 21.4(c).

The relative permittivity is then given by:

$$\varepsilon_r = \frac{C_p}{C_0} \tag{21.5}$$

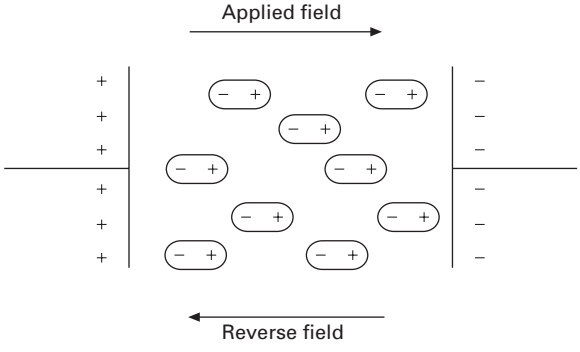

21.1 Polarisation of a medium.

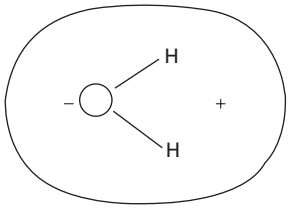

21.2 A permanent dipole – the water molecule.

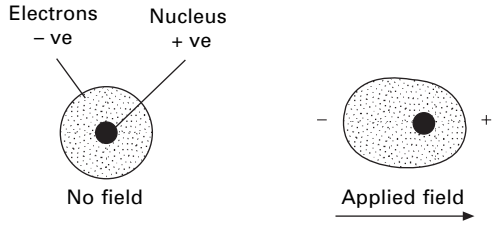

21.3 An induced dipole-distortion of the distribution of electrons round the nucleus of an atom.

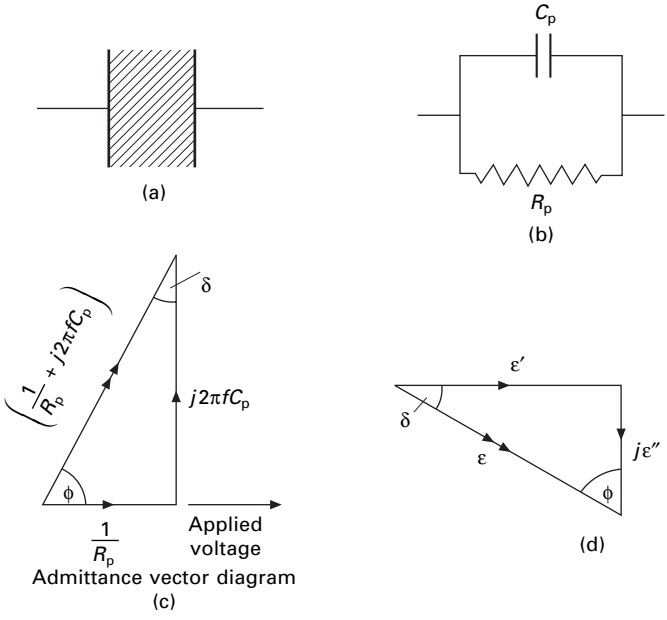

21.4 Representation of a real dielectric: (a) condenser with dielectric; (b) equivalent parallel circuit; (c) current vector diagram for circuit; (d) vector diagram – complex dielectric constant.

where C_0 = capacitance of the condenser with a vacuum (or, in practice, air) as dielectric.

The imperfection of the dielectric may be expressed as:

$$\text{dissipation factor, or loss tangent} = D = \tan\delta = \frac{1}{2\pi f C_p R_p} \tag{21.6}$$

where δ = loss angle, or as power factor = cos ϕ = [mean power dissipated in condenser/voltage × current (r.m.s. values)] = $D/\sqrt{(1 + D^2)}$, where ϕ = (π/2) – δ = phase angle. Table 21.1 shows the values of these quantities for pure capacitance and resistance; with real materials, the values lie between these limits.

An alternative method of expressing the properties of the material is in terms of a complex permittivity, **ϵ**, with the vector diagram of Fig. 21.4(d). We have:

Table 21.1 Dielectric properties

	Vector diagram	Power factor	Dissipation factor	Loss angle	Phase angle
Pure capacitance	$\uparrow j \cdot 2\pi f C_p$	0	0	0	$\pi/2$
Pure resistance	$\rightarrow 1/R_p$	1	∞	$\pi/2$	0

$$\epsilon = \varepsilon' - j\varepsilon'' \tag{21.7}$$

It can be shown that real part of permittivity = $\varepsilon' = \varepsilon$, as defined above, and imaginary part of permittivity = loss factor = $\varepsilon'' = 1/2\pi f C_p R_p$ and dissipation factor = tan δ = $\varepsilon''/\varepsilon'$.

21.3 Measurement

21.3.1 Experimental methods

To measure the dielectric properties, the material must be placed between the plates of a condenser and the impedance measured. For measurements on material in the form of film, a simple parallel plate condenser, with the plates fitting closely to the film, can be used. Fibres are less easy to handle. Balls [1] used parallel plates and carefully packed cotton fibres either perpendicular or parallel to the plates. Hearle [2] used conical electrodes. A layer of yarn, about 2 mm thick, was wound on the inner cone, and the outer cone was then pressed on it. With this arrangement, densities of packing of about 80% by volume were obtained with continuous-filament yarns, and of about 50% with staple-fibre yarns.

The method of measurement of impedance depends on the frequency being used for the test[1]. At audio-frequencies (from about 50 Hz to 100 kHz), a bridge method is suitable. Resonance methods can be used up to about 100 MHz. The condenser is connected in series with an inductance L in a resonant circuit, with the current measured by a high-impedance voltmeter across the condenser. At the resonant frequency f_0, the current has a maximum value. The capacitance $C = L/(2\ \pi\ f_0)^{1/2}$ and tan δ = $\Delta f/f_0$, where Δf = difference in frequency between the two values for which the current is $1/\sqrt{2}$ times the maximum value. Circuit-magnification meters, or Q-meters, can be used for this method. At very high frequencies (10 GHz), Shaw and Windle [3] used a cavity resonator. If a small dielectric specimen is placed along the axis of the cavity parallel to the electric field, the resonant frequency of the cavity is given by:

$$f = f_e\left[1 - 1.86\,(\varepsilon_r - 1)\,\frac{v_s}{v_e}\right] \tag{21.8}$$

where f_e = resonant frequency of empty resonator, v_s = volume of specimen and v_e = volume of cavity.

[1]The methods noted here are those used for the data in this chapter. Subsequent advances in electronics have changed the details of the technology, but not the principles.

At optical frequencies, the dielectric properties can be obtained from a study of refraction and absorption in the fibres by using the equations:

$$\varepsilon_r = n^2(1 - k^2) \tag{21.9}$$

$$\tan \delta = \frac{2k}{(1 - k^2)} \tag{21.10}$$

where n = refractive index and k = absorption index, defined by: $2\pi k = \lambda/x_0$, where λ = wavelength, and x_0 = distance in which amplitude decreases to 1/exp (x) times its original value.

21.3.2 Evaluation of results for an air-fibre mixture

The main difficulty in dealing with fibres is the interpretation of results found with a mixture of air and fibre in order to obtain the properties of the fibrous material itself. Depending on the particular assumptions used, different formulae can be obtained, and it is not easy to see how closely they should fit particular experimental conditions. Some of these relations are described below and shown in Fig. 21.5. We define ε_r as the relative permittivity of the fibre material (taken as 10 for the curves in Fig. 21.5), ε_m as the effective relative permittivity of the mixture, and P as the‘ volume fraction of fibre between the plates of the condenser.

- If the material is assumed to occupy only a fraction of the total area, but to be continuous between the plates, Fig. 21.5(a), and it is assumed that there is no distortion of the field, we have the parallel mixture law, Fig. 21.5A:

$$\varepsilon_m = 1 + (\varepsilon_r - 1)\, P \tag{21.11}$$

Balls [1] used this formula for fibres lined up perpendicular to the plates, but it

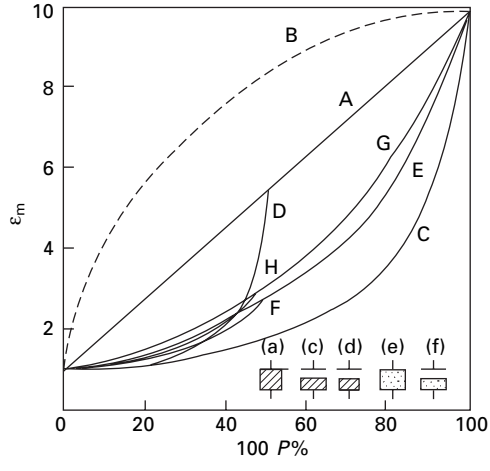

21.5 Theoretical curves for the variation of relative permittivity with density of packing.

seems unlikely that, under these conditions, one can neglect the distortion of the electric field. Owing to the high surface/volume ratio in fibres, there will be a large edge effect. The lines of force will concentrate on the region of high relative permittivity and increase the capacity above its expected value. Some curve such as Fig. 21.5B will be obtained.

- If the material is assumed to occupy the whole area, but only a fraction of the distance between the plates, Fig. 21.5(c), we have the series mixture law, Fig. 21.5C:

$$\frac{1}{\varepsilon_m} = (1 - P) + \frac{P}{\varepsilon_r} \tag{21.12}$$

- A combination of the above two cases, with α as the fraction of area occupied and β as the fraction of the distance between the plates (Fig. 21.5(d)), presents the problems of averaging referred to in Section 20.3.2 in relation to a mixture of mechanical properties. One model gives the following equation:

$$\varepsilon_m = \frac{\alpha}{[(1 - \beta) + \beta/\varepsilon_r]} + (1 - \alpha) = \frac{\alpha^2}{[(\alpha - p) + P/\varepsilon_r]} + (1 - \alpha) \tag{21.13}$$

With $\alpha = 0.5$, this gives Fig. 21.5 *D*.

- If molar polarisations are additive, the following equation holds [4]:

$$\frac{\varepsilon_m - 1}{\varepsilon_m + 2} = P\frac{\varepsilon_r - 1}{\varepsilon_r + 2} \tag{21.14}$$

This system is indicated in Fig. 21.5(e) and gives the curve Fig. 21.5E. It is not valid for large particles owing to the failure of the assumption on which it is based that the Lorentz internal field holds at all places. It has been shown to be a good approximation for small values of P [5]. Various improvements on this formula for particular conditions have been suggested [6–8], and Polder and van Santen [9] have discussed the problem more generally.

If ε_r is very nearly equal to 1, so that the difference between $\varepsilon_m + 2$ and $\varepsilon_r + 2$ is negligible. Equation (21.14) reduces to:

$$\varepsilon_m - 1 = P(\varepsilon_r - 1) \tag{21.15}$$

which is the same as equation (21.11) leading to Fig. 21.5A.

This is valid for a mixture of gases but would not be expected to be so for fibres, though it was used by Balls [1] for fibres arranged with their axes parallel to the plates.

- A combination of (C) and (E), illustrated in Fig. 21.5(f), would give the curve Fig. 21.5F.
- Licktenecker [10] proposed a logarithmic relation, which, for a mixture with one component having unit relative permittivity, reduces to Fig. 21.5G:

$$\log \varepsilon_m = P \log E_r \tag{21.16}$$

This has been applied, with experimental support, by Shaw and Windle [3] to the transverse relative permittivity of fibres wound solenoidally.

- A combination of (C) and (G) gives Fig. 21.5H. Hearle [2] obtained curves similar to, but not in quantitative agreement with, this when the density of packing between cones was varied by altering the pressure applied to the outer cone. Different curves, corresponding to different densities in the bulk of the material, can be obtained by using staple-fibre and continuous-filament yarns and by varying the winding tension. An example is given in Fig. 21.6.

Where the experimental arrangement approximates closely to one of the above models, it may be possible to obtain an accurate extrapolation formula, but, in general, the problem has not been solved.

For dry fibres having a comparatively low permittivity, Errera and Sack [11] overcame the problem by immersing the fibres in a mixture of liquids and adjusting the mixture until the introduction of the fibres made no difference. The permittivities of fibre and liquid were then equal.

21.4 The effect of frequency

21.4.1 General

Frequency has a most important influence on dielectric properties, in a way similar to its influence on dynamic mechanical properties. Owing to their inertia, and to restraints in the structure, the dipoles take a certain time to reverse direction. This is characterised as their relaxation time. At low frequency, the dipoles line up in the

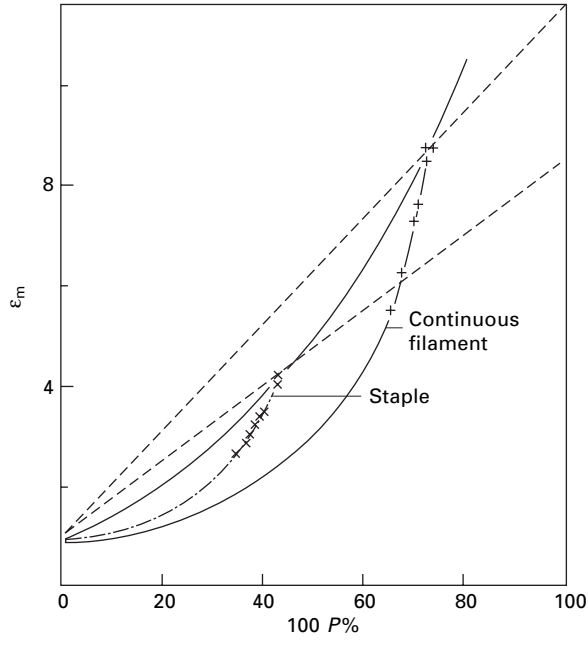

21.6 Practical variation of relative permittivity of viscose rayon with density of packing [2].

field, reverse direction when the field reverses, and so contribute to a high permittivity. At high frequencies, the dipoles will not follow the changes at all, and there will be no contribution to the permittivity. At intermediate, transitional frequencies the reversals of field take place at intervals comparable to the relaxation time, the response of the dipoles is sluggish, which gives a phase difference between voltage and current, and energy is dissipated due to internal friction. Different types of dipole will have different relaxation times, so that, as the frequency is raised, the permittivity drops in steps and the dielectric loss peaks. When the theory is worked out exactly, it is found that the maximum in ε'' occurs at the same frequency as the maximum rate of decrease of ε'; the maximum of $\cos \phi$ is displaced to a slightly higher frequency.

The general behaviour is illustrated by the results for water and ice. At low frequencies, the dipolar water molecules line up in the field, to give a relative permittivity of about 80. At higher frequencies, the permittivity drops in a step, and there is a maximum in the power factor. For ice, (Fig. 21.7), in which the considerable restraints in the structure limit the movement of the dipoles, this occurs at about 10 kHz; but, for liquid water, in which the molecules are less restrained, the permittivity remains constant up to about 1 GHz, and then drops rapidly and passes half its low-frequency value at about 20 GHz. Above these frequencies, there will still be electronic polarisation, but at high enough frequencies this will cease, and there will be a further decrease in permittivity.

21.4.2 Fibres

Figures 21.8 and 21.9 show results obtained by Hearle [2, 12] for cotton, viscose rayon, acetate, wool and nylon over the range of frequencies between 50 Hz and 10 MHz. Other values are included in the summary given later in Table 21.4. These results show the great influence of frequency on the dielectric properties, an influence

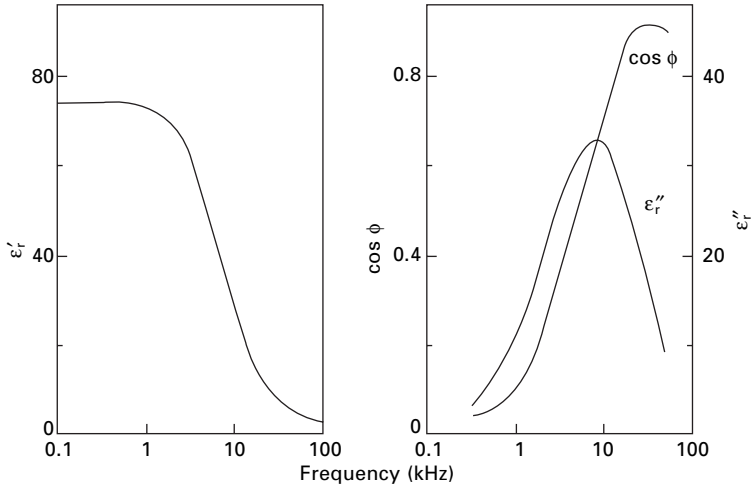

21.7 Dielectric properties of ice.

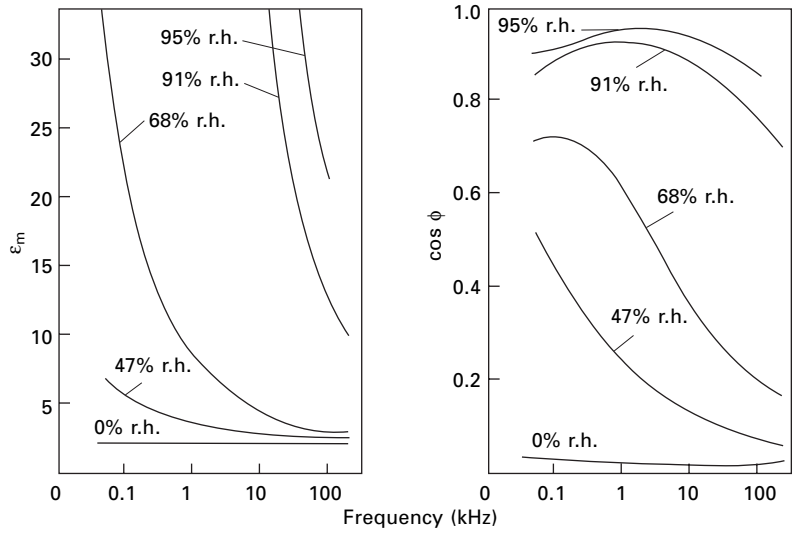

21.8 Dielectric properties of cotton yarn in cone condenser [2]. Cotton 44%; air 56%.

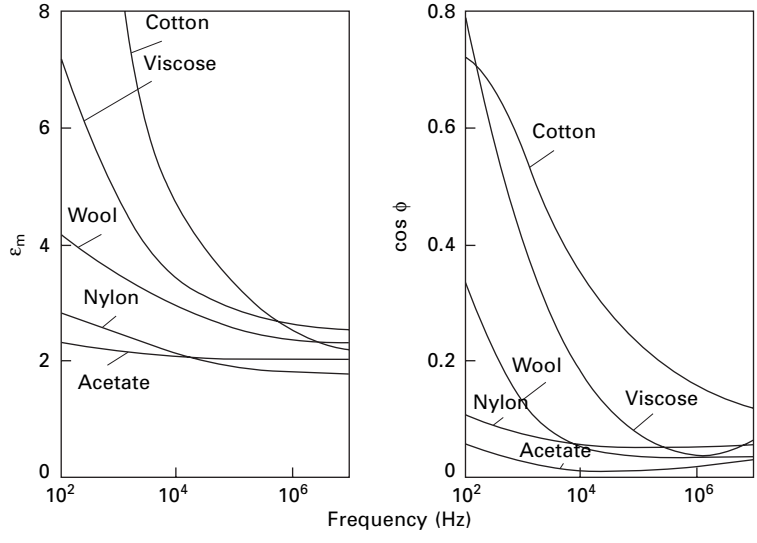

21.9 Variation of dielectric properties with frequency for various fibre–air mixtures at 65% r.h. [2, 12].

that becomes more marked the damper the specimen. The changes occur gradually and not in steps, which indicates that a range of relaxation times is involved.

Above 5 kHz, the permittivity decreases in a manner similar to that in ice, but, below 5 kHz, the permittivity curve does not flatten out, as does that of ice, but continues to increase as the frequency decreases. This must correspond to a comparatively large-scale polarisation phenomenon with a long relaxation time. The

maximum in the power factor for damp cotton at 50–100 Hz indicates that there must be a dominant relaxation time of the order of 1/100 second. These effects are probably due to a polarisation of the ion distribution in microscopic or sub-microscopic regions of the fibre structure, or possibly even across the whole fibre. This is the same as the Maxwell–Wagner effect, or interfacial polarisation, which occurs when there are heterogeneities in the conductivity and permittivity of a material between the plates of a condenser.

In several types of fibre (viscose rayon, acetate, fairly dry cotton), the power factor begins to increase with an increase in frequency in the region of 1 MHz. These results suggest that, at some frequency greater than 10 MHz, there will be a maximum in the power factor and a corresponding drop in the permittivity. The way in which the curves for viscose rayon and acetate at various humidities come together suggests that this effect is independent of the presence of water. It is probably associated with the lining-up of polar groups within the fibre.

In wool, Windle and Shaw [13, 14] found a decreasing power factor as the frequency increased from 3 to 26 GHz. This indicated the presence of a maximum in the power factor at some frequency below this. This is probably essentially the same effect as that which is suggested for viscose rayon, acetate and cotton by tests at lower frequencies.

It is interesting to notice that relaxation effects occur in the mechanical behaviour of fibres at similar frequencies to those found in the dielectric properties (see Section 16.5).

21.5 The effect of moisture

As would be expected, moisture has a marked effect on the dielectric properties; this is illustrated for cotton, acetate, wool and nylon in Figs 21.10 and 21.11. At the higher frequencies, the dielectric properties of the cellulosic fibres are consistent with the assumption that the water molecules are restrained in a manner similar to that in ice. For wool, the permittivity is lower, which indicates that the absorbed water molecules are more tightly held and cannot line up in the field. This behaviour

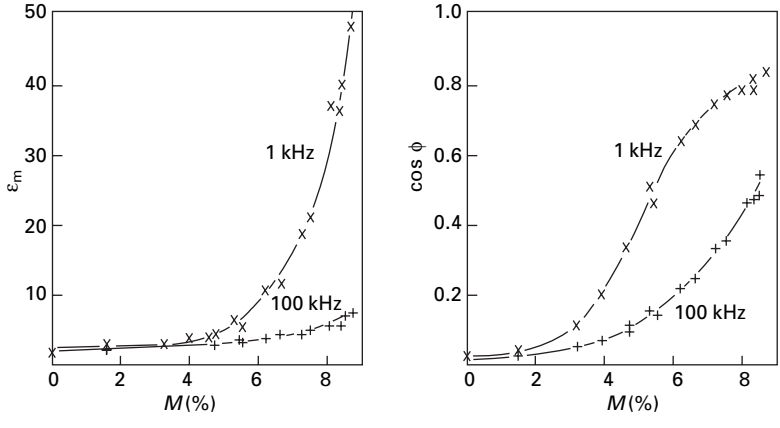

21.10 Variation with moisture content *M* of dielectric properties of cotton [2].

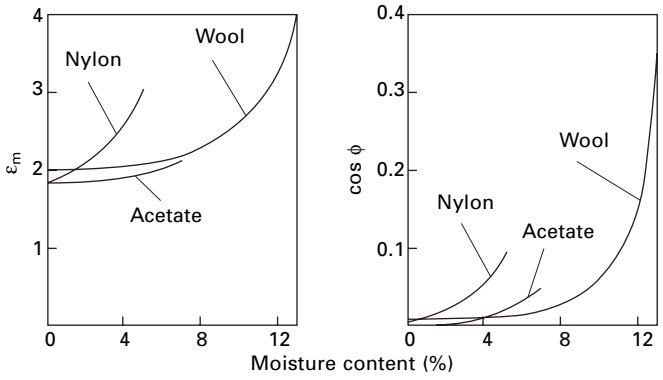

21.11 Variation with moisture content of dielectric properties of various fibres at 1 kHz [2].

is particularly marked at low moisture contents and is consistent with Speakman's suggestion (see Section 12.2.1) that the water first absorbed by wool is firmly bound to hydrophilic groups in the side chains of the keratin molecule. At the lower frequencies, in some materials (notably cotton, in which the permittivity reaches very high values), the effect of water becomes greater than it would be even if it were acting with a relative permittivity of 80, which indicates its importance in freeing other units in the structure so that they can polarise.

Windle and Shaw [14] have explained their results for wool at very high frequencies in terms of a three-phase theory of moisture absorption. The components of the system were regarded as dry wool, with experimentally determined properties; localised absorbed water, in which the molecules cannot rotate; intermediate absorbed water, in which the molecules are very little restricted; and mobile absorbed water, in which the molecules are as free as in liquid water. Using expressions for the dielectric properties of a mixture of dielectrics, assigning values for the dielectric properties of each component, and dividing up the absorbed water in proportions found theoretically, they obtained a good agreement between experiment and theory.

Of the non-absorbing fibres, polyester (PET) and polyvinylidene chloride (*Saran*) showed no variation in dielectric constant, and only a small change in power factor between 0 and 65% r.h. Polyvinyl chloride (*Vinyon*) and glass (*Fiberglas*) showed a marked change at low frequencies, which was presumably due to surface effects. In general, the effect of additives will have a major effect when the dielectric properties are not dominated by moisture absorption.

21.6 The effect of temperature

A rise in temperature, reducing the restraints on the dipoles, causes an increase in permittivity in solid materials. (In liquids and gases, where the intermolecular restraints are small, an increase of temperature causes a greater disorganisation, a less regular alignment of the dipoles, and thus a lower permittivity.) As for dynamic mechanical properties, the effects of temperature and frequency are often similar. This is shown

by Reddish's results [15] for polyethylene terephthalate (*Terylene*) film (Fig. 21.12). To include the effect of both variables, contour maps and solid models are used. It will be seen that there is a maximum in tan δ, occurring at about 1 MHz at room temperature and moving to lower frequencies at lower temperatures; this would correspond to the maximum suggested earlier Section (21.4.2) as being likely in the high-frequency region. At higher temperatures, there is another sharper maximum. These two ridges in tan δ in the 3D models correspond to the peaks in mechanical loss shown in Fig. 21.13. Corresponding to the maxima in tan δ, there are rapid dips in the values of the permittivity. Note that the permittivity plots are the inverse of dynamic modulus plots and would correspond to compliance plots. There is another

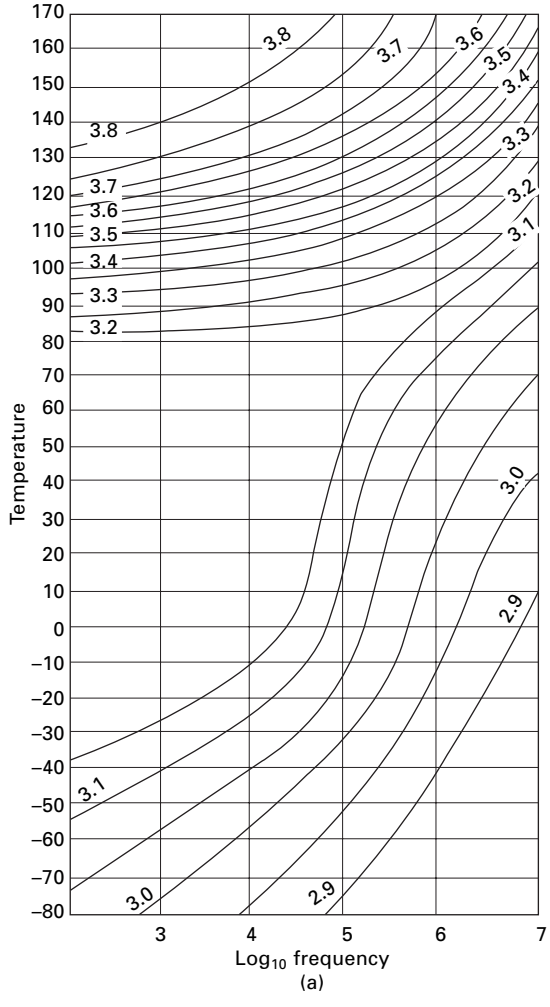

21.12 Influence of temperature and frequency on dielectric properties of polyester (*Terylene*) film: (a) relative permittivity contour map; (b) dissipation factor contour map; (c) relative permittivity solid model; (d) dissipation factor solid model. After Reddish [15].

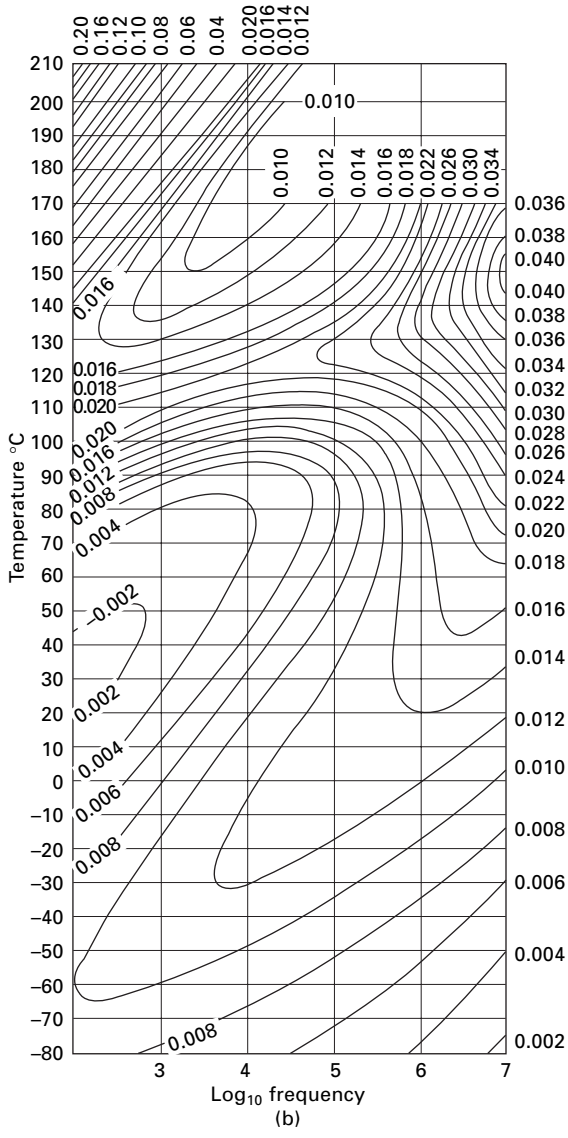

21.12 (Continued)

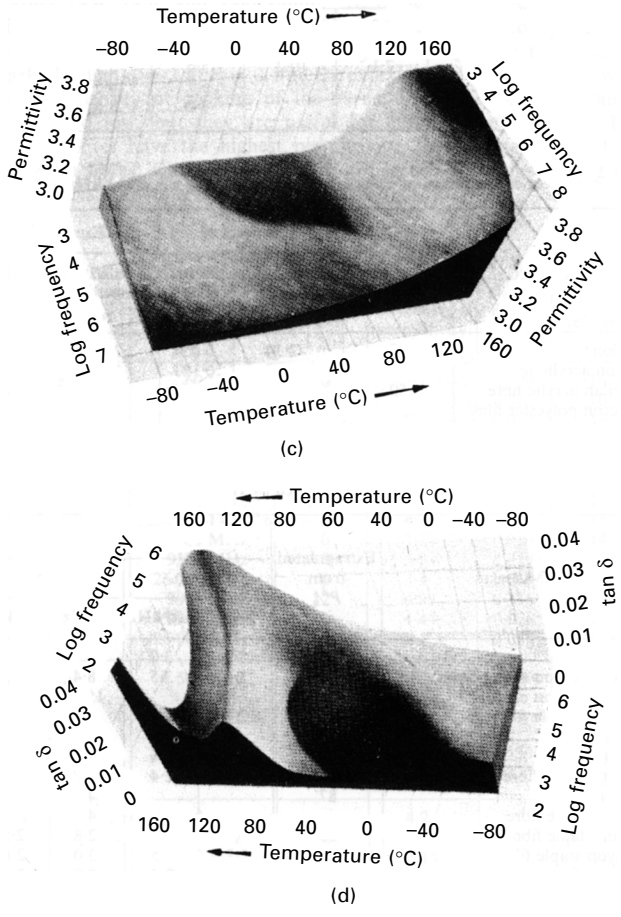

21.12 (Continued)

interesting feature: an increase in tan δ at low frequency at 160 °C. Although there is no observable maximum, this may indicate another transition at a higher temperature but below the melting point. This may be associated with permanent setting of polyester fibres. Figure 21.14 shows the results obtained by Stoops [17] for dry cellulose film (Cellophane). These also include a low-temperature maximum and, at 60 Hz, indications of a high-temperature maximum. Baker and Yager [18] obtained somewhat similar results with dry nylon 6.10. Table 21.2 shows values of the relative permittivity of nylon and keratin film at 25 and 40 °C at various moisture regains.

21.7 The effect of other factors

The permittivity of an anisotropic material, such as a fibre, would be expected to vary with the direction in which the electric field is applied. The results obtained by Balls [1] for cotton fibres indicate that the axial permittivity is about twice the transverse permittivity, but, as is indicated above Section (21.3.2), the extrapolation on which

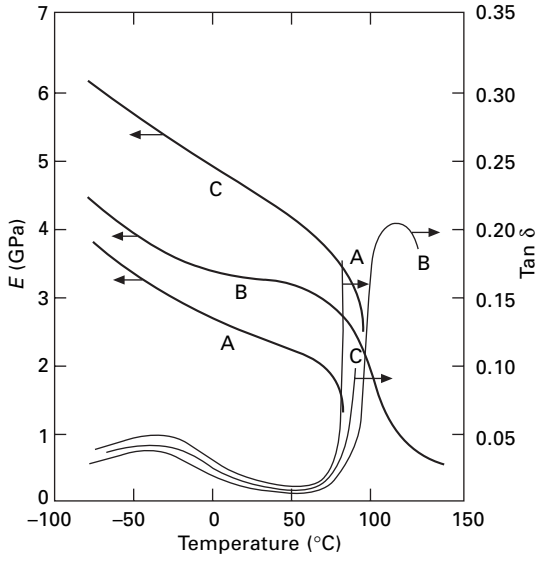

21.13 Dynamic mechanical modulus and tan δ of poly(ethylene terephthalate) as measured by Kawaguchi [16] at about 100 Hz: A, undrawn, 2% crystallinity; B, undrawn, 50% crystallinity; C, drawn 5×, 25% crystallinity.

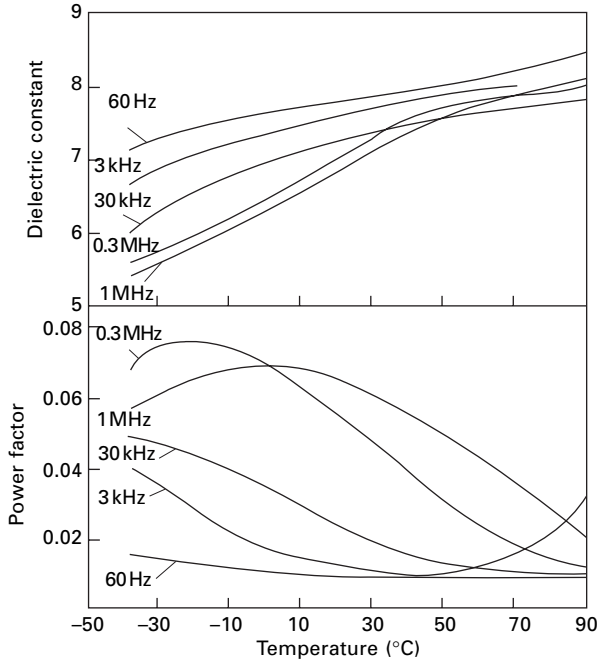

21.14 Variation of dielectric properties of cellophane. After Stoops [17].

Table 21.2 Effect of temperature on permittivity of nylon and keratin films [19]

Moisture regain (%)	Relative permittivity			
	Nylon film		Keratin film	
	25 °C	40 °C	25 °C	40 °C
0	4.2	4.5	4.7	4.8
1.8	5.0	6.0		
3.6	7.1	10.2	5.0	5.3
7.2			5.7	6.5
10.8			7.0	8.6

Table 21.3 Effect of extraction on dielectric properties at 65% r.h. and 1 kHz [2]

Material	Density of packing (%)	Unextracted		Extracted	
		Relative permittivity ε_m	Power factor $\cos \phi$	Relative permittivity ε_m	Power factor $\cos \phi$
Nylon	50	2.34	0.054	2.43	0.063
Acrylic fibre *Orlon*	40	2.28	0.123	1.73	0.0044
Acrylic fibre *Acrilan*	50	2.00	0.076	1.94	0.043
Polyester fibre *Dacron*	50	39.4	0.773	1.66	0.007

these results are based is of doubtful validity. At 3 GHz, Shaw and Windle [3] found that the relative permittivity of dry wool fibres was 3.88 ± 0.15 with the electric field parallel to the fibre axis and 4.41 ± 0.11 with the electric field perpendicular to the fibre axis.

The presence of impurities would be expected to alter the dielectric properties; in particular, ionic impurities would probably have a considerable effect at low frequencies. Table 21.3 shows the effect of the removal of surface dressings from some synthetic fibres by extraction in methanol and benzene. Only with the polyester fibre was there a large change, which was probably due to the removal of an anti-static finish, in the values obtained.

21.8 Summary of results for various materials

Tables 21.4, 21.5 and 21.6 summarise results for various materials at frequencies ranging from supply frequencies (50 Hz) to optical frequencies (10^{15} Hz). The figures given by Hearle [2] are extrapolated linearly through $\varepsilon_r = 1$ at $P = 0$, and the experimental point is found with maximum density of packing of the yarns, $P\%$: this will give values that are too low, but they are useful for comparative purposes. The cellulosic fibres have the highest permittivity, these being followed by the protein fibres, with the synthetic non-hygroscopic fibres having the lowest values. The power factors follow a similar order.

Table 21.4 Permittivities obtained by Hearle [2]

Material	Extrapolated from *P*%	Relative permittivity			
		0% r.h.		65% r.h.	
		1 kHz	100 kHz	1 kHz	100 kHz
Cotton	44	3.2	3.0	18	6.0
Viscose rayon staple fibre	44	3.6	3.5	8.4	5.3
Viscose rayon c.f.	73			15	7.1
Acetate staple fibre	45	2.6	2.5	3.5	3.3
Acetate c.f.	79			4.0	3.7
Wool	53	2.7	2.6	5.5	4.6
Nylon staple fibre	53	2.5	2.4	3.7	2.9
Nylon c.f.	87			4.0	3.2
Acrylic staple fibre *Orlon*	42	2.8	2.3	4.2	2.8
Acrylic staple fibre *Orlon* (extracted)	38			2.8	2.5
PVC staple fibre *Vinyon*	46	2.7	2.5	3.0	2.6
PCVD *Saran* c.f.	70	2.9	2.4	2.9	2.4
Polyester staple fibre *Dacron* (extracted)	48	2.3	2.3	2.3	2.3
Glass *fiberglass* c.f.	63	3.7	3.4	4.4	3.6

c.f. = Continuous-filament yarn

Table 21.5 Other values of dielectric properties

Material	Frequency	Moisture regain (%)	Relative permittivity	Power factor	Reference
Cellophane	60 Hz	0	7.7	0.009	15
film	10 kHz	0	7.3	0.016	15
	1 MHz	0	6.7	0.062	15
	3000 MHz	0	4.04		3
Wool	8 kHz	0	5.4		11
	60 kHz	0	4.4		11
	120 kHz-13 MHz	0	4.2		11
	3000 MHz	0	3.70	0.030	13
	9300 MHz	0	3.54	0.019	13
	26 000 MHz	0	3.4	0.0.15	14
	3000 MHz	12	4.99	0.146	13
	9300 MHz	12	4.44	0.076	13
	26 000 MHz	12	4.1	0.068	14
Keratin film	500 Hz	0	5		20
	11 kHz	0	4.5		20
	1 MHz	0	4		20
	500 Hz	12	9		20
	11 kHz	12	7.5		20
	1 MHz	12	5.5		20
Nylon	10 kHz	0	4.2		11
	500 kHz	0	3.26		11
	10 MHz	0	3.15		11
	3000 MHz	2	3.13		3
Nylon film	11 kHz	0	4		21
	11 kHz	4	8		21

Table 21.6 Relative permittivity at optical frequencies

Fibre	ε_r = 2 with light vibration:	
	Parallel to fibre axis	Perpendicular to fibre axis
Cotton	2.50	2.34
Viscose rayon	2.37	2.31
Acetate	2.19	2.16
Wool	2.40	2.37
Casein	2.37	2.37
Nylon	2.50	2.31
Polyester fibre *Terylene*	2.96	2.37
Acrylic fibre *Orlon*	2.25	2.25
Polyethylene	2.43	2.28
Glass	2.40	2.40

* From refractive indices in Table 24.3

21.9 References

1. W. L. Balls. *Nature*, 1946, **158**, 9.
2. J. W. S. Hearle. *Text. Res. J.*, 1954, **24**, 307.
3. T. M. Shaw and J. J. Windle. *J. Appl. Phys.*, 1950, **21**, 956.
4. C. J. F. Böttcher. *Theory of Electric Polarization*, Amsterdam, Netherlands, 1942, p. 415.
5. J. W. Rayleigh. *Phil. Mag.*, 1892, **34**, 481.
6. C. J. F. Böttcher. *Res. Trav. Chim.*, 1945, **4**, 47.
7. E. Stöcker. *Z. Physik.*, 1920, **2**, 236.
8. O. Wiener. *Abhandl. math. phys. – Klasse sachs. Akad. Wiss. Leipzig.*, 1912, **32**, 509.
9. D. Polder and J. H. van Santen. *Physica*, 1946, **12**, 257.
10. K. Licktenecker. *Physik. Z.*, 1926, **27**, 115.
11. J. Errera and H. S. Sack. *Industr. Engng Chem.*, 1943, **35**, 712.
12. J. W. S. Hearle. *Text. Res. J.*, 1956, **26**, 108.
13. J. J. Windle and T. M. Shaw. *J. Chem. Phys.*, 1954, **22**, 1752.
14. J. J. Windle and T. M. Shaw. *J. Chem. Phys.*, 1956, **25**, 435.
15. W. Reddish. *Trans. Faraday Soc.*, 1950, **46**, 459.
16. T. Kawaguchi. *J. Polymer Sci.*, 1958, **32**, 417.
17. W. N. Stoops. *J. Amer. Chem. Soc.*, 1934, **56**, 1480.
18. W. O. Baker and W. A. Yager. *J. Amer. Chem. Soc.*, 1942, **64**, 2171.
19. G. King and J. A. Medley. *J. Colloid Sci.*, 1949, **4**, 9.
20. G. King. *Trans. Faraday Soc.*, 1947, **43**, 601.
21. G. King. J. *Colloid Sci.*, 1947, **2**, 551.

22.1 Introduction

When electricity was first intentionally conducted from one place to another (from an electrified tube to an ivory ball) by Stephen Gray in 1729, the material used as the conductor was hempen pack-thread. Gray eventually covered distances of up to 233 m along the corridors of his house. In order to do this, he had to support the pack-thread and, after an abortive attempt in which fine copper wires were used, he suspended the thread by silk filaments. Thus both the conductor and the insulator were textile fibres. Soon afterwards, Du Fay found that pack-thread was a better conductor when it was wet. Then, in 1734, Gray discovered metallic conductors, and, apart from some use for insulating purposes, interest in the electrical resistance of fibres did not revive for nearly 200 years [1].

22.2 Definitions

The electrical resistance of a specimen, i.e. the voltage across the specimen divided by the current through it, is determined both by the properties of the material and the dimensions of the specimen. For most substances, the property of the material is best given by the specific resistance ρ (in Ω m), which is defined as the resistance between opposite faces of a 1 m cube, but, as with mechanical properties (see Section 13.3.1), it is more convenient with fibres to base a definition on linear density (mass per unit length) than on area of cross-section. A *mass-specific resistance* R_s is therefore defined as the resistance in ohms between the ends of a specimen 1 m long and of mass 1 kg, giving units of Ω kg/m^2. The two quantities are related as follows:

$$R_s = \rho d \tag{22.1}$$

where d = density of material in kg/m^3.

In practice, it is more convenient to express R_s in Ω g/cm^2, when the numerical values for most fibres will differ by less than 50% from the values of ρ expressed in Ω cm. With these units, the resistance R of an arbitrary specimen is given by the relation

$$R = R_s \frac{l}{NT} \times 10^5 \tag{22.2}$$

where l = distance between the ends of the specimen in cm, N = number of ends of yarn or fibre and T = linear density of yarn or fibre in tex.

Because of the wide range of resistance values, results are frequently expressed in terms of the logarithm of resistance.

22.3 Methods of measurement

22.3.1 Measurement of resistance

Ideally, the resistance should be measured accurately, instantaneously and at a constant voltage. The difficulties of doing this are increased by the high values of resistance that have to be measured and the wide range that is covered. A variety of methods has been used [1].

The simplest method of measurement is the use of an ammeter in series and a voltmeter across the resistance. This can be done when the resistance of the material is low. With a sensitive galvanometer, the method has been used for resistances up to $10^9\,\Omega$, but the time taken for the galvanometer to come to rest may be a disadvantage. Wheatstone bridge methods may also be used for fairly low resistances. The charging or discharging of a capacitor through the resistance is a method of measurement of high resistance. The general relation for the charge Q on a capacity C to which a voltage V_0 has been applied through a resistance R for a time t is:

$$Q = V_0 C\,(1 - e^{-t/CR}) \tag{22.3}$$

For the capacity discharging, $Q = V_0 C\, e^{-t/CR}$. Various arrangements may be used to apply these relations, but they all suffer from the defects that the test must last for a measurable time and that the voltage varies during the test.

With high-resistance stable resistors, comparison methods can be used. Fig. 21.1 shows the circuit used by Hearle [2]. The voltage V_1 can be measured by a low-resistance voltmeter. The voltage V_2 must be measured by a voltmeter whose resistance is much greater than that of the unknown resistance R. The resistance to be measured is given in terms of the standard resistance R' by the relation

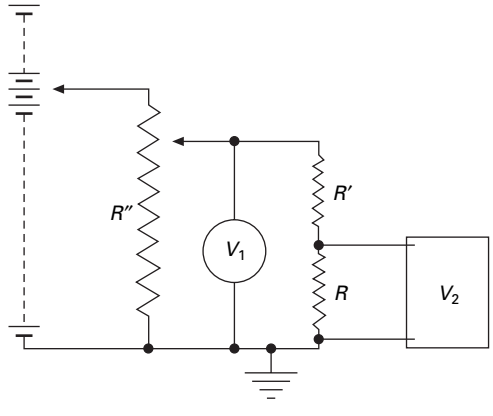

22.1 Circuit for measurement of high resistances.

$$R = R'\left(\frac{V_2}{V_1 - V_2}\right) \tag{22.4}$$

By this method, high resistances can be measured quickly with a known voltage V_2 adjustable by the potentiometer R'' across the specimen. Hersh and Montgomery [3] used a slightly more complicated circuit in a null method, which does not require such a high-resistance detector.

In measuring high resistances, great care must be taken to avoid the pick-up of stray voltages, which necessarily take a long time to discharge.

22.3.2 Arrangement of specimens

Many different arrangements of the material to be tested have been used [1]. The resistance has been measured along single fibres, along many fibres in parallel, along single ends of yarn, along many ends in parallel, parallel to the weft and parallel to the warp in cloth, across yarn and across cloth, and with special electrodes, such as those of the Shirley Moisture Meter (see Section 7.3.5).

In most of his experiments, Hearle [2, 4] used yarn wound on a polythene former and then held between bulldog clips, lined with tinfoil, 1 cm apart. Hersh and Montgomery [3] stuck fibres or pieces of yarn onto brass tabs with silver conducting paint.

The specimens must be conditioned by being placed in a suitable atmosphere. A simple conditioning chamber is satisfactory for work at constant temperature. Hearle [2] used a glass jar containing saturated salt solutions to control humidity. Leads were brought out through a tight-fitting stopper. A sample of the fibre was suspended in the jar and removed to measure moisture content. Alternatively, the resistance may be measured immediately after removal of the specimen from the conditioning atmosphere.

Securing constant moisture conditions at different temperatures is more difficult. The most satisfactory method is to enclose the specimen in a space so small that no appreciable evaporation can take place, which thus keeps the moisture content constant. Hearle [5] sealed specimens between sheets of rubber, brought out fine copper leads, and immersed the whole in a bath of paraffin.

22.4 Results of experiments

22.4.1 The influence of moisture

Moisture is the most important factor in determining the resistance of most textile materials and causes a variation over a range of at least 10^{10} times. Even the difference between 10 and 90% r.h. will cause a million-fold difference of resistance, namely, a tenfold decrease in resistance for every 13% increase in relative humidity.

For most hygroscopic textile fibres between 30 and 90% r.h., relations of the following form hold:

$$\log R_s = -n \log M + \log K \tag{22.5}$$

$$R_s \cdot M^n = K \tag{22.6}$$

where M = moisture content (%), and n and K are constants.

When plotted over a wider range of moisture conditions, a sigmoidal relation between log R_s and log M is obtained (Fig. 22.2). At low moisture contents (below 3.5% for cotton, 7% for viscose rayon and 4% for wool and silk), the following form fits the results:

$$\log R_s = -n' M + \log K' \tag{22.7}$$

where n' and K' are constants. A relation of this form was also found to fit the results for acetate and some specimens of nylon [6].

The resistance of a specimen at constant temperature has been found to be a single-valued function of moisture content, no hysteresis being detectable. It follows that there must be hysteresis between resistance and humidity. Nevertheless, for a given part of the hysteresis loop, relations of the following form are found to fit the experimental data fairly well:

$$\log R_s = -aH + b \tag{22.8}$$

where H = relative humidity, and a and b are constants.

22.4.2 Comparison of different materials

Figure 22.2 shows results for various materials plotted in terms of moisture content; Fig. 22.3 shows them in terms of relative humidity. Table 22.1 gives values of log R_s at 65% r.h., and of n and (log $K - n$). The latter quantity, which is equal to the value of log R_s at $M = 10\%$, is more useful for comparative purposes than the value of log

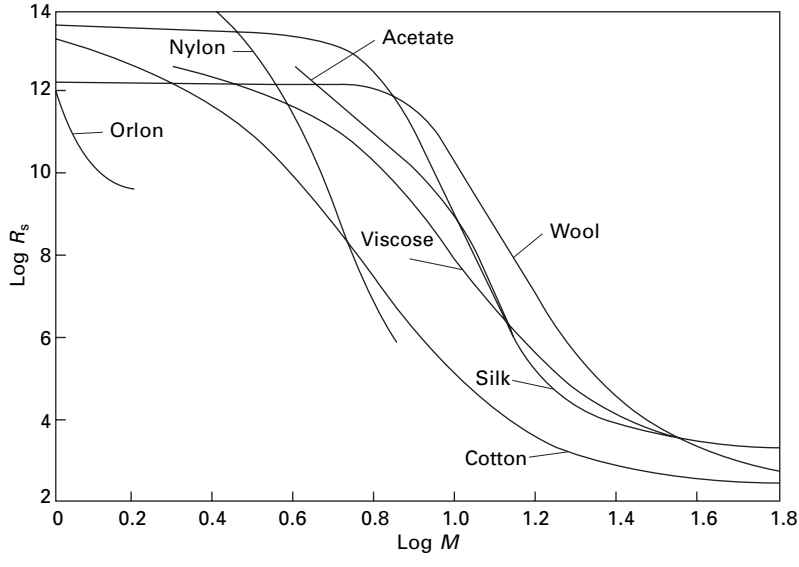

22.2 Variation of resistance of fibres with moisture content [2, 6].

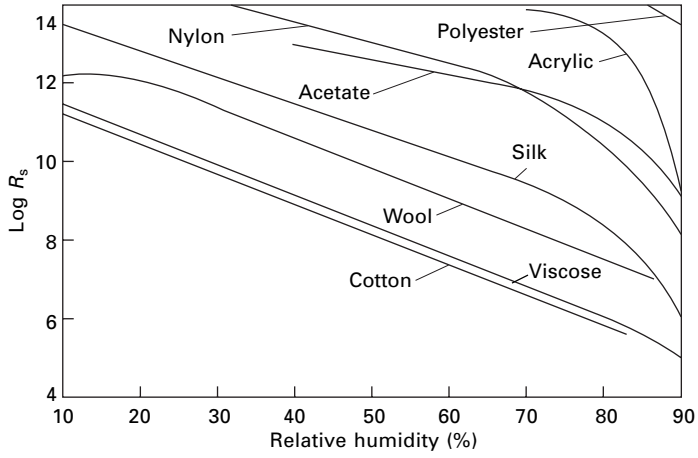

22.3 Variation of resistance of fibres with relative humidity [2, 7].

Table 22.1 Electrical resistance results, along yarn [2, 6, 7]

Material	n	(log K – n) = log R_s at M = 10%	log R_s at 65% r.h.	r.h. % for $R_s = 10^{10}\ \Omega\ g/m^2$
Cotton	11.4	5.3	6.8	30
Washed cotton	10.7	6.0	7.2	30
Mercerised cotton	10.5	6.8	7.2	30
Flax	10.6	6.8	6.9	30
Viscose rayon	11.6	8.0	7.0	30
Washed viscose rayon	12.0	9.0	7.5	30
Acetate		9.0	11.7	85
Silk	17.6	9.0	9.8	65
Wool	15.8	10.4	8.4	55
Washed wool	14.7	11.9	9.9	60
Nylon			9–12	85
Orlon acrylic fibre (as received)			8.7	85
Purified *Orlon* acrylic fibre			14	95
Terylene polyester fibre (as received)			8.0	85
Purified *Terylene* polyester fibre			14	95

K, which has to be obtained by extrapolation and is greatly affected by any error in the value chosen for n. Table 22.2 gives values of n' and log K' obtained at low moisture contents.

The values of n for the different cellulosic fibres are very nearly the same. Hearle [2] found that they can all be fitted with reasonable accuracy by the relation:

$$\log R_s = -11.2 \log M + \log K \tag{22.9}$$

where the value of log K can be found by measuring the resistance at one moisture content.

Table 22.2 Electrical resistance results: low moisture contents [8]

Material	n'	log K'	Upper limit of relation, M%	Lower limit of tests, M%
Cotton	1.90	16.0	3.5	1.3
Viscose rayon	0.47	13.6	7	2.2
Wool	0	12.7	4	0
Silk	0.15	13.9	4	1.4
Acetate [6]	0.72	16.5	> 12	4

Within the limits of experimental error, Hearle found no difference between 12 different cottons (two American, five Pakistani, two Egyptian, Brazilian, Tanguis and Uganda). A comparison of the results for cotton and viscose rayon shows that they are in reasonable agreement with the assumption that the conduction is in the non-crystalline region of the fibre, which will have a resistance determined by its own moisture content. Cellulose acetate shows a rather high resistance when considered in terms of either moisture content or relative humidity.

The protein fibres have larger values of n (between 16 and 18 in most cases), and, except at very low moisture contents, they have a much higher resistance than the cellulosic fibres. The change in resistance with moisture content at low moisture contents becomes very small, and in wool it is almost non-existent.

There is a wide variation, depending on their history and the presence of additives, in the resistance of different specimens of nylon. Nylon has a high resistance at a given humidity, but, when plotted against moisture content, the resistance values fall below those of viscose rayon. The curves of log R_s against log M show no linear portion. It has been shown by Sharman *et al.* [9] that the resistance of nylon increases as the draw-ratio increases; they consider that the change is greater than would be explained by a change of regain.

The acrylic fibres show a low resistance at a given moisture content, and at a given relative humidity they may even have a resistance as low as that of wool.

Fibres such as polyester or vinyl fibres, which absorb little water, all have very high resistances. Their resistances decrease at a rate of about ten times for every 10% increase in relative humidity up to about 80% r.h.; above this humidity, the resistance decreases more rapidly. However, for these fibres, anti-static finishes are commonly applied to lower the resistance, as indicated by the million-fold increase in the resistance on removing finish from the polyester fibre in Table 22.1.

The high-modulus, high-tenacity (HM–HT) polymer fibres are inherently good insulators, though there is some effect of moisture in aramid fibres. Glass and ceramic fibres are also good insulators. Surface finishes can, of course, cause a modification of properties. Carbon fibres are fairly good conductors of electricity, with a resistivity of about 15 Ω m.

22.4.3 Effect of impurities

The resistance of the hygroscopic fibres depends on their electrolyte content, as is illustrated by the results for cotton and wool in Fig. 22.4. The addition of a salt such

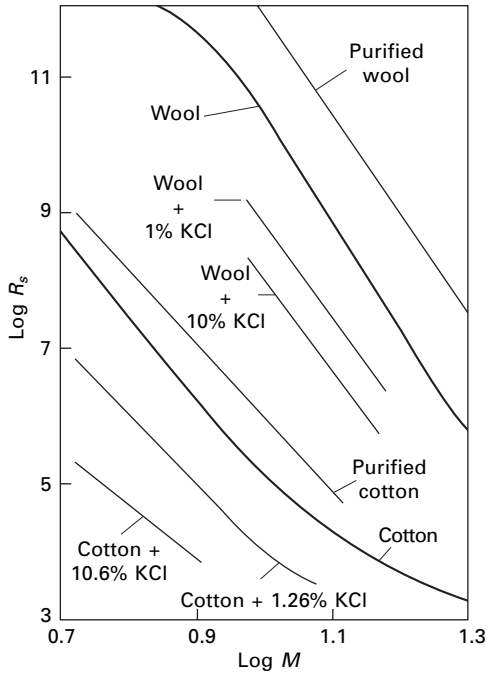

22.4 Resistance of wool and cotton as received, purified, and with added electrolyte [2].

as potassium chloride lowers the resistance. At low salt contents, the evidence indicates that conductivity is approximately proportional to electrolyte content, but, at high salt contents (greater than 1%), O'Sullivan [10] found that the resistance of cellulose film at a given moisture content was independent of the nature or amount of salt present.

Washing in distilled water increases the resistance, and a further increase may be obtained by washing in calcium sulphate solution. Walker and Quell's results [11] show the increase in resistance between raw cotton (0.4% of sodium and potassium salts) and washed cotton:

	R_s, MΩ g/cm^2
raw cotton	0.5
after washing 200 g in 5 litres distilled water	14
after washing 200 g in 40 litres distilled water	12–25
after washing in $CaSO_4$ solution followed by distilled water	18–37

The action of the calcium sulphate solution is to replace the monovalent ions left behind after washing in distilled water by less conducting bivalent ions (see Section 22.5.3). The residual ions are probably associated with ionic groups in the fibre molecule, for example, carboxyl (—COO—) groups present as impurities in cellulose molecules. Church [12] found that, when hydrogen ions were replaced by calcium ions in paper, the resistance increased six times.

Any wet processing, such as bleaching or dyeing, that alters the electrolyte content will alter the electrical resistance. The resistance of the synthetic fibres is much affected by the presence of surface finishes. For example, Hayek and Chromey [13] found a reduction of 10 000 times by a suitable anti-static agent.

Boyd and Bulgin [14] have shown that, when about 30% of carbon black is included in viscose rayon fibres, their specific resistance at 0% r.h. falls from between 10^{14} and $10^{15}\,\Omega$ cm to less than $10^{6}\,\Omega$ cm. This must be due to the presence of a continuous conducting path of carbon black. With increase of humidity, the resistance increases slightly, presumably owing to a greater dispersion of the carbon black. There is also a change with humidity in the critical concentration of carbon black at which the resistance begins to drop markedly: this rises from 26% carbon black in the dry state to 30% at saturation.

22.4.4 Effect of temperature

The resistance of fibres decreases as the temperature increases, a rise of 10 °C causing a fall of the order of five times. A typical set of results is shown for cotton in Fig. 22.5.

For cotton, viscose rayon and wool, Hearle [5] found that the rate of change of log R with temperature varied separately with moisture content M and temperature θ C.

$$\frac{-\mathrm{d}(\log R)}{\mathrm{d}\theta} = a - bM - c\theta \tag{22.10}$$

where a, b and c are constants for a given material. Values of a, b and c are given in Table 22.3. The value of a gives the rate of change of log R with temperature under dry conditions at 0 °C, and the values of b and c give the change of d(log R)/dθ with moisture content and temperature, respectively.

Clark and Preston [15] have found that the same equation fits the results for

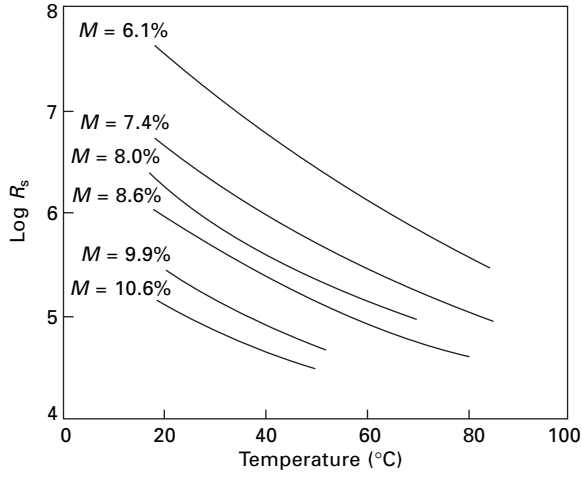

22.5 Variation of resistance of cotton with temperature [5].

Table 22.3 Values of *a*, *b* and *c* [5]

Material	*a* (per deg C)	*b* (per deg C per unit moisture content)	*c* (per deg C per deg C)
Cotton	0.0863	0.005 35	0.000 35
Viscose rayon	0.0707	0.001 86	0.000 37
Wool	0.0960	0.002 12	0.000 57
Acetate*	0.0528	0.000 80	0.000 25
Silk†	0.0934	0.002 87	0.000 82

*Only tested over small range.
†Near 20 °C and 10% moisture content.

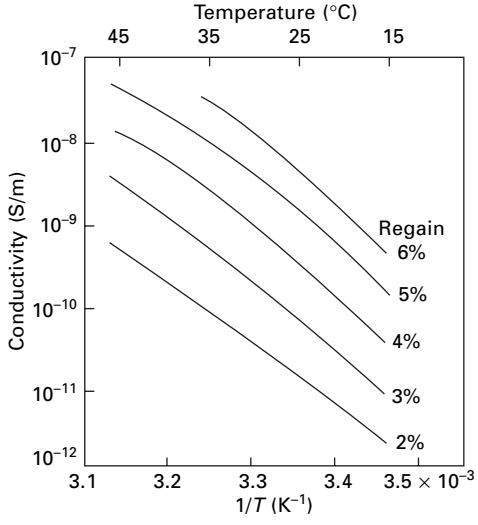

22.6 Variation of conductivity of drawn nylon with temperature [9].

viscose rayon at 24.5% regain down to – 60 °C. For silk, a relation of the above form is not strictly accurate. For nylon at 20 °C and 6% moisture content, it was found that $d(\log R)/d\theta = 0.05$ per °C. Sharman *et al.* [9] found that curves of log (conductivity) against the reciprocal of temperature were approximately parallel at different regains, as is shown in Fig. 22.6.

22.4.5 Arrangement of specimen

One would expect the specific resistance of fibres to vary with the direction of measurement, but, owing to the experimental difficulties, no values for the transverse specific resistance of fibres are available. O'Sullivan [10] found that the resistance of cellulose film parallel to the direction of extrusion was 0.8 times that perpendicular to the direction of extrusion. Hearle and Jones [16] found that the ratios of resistances with three different electrode systems varied with the material and the moisture

content, which indicated that the ratios of specific resistances in different directions varied with these factors.

All the results in the literature, except for those in one paper [17], indicate that the experimentally obtained specific resistance of fibres is independent of the dimensions and form of the specimen. In other words, there is no composite specimen effect, and the resistance of a specimen is proportional to its length and inversely proportional to its area of cross-section (or mass per unit length). This relation will break down if the contact resistance between electrode and specimen becomes comparable with the resistance of the specimen.

Hersh and Montgomery [3] tested nylon specimens ranging in linear density from 3 to 340 den (from 0.33 to 38 tex) and showed that they all gave the same specific resistance. Hearle [4] found only a very small change in resistance when cotton and viscose rayon were subjected to tensions up to near their breaking point.

22.4.6 Polarisation and related effects

If polarisation, whether electrolytic or electrostatic, causes a back electromotive force (e.m.f.) to occur, it will be detectable in three ways: the resistance will increase with time as the back e.m.f. develops; the resistance will decrease with voltage; and the back e.m.f. will be present, dying away, after the applied voltage has been removed.

Several workers have found that the variation of resistance with time is undetectable or very slight, except at low and high humidities. For raw cotton with tin electrodes, Hearle [4] obtained a significant variation of resistance with time only above 90% r.h. At 17.4% moisture content, the resistance doubled in 30 s. With cotton containing added potassium chloride, the resistance increased with time down to below 50% r.h. With one specimen of wool, the resistance remained constant even at 27% moisture content, but, with another specimen, there was an increase of 7% per minute at 17% moisture content. The nature of the electrodes is an important factor in polarisation effects. The curves in Fig. 22.7 show that, at 9.3% moisture content, the resistance of cotton between copper and zinc electrodes increases rapidly with time, but that, with tin, aluminium, or platinum electrodes, it changes only very slowly. Jones [18] found that a large stainless-steel anode was most effective in eliminating polarisation. On ashing polarised cotton fibres, Williams and Murphy [19] found most of the ash near the electrodes.

The above effects are typical of polarisation as it occurs in electrolytic solutions, when it is most marked if there is a rapid discharge of ions at the electrodes. It is due to the prevention of the rapid attainment of equilibrium by a slow process at the electrode and is much affected by the nature of the electrodes.

Other effects, such as heating, which will change the temperature and may cause drying, and the transport of water or ions in the specimen, have been suggested as a cause of variation of resistance with time. Although it is likely that these effects may be appreciable in some conditions, they have never been definitely observed.

Back e.m.f. of the order of 2 V has been found by Hearle [4] and others. A set of results for cotton is shown in Fig. 22.8. At low moisture contents, there is only a small back e.m.f. As the moisture content increases, the back e.m.f. also increases

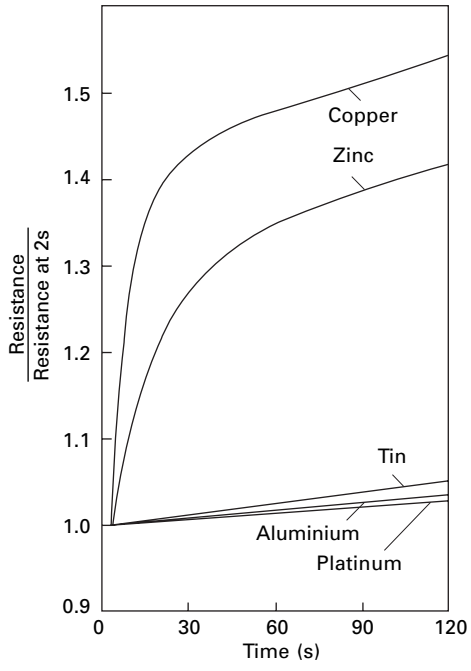

22.7 Variation of resistance of cotton with time for various electrodes [4]. Moisture content = 9.3%.

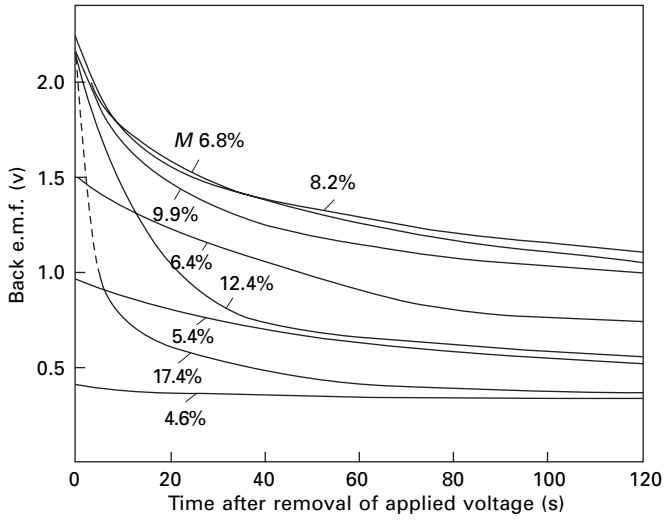

22.8 Back e.m.f.s in cotton, at various moisture contents, after applying 122 V for 1 min [4].

and reaches a value of about 2 V at 7% moisture content. At higher moisture contents, the back e.m.f. remains the same, but above 9% moisture content it dies away more rapidly after the removal of the applied voltage. The value of the back e.m.f. was found to be different with electrodes of different metals.

Polarisation effects have also been reported below 25% r.h. for cotton and wool. Murphy [20], working with cotton, found that, under these conditions, the back e.m.f. varied with the applied voltage, and he obtained values of over 100 V. This behaviour indicates electrostatic polarisation.

The variation of resistance with voltage in fibres was observed by Evershed [21] in 1913. Fig. 22.9 shows a typical result for cotton. The decrease of resistance with voltage up to 50 V is adequately explained by the presence of a back e.m.f. of the order of 2 V (Fig. 22.10). Similar effects are observed with other fibres, though with wool the resistance does not vary with voltage below 80% r.h.

The continuing decrease at higher voltages found by Evershed and others is greater than that due to a small back e.m.f. By testing specimens of various lengths, Hearle [4] showed (Fig. 22.11) that the specific resistance depended on the average field strength (or what comes to the same thing, the current density) rather than on the actual applied voltage.

Hersh and Montgomery [3] have found the resistance of cotton yarns to be ohmic in the range 50–2000 V. However, Cusick and Hearle [22] have suggested that this is because they allowed some time to elapse before measuring the resistance, and consequently an increase of resistance with time fortuitously masked the decrease with voltage. In a later comment, Hersh and Montgomery [23] have suggested that the change in resistance is due to a heating of the specimen. This would be influenced by the air velocity in the neighbourhood of the specimen.

Cusick and Hearle [22] also found that the rate of change of resistance of cotton with time increased as the voltage increased, as shown in Fig. 22.12. When the specimen is left with no voltage applied, the resistance recovers at a similar rate to its previous increase.

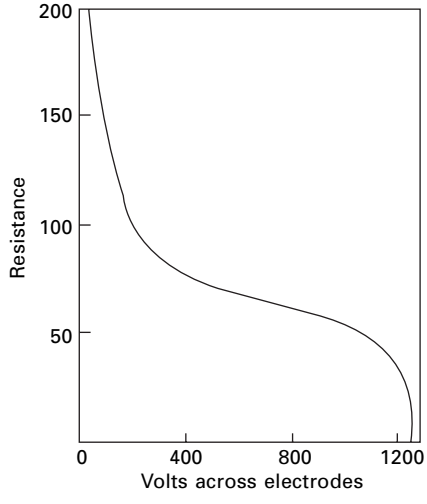

22.9 Variation of resistance of cotton with applied voltage. After Evershed [21].

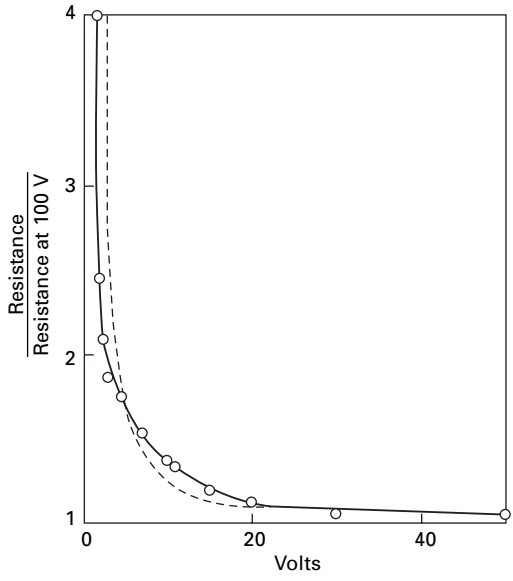

22.10 Variation of resistance of cotton (moisture content = 6.4%) with applied voltage up to 50 V. The dotted line is the theoretical curve for a back e.m.f. of 2 V [4].

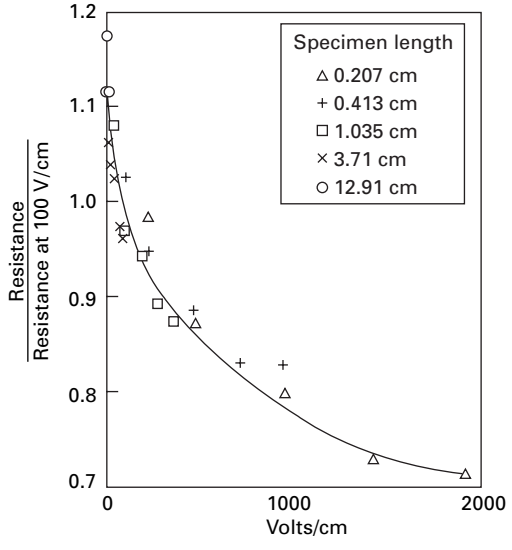

22.11 Variation of resistance with field strength. The points are four specimens of various lengths [4].

22.4.7 Electrolytic effects

During conduction in cellulose film impregnated with salts, O'Sullivan [24] observed phenomena similar to those occurring in the electrolysis of salt solutions. When the film is soaked in sodium chloride, an acid region develops at the anode and an

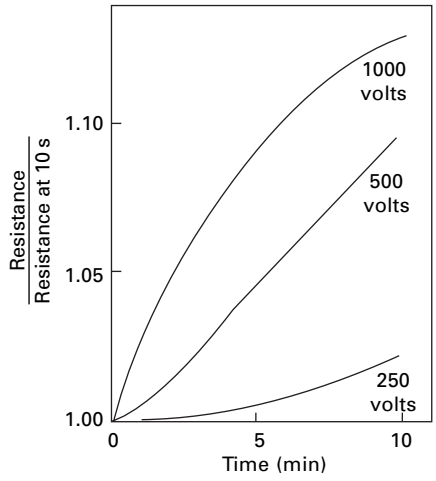

22.12 Effect of voltage on change of resistance of cotton with time [22].

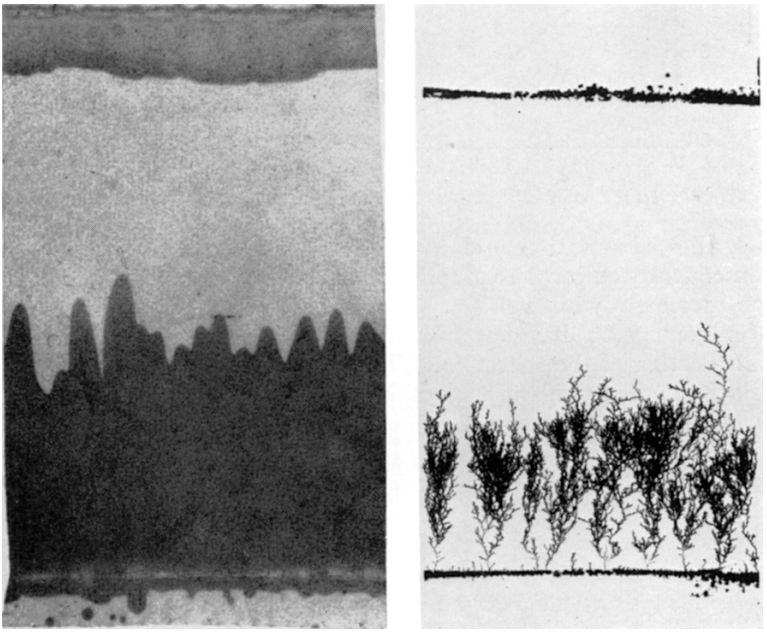

22.13 Electrolytic effects during conduction in cellulose film. (a) Film impregnated with sodium chloride and an indicator, showing acid and alkaline regions at electrodes. (b) Film impregnated with silver nitrate, showing deposition of silver at cathode and entry of copper at anode.

alkaline region at the cathode. Figure 22.13(a). With silver nitrate in the film, 'treeing' occurs (Fig. 22.13(b)) as the silver is deposited at the cathode. The conditions are just those which would cause 'treeing' in electroplating (high potential gradient, unstirred bath and low conductivity) and, as in electroplating, it may be avoided by using potassium silver cyanide instead of silver nitrate.

King and Medley [25] measured the amount of hydrogen liberated during conduction in keratin film and found that it was about 90% of that expected from the quantity of electricity passed. There were also small quantities of oxygen and carbon dioxide from the anode reactions.

O'Sullivan [26, 27] measured the bulk mobilities of ions in cellulose film. Typical results are given in Table 22.4.

22.4.8 Resistance noise

Owing to the arrival of current in discrete charges, there is a variable component in direct current. This gives rise to resistance noise, which is one of the factors limiting the amplification of small signals. The magnitude of these random fluctuations has been worked out by Schottky [28] for current carried by electronic charges.

Boyer [29], working with films of various polymers, including cellulose and nylon, has found that the noise level is much higher than that given by Schottky's formula and that the noise has a frequency distribution characteristic of the particular polymer. He concludes that this is due to the arrival of ions at the electrodes in 'avalanches', owing to their being held up at places in the polymer until some movement of the structure allows them to continue to flow.

22.5 Theoretical

22.5.1 Nature of the conduction

In a consideration of the mechanism of conduction of electricity, the first questions to be answered are: 'Where is the current flowing'? and 'What is carrying the current?' Both of these problems have to be solved mainly by circumstantial evidence.

Hersh and Montgomery [3] have shown that for nylon filaments the resistance is inversely proportional to the area of cross-section. This indicates that conduction is predominantly a volume effect, with the current flowing through the bulk of the material. If conduction had been a surface effect, the resistance would have been inversely proportional to the circumference (i.e. the square root of the area or cross-

Table 22.4 Bulk mobility of ions in cellulose film [26, 27]

Ion	Mobility in $cm^2\ s^{-1}\ V^{-1}$ at moisture content of:			
	10%	20%	30%	40%
H^+	3×10^{-8}	4×10^{-6}	2.5×10^{-5}	8×10^{-5}
OH^-	1.6×10^{-8}	1.6×10^{-6}	8×10^{-6}	2.5×10^{-5}
K^+	3×10^{-6}	6×10^{-7}	3×10^{-6}	6×10^{-6}
Ag^+	1.6×10^{-7}	4×10^{-6}	1.3×10^{-5}	2.5×10^{-5}
Cl^-	3×10^{-9}	8×10^{-7}	8×10^{-6}	2×10^{-5}
Fe^{2+}		2.5×10^{-7}	1.3×10^{-6}	1×10^{-5}
Cu^{2++}		2.5×10^{-8}	1×10^{-6}	5×10^{-6}
SO_4^{2--}, CrO_4^{2--}		2×10^{-7}	2.5×10^{-6}	1×10^{-5}
Ca^{2++}				5×10^{-7}

section). Different types of cotton also have the same specific resistance, though here the range of fineness covered is smaller; different qualities of wool differ to an appreciable extent only at low moisture contents, when the influence of impurities is great. Indirect evidence that conduction is a volume effect is provided by the lack of hysteresis between resistance and moisture content (which is a volume, not a surface, quantity), despite the hysteresis between moisture content and relative humidity. Thus, in the hygroscopic fibres, it appears that volume conduction is the dominant effect, surface conduction being negligible in comparison.

Both the close association between resistance and moisture content and the relation between the resistances of cotton and viscose rayon indicate that the current will be flowing in the non-crystalline regions of the fibre. Indeed, the ordered arrangements of cellulose molecules in a crystalline region would be expected to be highly insulating.

In the synthetic fibres, with higher resistance and negligible moisture absorption, surface conduction is likely to be more important and may be the dominant mechanism. Certainly when conducting surface finishes are applied, the current will be almost entirely on the surface.

Current may be carried either by electrons or by ions. Baxter [30], in 1943, put forward a theory that conduction in wool was by electrons, the water molecules acting as impurity centres in an electronic semiconductor, but most workers have assumed that conduction is by ions. Where the products of electrolysis have been directly observed by O'Sullivan [24], using cellulose film, and by King and Medley [25], using keratin film, the current must be ionic. The variation of resistance with electrolyte content and the polarisation effects also support this view. Thus, where there is evidence, it indicates that conduction is ionic, but, where there is no special evidence (for example, at low moisture contents), it cannot be definitely stated that conduction is not electronic. A specialised mechanism that Baker and Yager [31] have suggested for the polyamides is the mobility of hydrogen atoms (protons) from hydrogen bonds. This can, however, be regarded as equivalent to other forms of ionic conduction, since it is essentially an ionisation at the hydrogen bond:

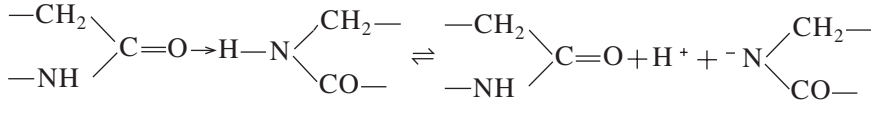

With the possible exceptions noted above, the general picture is of ionic conduction taking place through the bulk of the material. The next step is to consider theories that will explain the enormous variation of resistance with moisture content, the large variation with temperature, and other effects, such as the higher resistance of protein fibres and the low conductivity of bivalent ions. There are two possible causes of variation of resistance: there may be changes in the number of ions available for conduction or there may be changes in the rate at which the ions move through the material under a given applied voltage.

For a specimen having v ions per unit length available for conduction, with z as the valency of the ions and e as the electronic charge, and on the assumption that the ions move with an average velocity u under a potential difference V between the ends of the specimen, the current I and resistance R are given by:

$$I = vzeu \tag{22.11}$$

$$R = \frac{V}{I} = \frac{V}{vzeu} \tag{22.12}$$

For further study, it is convenient to separate the factors by taking logarithms:

$$\log R = \log V - \log v - \log ze - \log u \tag{22.13}$$

22.5.2 Influence of permittivity on dissociation of ion pairs

There has been no success in attempting to explain the enormous changes of resistance with moisture content on the basis of changes in rate of ion movement. The most likely theory, proposed by O'Sullivan [32] and based on breaks in conducting water paths, was shown by Hearle [33] to be impossible because of the polarisation that would occur. For a successful theory, we must look to changes in the number of available ions.

Strong electrolytes are completely ionised, and the ions can be held together in molecules only by electrostatic forces. In solutions in liquids of high permittivity, such as water, these forces are so weak that there is no close association of ions, but even weak inter-ionic forces prevent the ions from acting as completely free particles.

If the permittivity of the solvent is lower, the electrostatic forces will be stronger, and we may consider an equilibrium between ion pairs and free ions

$$A^+ B^- \rightleftharpoons A^+ + B^-$$

The variation in this equilibrium offers a possible explanation of variations in resistance. A rise in permittivity would cause more dissociation, making more free ions available for conduction and consequently lowering the resistance. This is illustrated diagrammatically in Fig. 22.14.

A simplistic theory, which applies macroscopic ideas to molecular phenomena and does not take account of the interaction of all the ions present, has been put forward by Hearle [33]. Let α be the degree of dissociation of the ion-pairs:

$$\underset{(1-\alpha)}{A} + B^- \overset{U}{\rightleftharpoons} \underset{\alpha}{A^+} + \underset{\alpha}{B^-}$$

It can be shown that, as a consequence of the Law of Mass Action:

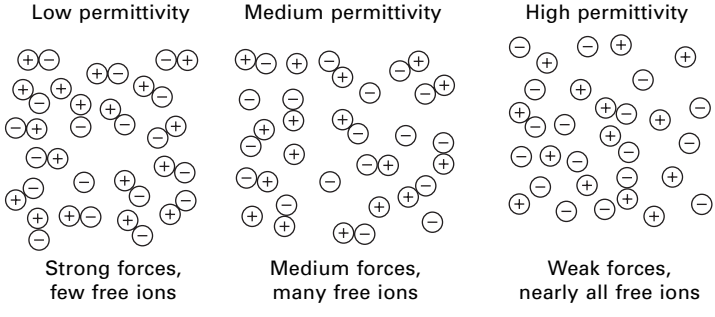

22.14 Effect of permittivity on association of ions.

$$\frac{\alpha^2}{1-\alpha} = A\,\mathrm{e}^{-U/kT} \tag{22.14}$$

where U = the energy of dissociation, k = Boltzmann's constant, T = absolute temperature and A = a constant, of the order of the ratio of the total volume to the volume occupied by ions.

The energy needed to separate two electrostatic charges in a medium of relative permittivity ε_r is given by:

$$U = \frac{U_0}{\varepsilon_r} \tag{22.15}$$

where U_0 = the energy needed to separate the ions in a medium of unit relative permittivity and is thus a constant. Hence:

$$\frac{\alpha^2}{1-\alpha} = A\,\mathrm{e}^{-U_0/\varepsilon_r kT} \tag{22.16}$$

If $\alpha << 1$, that is when most of the ions are associated in pairs:

$$\frac{\alpha^2}{1-\alpha} \approx \alpha^2 \tag{22.17}$$

Hence:

$$\alpha = A^{1/2}\,\mathrm{e}^{-U_0/2\varepsilon_r kT} \tag{22.18}$$

But, if v_0 is the total number of electrolyte molecules per unit length of specimen, then the number of ions available for conduction is given by:

$$v = 2\,\alpha\,v_0 \tag{22.19}$$

and, substituting in equation (22.13), we get:

$$\begin{aligned}\log R &= \log\frac{V}{uze} - \log\alpha - 2\log v_0 \\ &= \log\frac{V}{2A^{1/2}uzev_0} + \frac{U_0\log e}{2kT}\frac{1}{\varepsilon_r}\end{aligned} \tag{22.20}$$

This may be written:

$$\log R = \frac{\Psi}{\varepsilon_r + \chi} \tag{22.21}$$

where $\Psi = (U_0 \log \mathrm{e})/(2\,k\,T)$ and $\chi = \log\,(V/2\,A^{1/2}\,u\,z\,e\,v_0)$.

After suitable values for Ψ and χ have been chosen, equation (22.21) can be tested with experimental results. Figure 22.15 shows a comparison of Hearle's values of resistance with theoretical predictions in which Balls's values [34] of the permittivity of cotton and King's values [35] of the permittivity of keratin film have been used. For cotton, there is a good fit with $\Psi = 76.8$ and $\chi = 1.1$ and for wool with $\Psi = 42.2$ and $\chi = 3.6$. The coincidence of the bending-over of the curve for wool is particularly striking.

From the value chosen for Ψ, the values of U_0 can be calculated. With $\Psi = 76.8$

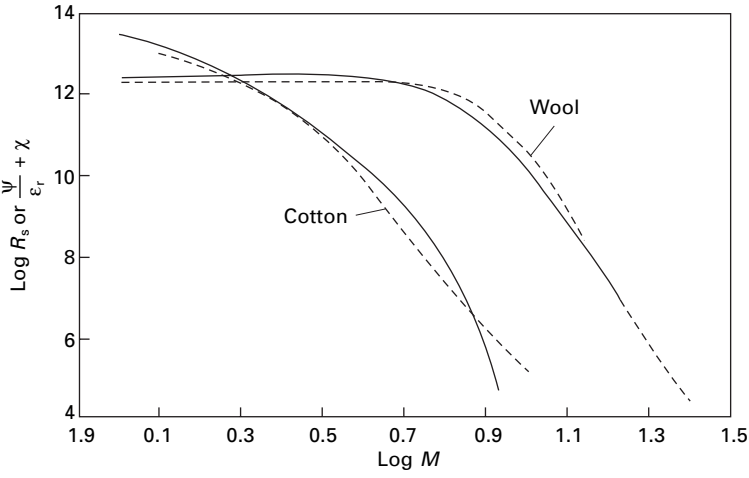

22.15 comparison of experimental (full lines) and theoretical (dotted lines) curves for variation of resistance of cotton and wool with moisture content [33].The theoretical expressions are:

Cotton: $\log R_s = \frac{76.8}{\varepsilon_r} + 1.1$

Wool: $\log R_s = \frac{42.2}{\varepsilon_r} + 3.6$

and at room temperature, $T \approx 300$ K, this gives $U_0 \approx 1.5 \times 10^{-18}$ J. This may be compared with the energy required to separate two electronic charges, initially at a distance apart equal to the ionic diameter, i.e. of the order of 5×10^{-10} m, which gives $U_0 \approx 5 \times 10^{-18}$ J. Thus the chosen value of Ψ proves to be of the right order of magnitude.

This theory will explain the high resistance of multivalent ions. If the ions have valencies z_1 and z_2, then, considering isolated charges separated by a distance X, we have

$$U = \frac{z_1 z_2 U_0}{\varepsilon_r} \approx \frac{z_1 z_2 e^2}{\varepsilon_r X} \tag{22.22}$$

where U_0 is assumed to be the value for monovalent ions.

Equation (22.21) therefore becomes:

$$\log R = \frac{z_1 z_2 \Psi}{\varepsilon_r + \chi} \tag{22.23}$$

The value of $\log R$ is thus increased by an amount $(z_1 z_2 - 1)\, \Psi/\varepsilon_r$ compared with the value with the same number of monovalent ions present. Some values of this quantity are given in Table 22.5. These figures, being differences in $\log R$, give the number of powers of 10 by which the resistance with multivalent ions would be greater than the resistance with monovalent ions. It will be seen that, in almost all cases, conduction by multivalent ions would be negligible.

Although the constants Ψ and χ would not be expected to be exactly the same for different materials, Hearle [36, 37] has shown that, when values of $\log R_s$ are plotted

Table 22.5 Values of $(z_1z_2–1)\ \Psi/_r$ [33]

ε_r	Ψ = 76.8		Ψ = 42.2	
	z_1z_2 = 2	z_1z_2 = 4	z_1z_2 = 2	z_1z_2 = 4
1	76.8	229	42.9	126
5	15.4	46	8.4	25
10	7.7	23	4.2	13
15	5.1	15	2.8	8
20	3.8	11	1.1	3

against values of $1/\varepsilon_r$ (all determined under the same conditions), the straight lines do group closely together. In particular, the differences in their permittivities explain the differences in resistance between cellulosic and protein fibres under similar moisture conditions.

22.5.3 Conduction at high moisture contents

At high moisture contents, when the permittivity becomes high, the condition $\alpha << 1$ will break down, and dissociation will become almost complete. Equation (22.21) will then cease to apply, and the effect of the permittivity will be small. Theoretical estimates, based on the value of A, and experimental results for the dissociation of electrolytes in liquids both indicate that α becomes near to unity for permittivities greater than 20. Under these conditions, an alternative mechanism will be limiting the conduction. The theory of breaks in conduction paths would also break down at high moisture contents, when breaks become negligible.

At high moisture contents, the ions will be moving along water paths and their speed will be limited by viscous hindrance to their flow. If the paths are narrow and the water is moving with the ions, Poiseuille's equation for the flow of liquids along tubes should apply to the velocity u of the ions, to give:

$$u \propto (\text{radius of tube})^4 \propto (\text{volume of water})^2 \propto (\text{regain})^2$$

Note that it is regain r (mass of water per mass of fibre), which tends to infinity as a maximum, and not moisture content M (mass of water per mass of water + fibre), which tends to 1, that is the relevant quantity.

Thus, from equation (22.13):

$$\log R = \log(\text{constant}) - 2 \log r = \log(\text{constant}) - 2 \log M + \log (1 - M) \tag{22.24}$$

As shown in Fig. 22.16, an equation of this form does have approximately the right slope for a plot of log R against log M over a range of about 15–30% moisture content for cotton, when the experimental plot starts to level off. Equation (22.24) then has a rapid fall as $\log(1 - M)$ tends to minus infinity. However, at high moisture contents, the tubes become much wider, the ions would effectively be moving through an infinite medium, and the velocity would tend to a constant value, determined by Stokes' equation and giving a constant resistance.

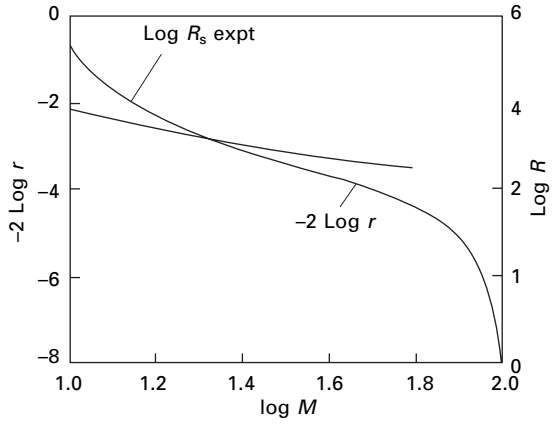

22.16 Comparison of variation of log R_s and (–2 log r) with moisture content [33].

22.5.4 An alternative theory

Baxter's [30] theory for wool was that conductance C was due to electrons jumping between absorbed water molecules, so that the decrease in resistance as moisture regain r increased was due to the reduction in distance between absorbed water molecules. His result given below can be transformed into an expression for resistance R:

$$C = A \exp\left(\frac{-B}{r^{1/3}}\right) \tag{22.25}$$

$$\log R = \frac{b}{r^{1/3} - a} \tag{22.26}$$

where r = regain and A, B, a and b are constants.

Christie and coworkers [38, 39] argue that conduction is by mobile protons. Since Baxter's model is independent of the charge carrier, they adapt his equation. For cellulose fibres [38], they find that it is necessary to offset the regain by an amount r_0, for which they offer possible explanations. The equations become:

$$C = A \exp\left[\frac{-B}{(r - r_0)^{1/3}}\right] \tag{22.27}$$

$$\log R = \frac{b}{(r - r_0)^{1/3} - a} \tag{22.28}$$

This equation gives good agreement with the experimental results for cotton over the measured range to 20% regain. For viscose rayon there is agreement up to 40% regain, but then the conductance levels off.

In order to fit data for wool and silk [39], it was necessary to introduce extra terms to allow for conductivity at zero regain C_0 and for strongly and weakly bonded water:

$$C = C_0 + A_s \exp[- B_s/(r_s)^{1/3}] + A_w \exp[-B_w/(r_w)^{1/3}] \quad (22.29)$$

This accords with two-phase theories of moisture absorption (see Chapter 12). Although the model could be interpreted as defining the rate at which protons move through the material, it can also be related to the numbers available to jump in a given time, which fits the dissociation model. Introduction of the dependence of dielectric constant on regain might show that there was less difference between the theories than is first apparent.

22.6 References

1. J. W. S. Hearle. *J. Text. Inst.*, 1952, **43**, P194 (review of literature).
2. J. W. S. Hearle. *J. Text. Inst.*, 1953, **44**, T117.
3. S. P. Hersh and D. J. Montgomery. *Text. Res. J.*, 1952, **22**, 805.
4. J. W. S. Hearle. *J. Text. Inst.*, 1953, **44**, T155.
5. J. W. S. Hearle. *J. Text. Inst.*, 1953, **44**, T144.
6. G. E. Cusick and J. W. S. Hearle. *J. Text. Inst.*, 1955, **46**, T699.
7. G. E. Cusick and J. W. S. Hearle. *J. Text. Inst.*, 1955, **46**, T369.
8. E. J. Murphy and A. C. Walker. *J. Phys. Chem.*, 1928, **32**, 1761.
9. E. P. Sharman, S. P. Hersh and D. J. Montgomery. *Text. Res. J.*, 1953, **23**, 793.
10. J. B. O'Sullivan. *J. Text. Inst.*, 1947, **38**, T271.
11. A. C. Walker and M. H. Quell. *J. Text. Inst.*, 1933, **24**, T123.
12. H. F. Church. *J. Soc. Chem. Industr.*, 1947, **66**, 221.
13. M. Hayek and F. C. Chromey. *Amer. Dyest. Rep.*, 1951, **40**, 164.
14. J. Boyd and D. Bulgin. *J. Text. Inst.*, 1957, **48**, P66.
15. J. F. Clark and J. M. Preston. *Text. Res. J.*, 1955, **25**, 797.
16. J. W. S. Hearle and E. H. Jones. *J. Text. Inst.*, 1949, **40**, T311.
17. F. Weidmann. *Kunstoffe*, 1939, **29**, 133.
18. E. H. Jones. *J. Sci. Instrum.*, 1940, **17**, 55.
19. R. R. Williams and E. J. Murphy. *Bell Syst. Tech. J.*, 1929, **8**, 225.
20. E. J. Murphy. *J. Phys. Chem.*, 1929, **33**, 200.
21. S. Evershed. J. Instn Elect. Engrs, 1913, **52**, 51.
22. G. E. Cusick and J. W. S. Hearle. *Text. Res. J.*, 1955, **25**, 563.
23. S. P. Hersh and D. J. Montgomery. *Text. Res. J.*, 1955, **25**, 566.
24. J. B. O'Sullivan. *J. Text. Inst.*, 1947, **38**, T285.
25. G. King and J. A. Medley. *J. Colloid Sci.*, 1949, **4**, 1.
26. J. B. O'Sullivan. *J. Text. Inst.*, 1947, **38**, T291.
27. J. B. O'Sullivan. *J. Text. Inst.*, 1947, **38**, T298.
28. S. Schottky. *Ann. der. Phys.*, 1918, **57**, 541.
29. R. F. Boyer. *J. Appl. Phys.*, 1950, **21**, 469.
30. S. Baxter. *Trans. Faraday Soc.*, 1943, **39**, 207.
31. W. O. Baker and W. A. Yager. *J. Amer. Chem. Soc.*, 1942, **64**, 2171.
32. J. B. O'Sullivan. *J. Text. Inst.*, 1948, **39**, T268.
33. J. W. S. Hearle. *J. Text. Inst.*, 1953, **44**, T177.
34. W. L. Balls. *Nature*, 1946, **158**, 9.
35. G. King. *Trans. Faraday Soc.*, 1947, **43**, 601.
36. J. W. S. Hearle. *Text. Res. J.*, 1954, **24**, 307.
37. J. W. S. Hearle. *J. Text. Inst.*, 1957, **48**, P40.
38. J. H. Christie and I. M. Woodhead. *Textile Res. J.*, 2002, **72**, 273.
39. J. H. Christie, I. M. Woodhead, S, Krenek and J. R. Sedcole. *Textile Res. J.*, 2002, **72**, 303.

23
Static electricity

23.1 Introduction

Some of the effects of static electricity were described by Thales in about 600 BC, and the first understanding of the nature of electricity came from the study of the phenomenon of static electricity in the 18th century. After the discovery of current electricity, however, the study of static electricity, with all its experimental difficulties, was neglected, but the increasing amount of trouble in industry that is due to static, resulting from the introduction of new materials, particularly synthetic fibres, led to a revived interest in it [1–3]. Holme *et al*. [4] have published a more recent review. Through its effects, static causes a variety of troubles in textile materials and processing.

Similar charges repel one another. This causes difficulty in handling materials. The filaments in a charged warp will bow out away from one another. There will be 'ballooning' of a bundle of slivers. Cloth will not fold down neatly upon itself when it comes off a finishing machine and so on. Unlike charges attract one another. This has caused difficulty in the opening of parachutes. It will also cause two garments, oppositely charged, to stick to one another, and in movement one garment may ride up on the other and cause embarrassment to the wearer. Another consequence is the attraction to a charged material of oppositely charged particles of dirt and dust from the atmosphere (Fig. 23.1). After 15 days, the soiling of a cotton fabric held at +1.2 kV was over twice as severe as at 0 kV. At –12 kV it was 13 times worse, but at +12 kV it was 19 times worse owing to the preponderance of negatively charged dirt particles in the atmosphere [5]. This fine dirt adheres so firmly that it is difficult to remove and causes serious soiling. When this occurs on the portion of cloth in a loom that is left exposed overnight, it is known as 'fog-marking'. The effects of attraction and repulsion were described by Robert Symmer in 1759, who used to wear two pairs of stockings, white worsted for comfort and black silk for appearance: on separating the stockings: 'the repulsion of those of the same colour, and the attraction of those of different colour, throws them into an agitation that is not unentertaining'.

Charged bodies are attracted to uncharged bodies. Consequently, fibres will stick to earthed parts of machines; this happens particularly in carding. When a charged yarn is passing through a guide, the extra-normal force due to this attraction may notably increase the friction. Another consequence is that uncharged particles in the atmosphere will be attracted to a charged material.

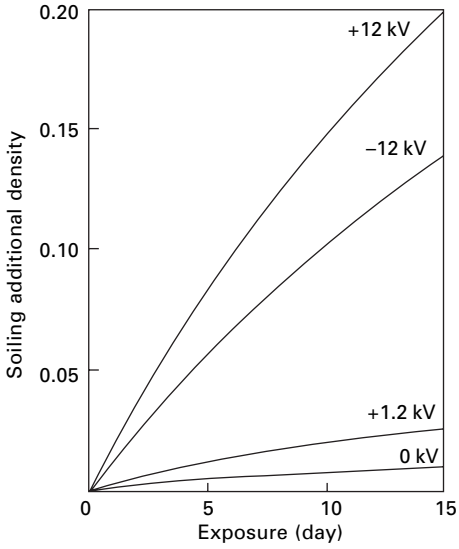

23.1 Effect of potential on soiling of cotton fabric. After Rees [5].

When high enough fields occur, discharge in air will take place with accompanying sparks. This is easily noticeable on taking off charged clothing. The noise of the discharge may be a nuisance in some special cases, for example in the fur hoods worn in arctic conditions. There is also a risk of fire or explosion owing to the sparks. This is a danger in the textile industry only in exceptional circumstances, but sparks from clothing are a source of danger where inflammable vapours are present, as in the operating theatres of hospitals. Shocks will be given to people coming into contact with static charges. These are only serious where a large insulated conductor (for example, a machine on an insulating floor) has become charged up. The remedy is to earth the machine. More commonly, individuals act as condensers with a large capacity. Walking on a carpet or sliding off a car seat can lead to accumulation of a large charge. On touching metal, a door handle or whatever, the discharge gives a nasty shock.

As discussed below, the limiting condition for high static charges, and hence the susceptibility to troubles in use, has been shown to depend on the resistance of the material. Low-resistance materials such as cotton and viscose rayon will rarely give static troubles; higher-resistance materials such as wool, silk and acetate will give trouble more often; and the very high-resistance synthetic fibres will give most trouble. The speed of the process is also important: thus, to avoid fog-marking in weaving, dissipation in 10 minutes, needing a total current of 0.003 μA, is adequate, but, to avoid trouble in carding, dissipation must take place in 0.1 s, which needs 0.07 μA; to avoid trouble in warping, it must take place in 0.01 s, which needs 5 μA.

Methods of getting rid of static charges depend upon increasing the leakage by lowering the resistance of either the material or the air, or by providing a conducting liquid at the separation. The resistance of the material may be lowered by raising the humidity or by moistening it. The resistance of the air may be lowered by ionising it,

either by using a high-voltage static eliminator or by the presence of a radioactive material. Safe concentrations of the latter are only sufficient to cause a slow discharge. The use of electrostatic eliminators in the textile industry has been described by Henry [6]. The use of anti-static agents is discussed by Sagar [7], Götze *et al*. [8] and Holme *et al*. [4]. Unfortunately, the hygroscopic salts that are the most effective anti-static agents are usually unsuitable for other reasons.

23.2 Measurement of static

The methodology can be illustrated by methods used in the earlier studies of textile charging. The principles remain the same, but advances in electronics have changed the devices used in electrical measurements [9]. The amount of static present should be expressed by the magnitude of the charge on the material. This may be measured by the use of a Faraday cylinder. Figure 23.2 shows the apparatus used by Keggin *et al.* [10] to measure the charge on card sliver after carding. The charged material in the cylinder induces an equal opposite charge on the inside of the cylinder (since there can be no net charge inside a closed conductor), and this leaves an equal charge, of the same sign as that on the material, to be shared between the outside of the cylinder and a condenser, which give a total capacitance C. The potential V is measured by a voltmeter and the charge Q can be calculated from the usual expression $Q = CV$.

When the specimen cannot be surrounded, even approximately, by a conductor, the potential to which a neighbouring conductor, the 'probe' electrode, comes may be used as a measure of the charge on the specimen. Unless the geometry is simple enough for the induction coefficients to be calculated, this can give only an arbitrary value. However, when the position, size, shape and charge distribution of the specimen remain constant, it is a useful method for obtaining relative values under different conditions. Some authors have replaced the specimen by a conductor of the same size and shape and, by raising this to known potentials, have obtained a calibration for what they refer to as 'the potential of the specimen'. It is, however, meaningless to

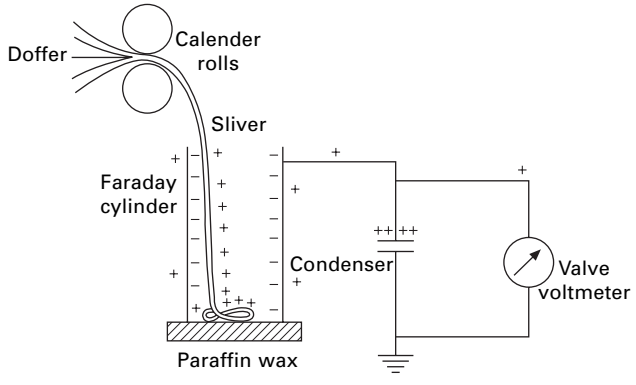

23.2 Measurement of charge by means of a Faraday cylinder. After Keggin *et al*. [10].

talk about the potential of an insulator, since only conductors come to an equal potential at all points.

The potential of the probe electrode may be measured either with a d.c. electrometer or by converting it into an alternating potential. Hayek and Chromey's method [11] (Fig. 23.3(a)), illustrates the latter technique. When the specimen, which has been charged by contact with the paddle, passes the probe electrode, an impulse is transmitted to the measuring circuit. The reading of the detector gives an arbitrary measure of the charge on the specimen. Since the input acts as a resistance/capacity differentiating circuit (Fig. 23.3(b)), it is important that the speed of the drum should be constant.

Another method of obtaining the charge on a specimen, which has been used by Medley [12] and by Gonsalves and van Dongeren [13], is to measure the charge remaining on the conductor from which the specimen is separated. This is illustrated in Fig. 23.4. The potential difference between the rod and earth is indicated on the electrometer, *V*. From a knowledge of the total capacity to earth, the charge left on the rod and the condenser can be calculated. It will be equal and opposite to the charge on the material, provided that no leakage has occurred to other points. If the capacity to earth is large, the rod will remain close to earth-potential but measurable during a test.

The use of electrostatic field meters and voltmeters to measure surface charge distributions is discussed by Seaver [14] and Durkin [15]. Ellison [16] describes a robotic method.

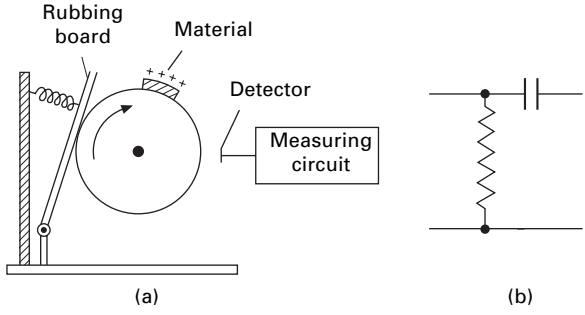

23.3 (a) Intermittent detection by probe electrode. After Hayek and Chromey [11]. (b) Effective input circuit.

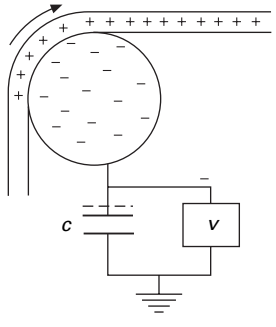

23.4 Measurement of charge remaining on conductor.

23.3 Results

23.3.1 Formation of charge

It was once thought that the conditions necessary for charges to appear were a difference between the nature of the surfaces and rubbing between them. It is now clear that either of these conditions by itself is sufficient. The mere separation of two unlike surfaces has been shown to result in a separation of charge, and Henry [17] and others have shown that the asymmetric rubbing of two identical surfaces results in a transfer of charge.

A familiar idea is that of an electrostatic series, in which materials can be arranged in an order such that, on the separation of any two materials, the higher on the list will be positively charged and the lower negatively charged. However, many workers have produced series that are inconsistent with one another, or have found it impossible to produce self-consistent lists. Henry [17] has shown that, provided that care is taken to minimise non-equilibrium effects due to friction, a series of ten materials could be placed in order with no significant inconsistencies. If the equilibrium charge separations at contact could be measured, not only should they be self-consistent in sign, but the magnitude of the charges should also be additively related to one another. Leakage usually prevents the testing of such a relation, but Harper [18] has shown that it holds for a number of metals. Hersh and Montgomery [19] also found a correlation of the magnitude of the charge generated when metals were rubbed on insulators with the work function[1] of the material and the position of the insulator in the series. Arridge [20] confirmed the correlation with the work function of the metal in experiments on nylon.

Table 23.1 gives the series found in three investigations. Polyamides and wool, which both contain —CO·NH— groups, are at the positive end; cellulose, acrylics and similar materials are in the middle; and the more inert polymers are at the negative end. Cohen [23] suggested that, on the separation of two materials, the one with the high permittivity would become positive; this rule is not of universal validity but may apply to a limited class of materials.

Reversals of the signs of charges owing to very slight (and sometimes undetected) changes of conditions have often been reported. These reversals must be associated with a change in the mechanism of charge transfer. Gonsalves and van Dongeren [13] frequently found a change from positive to negative, as shown later in Fig. 23.9(B)), on an insulator rubbed against a metal as the pressure increased, but they did not find the reverse change.

Martin [24] found that, when a wool fibre was pulled out by the root end from a bundle of wool fibres, all lying in the same direction, it became positively charged, whereas when it was pulled out by the tip end, it became negatively charged.

Owing to slight differences in the surface or the asymmetry in the rubbing, charges may easily be generated by inter fibre contact between apparently identical fibres.

[1]The work function of a metal is the energy needed by an electron in order to free itself from the metal.

Table 23.1 Electrostatic series

	Smith *et al.* [21]	Tsuji and Okada [22]	Hersh and Montgomery [19]
Positive (+)	Wool	Glass	Wooll
	Hercosett wool	Nylon 6.6	Nylon
	Nylon 6.6	Nylon 6	Viscose
	Nylon 6	Wool	Cotton
	Silk	Silk	Silk
	Regenerated cellulose	Viscose	Acetate
	Cotton	*Vinylon* (PVAlc)	*Lucite* (PMMA)
	Poly(vinyl alcohol) (PVA)	*Acrilan* (acrylic)	PVAlc
	Chlorinated wool	Steel	*Dacron* (polyester)
	Cellulose triacetate	Cotton	*Orlon* (acrylic)
	Calcium alginate	*Orlon* (acrylic)	PVC
	Acrylic	Acetate	*Dynel* (VC/AN)
	Cellulose acetate	*Dynel* (VC/AN)	*Velon* (VDC/VC)
	Polytetrafluoroethylene (PTFE)	*Saran* (PVDC)	Polyethylene
	Polyethylene	*Rhovyl* (PVC)	*Teflon* (PTFE)
	Polypropylene	Rubber	
	Poly(ethyleneterephthalate)		
	Poly(1,4-butylene terephthalate)		
	Modacrylic		
Negative (–)	Chlorofibre		

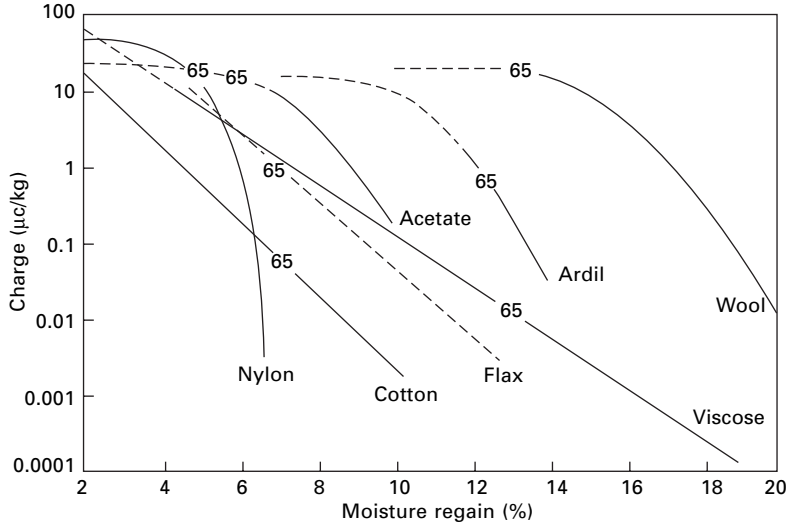

23.5 Charge left on sliver after carding, marking 65% at r.h. level. After Keggin *et al.* [10].

23.3.2 Magnitude of charge

Figure 23.5 shows the charges remaining on the sliver emerging from a card as measured by Keggin *et al.* [10]. It will be seen that at low regains all the materials acquire approximately the same charge. This charge remains constant as the regain

increases until a certain value is reached, and it then drops rapidly for further increases of regain. The points corresponding to 65% r.h. have been marked on the graph, and they illustrate the susceptibility of different fibres to static under the same atmospheric conditions. The amount of static necessary to cause processing difficulties varies from one material to another and is affected by the amount of crimp in the fibre.

Results similar to these have been obtained by Gonsalves and van Dongeren [13] and Medley [12, 25, 26]. The most convenient way of expressing the results is as surface-charge density in microcoulombs per square metre ($\mu C/m^2$). Figure 23.6 shows the charge on nylon film and Fig. 23.7 the charge on single fibres, drawn over platinum rods. It appears that, when the conductance is above a certain value, the charge observed falls rapidly as the conductance increases. A similar result (Fig. 23.8) is obtained when a wool roving that has been coated with a surface-conducting agent emerges from between rollers. The conductance necessary for the rapid drop in charge to start is affected by the speed with which the material is passing through the rollers; the higher the speed, the greater is the conductance necessary. This is shown by the results in Table 23.2. In practice, it is found that the cellulosic fibres are least troubled by static charges; wool and silk are intermediate; and acetate, nylon, polyester, acrylic and other synthetic fibres are most affected. This accords with their electrical resistances as given in Chapter 22.

Medley [26] found that the charge increased with the pressure applied to the rollers, probably owing to an increase in the true area of contact. Gonsalves and van Dongeren [13] found similar results (Fig. 23.9) when the contact pressure for rayon and nylon threads wrapped round a cylinder was increased by increasing either the pre-tension or the angle of wrap. The unfinished rayon thread is an example of the sign change with pressure mentioned earlier (Section 23.3.1). In his experiments

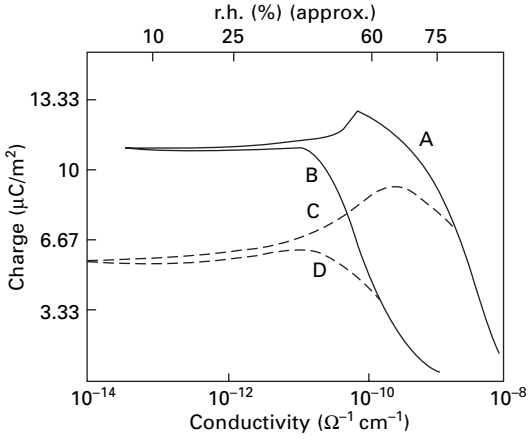

	A	B	C	D
Cylinder diameter (cm)	0.12	0.12	1.25	1.25
Film width (cm)	1	1	2	2
Load (mN)	150	150	50	50
Speed (cm/s)	10	0.5	10	0.5

23.6 Charge developed on nylon film pulled over platinum cylinder [12].

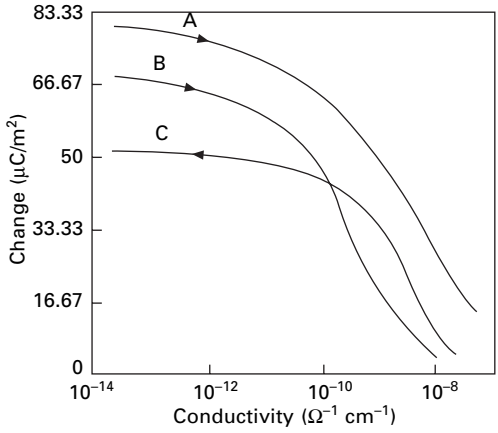

	A	B	C
Material	Nylon	Nylon	Wool
Diameter	20	20	45
Speed (cm/s)	10	0.5	10

23.7 Charge developed on single fibres pulled over 0.1 cm diameter platinum cylinder [12].

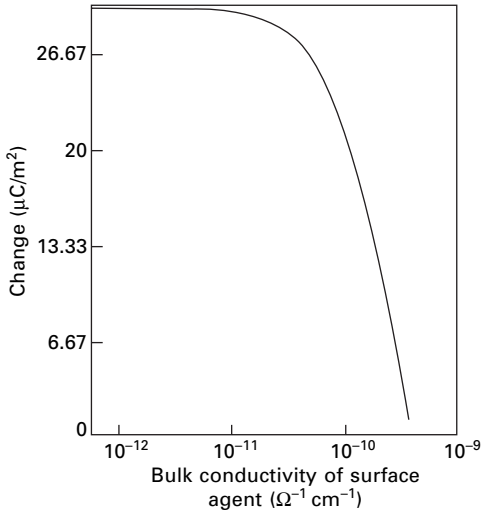

23.8 Electrification of wool roving coated with surface-conducting agent, on pulling through rollers at 10 cm/s [26].

with material emerging from rollers, Medley [26] also measured the charge lost to neighbouring conductors. When charged roving was passed through a small metal loop, its charge was reduced to less than 0.67 μC/m^2: a metal wire held 5 mm below the roving and a metal sheet held 5 cm below it were less effective in discharging the roving.

Lowering the atmospheric pressure reduces the charges that are obtained, as is shown in Fig. 23.10, except at low pressures. In a high vacuum large charges are

Table 23.2 Critical conditions for electrostatic charges (after Medley [25])

(a) Without surface-conducting agents

Material	Rollers	Speed (cm/s)	*Charge halved at:* r.h. (%)	conductance	$\frac{kt}{\varepsilon_0 \upsilon}$ or $\frac{ka}{2\varepsilon_0 \upsilon}$ (see Section 23.5.2) ($\Omega^{-1}\,m^{-1}\,s$)
Woollen taffeta	Steel	5.0	40	$1.2 \times 10^{-12*‡}$	2.8
		2.0	75	$0.4 \times 10^{-12*}$	2.1
		11.0	75	$1.6 \times 10^{-12*}$	1.6
Filter paper	Steel	11.0	40	$1.7 \times 10^{-12*}$	1.8
		15.0	40	$3.4 \times 10^{-12†‡}$	2.0
Wool roving	Cork	11.0	70	$3.6 \times 10^{-12†}$	2.9
a = 0.2 cm		1.25	70	$0.6 \times 10^{-12†}$	4.0

* Ω^{-1} for 1 cm length and breadth equals kt.
† Ω^{-1} for 1 cm length, equals $2\pi a$ (ka).
‡ KC1-treated.

(b) For wool roving with surface-conducting agent. Cork rollers

Aerosol *OT* in combing oil (%)	Bulk conductivity of agent ($\Omega^{-1}\,cm^{-1}$)	Speed at which charge reduced to 12 μC/m^2 (cm/s)
0	2×10^{-12}	Unobtainable
1	1×10^{-10}	3
3	2.5×10^{-10}	10

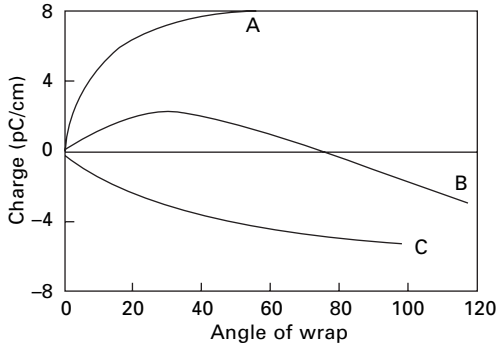

23.9 Effect of wrap on charge on yarn rubbed over steel rod [13]: A, finished rayon; B unfinished rayon; C nylon (approximately 20% r.h.).

obtained. Medley [25] found that, when the air was saturated with carbon tetrachloride, the charge on nylon film increased by 50%. On the other hand, ionising the air reduces the charges that can be obtained.

The maximum charge densities obtained by Medley were about 30 μC/m^2 on films, cloth, and roving and about 160 μC/m^2 on single fibres. Other workers have also found limiting values of about this amount. However, by an ingenious technique,

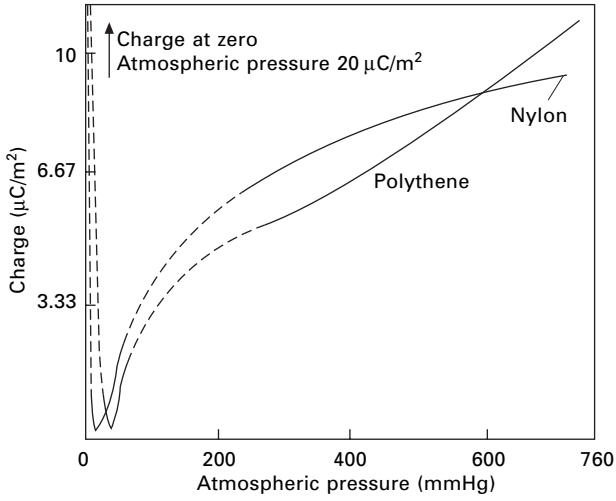

23.10 Effect of atmospheric pressure on charge left on films pulled over platinum wire [12].

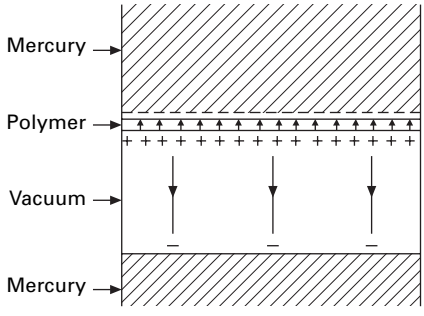

23.11 Charge distribution after separation of mercury from lower surface of polymer.

designed to reduce leakage, Medley [27] was able to obtain much higher values. He separated mercury from a thin layer of polymer, which had another layer of mercury on its opposite side. The whole experiment was carried out in a vacuum. After separation, the charge distribution and electric field will be as shown in Fig. 23.11. The almost equal charge induced on the adjacent layer of mercury after separation can be measured by the usual arrangement of an electrometer and condenser. As soon as the separation has become large compared with the thickness of the polymer, the field in the vacuum will be very small, so that leakage will be negligible. Leakage is possible when the separation is still small, but, under these conditions, the dielectric strength is greater and the insulation is very good. The larger the capacity of the polymer film, the smaller is the chance of leakage. Figure 23.12 shows the results of the experiments. Values of up to 1500 $\mu C/m^2$ were obtained, and it appears that higher values still are possible. If an external electric field is applied, there will be a charge transfer due to the field superimposed on the charge transfer due to the

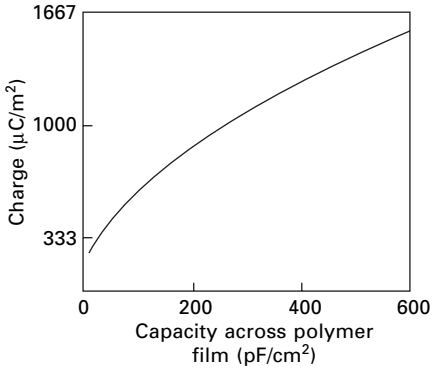

23.12 Charge left after separating polymer film from zinc amalgam [27].

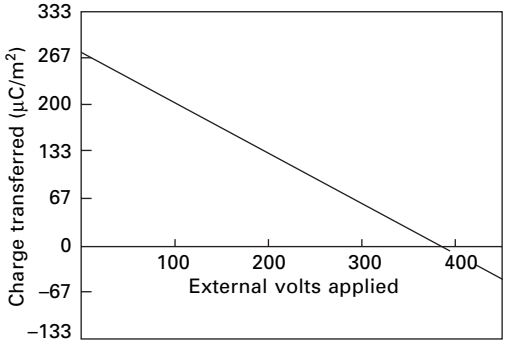

23.13 Effect of applied field on electrification of a nylon film [27].

difference in the two surfaces. According to the direction of the field, this may increase or reduce the charge transfer, and, if large enough, it can even reverse it (Fig. 23.13).

23.3.3 Anti-static treatments

The presence of oil on the surface will influence the charge obtained, as is shown in Table 23.3. Insulating oils may increase the charge, but conducting oils will decrease it. Table 23.4 gives some practical results for various types of anti-static agent. Values for the best and worst material of each type are included. For continued efficacy, finishes must not be lost by washing or wear.

Permanent anti-static behaviour is achieved by the use of conducting fibres. Fibres with moderate conductivity can be used instead of regular fibres in a product, but it is more common to use more highly conducting fibres in small quantities in a blend with other fibres. The inclusion of carbon black to give a conducting path, provided the particles are close enough together, was referred to in Section 22.4.3. However, this has the disadvantage of making the material black. Conductivity can be increased by incorporating hydrophilic groups by copolymerisation or by co-extrusion with a

Table 23.3 Effect of insulating and conducting oil [12]

Insulating oil – liquid paraffin Cowtail fibre – 140 μm diameter Platinum cylinder – 0.123 cm diameter				Conducting oil (180 μm fibre)		
Load on fibre (MPa)	Rubbing	Charge ($\mu C/m^2$) on:		Conductivity of oil ($\Omega^{-1}\,cm^{-1}$)	Rubbing speed (cm/s)	Charge (arbitrary units)
		clean fibre	oiled fibre			
0	Single	0	0	7.5×10^{-13}	5	28
1	Single	13	17	3×10^{-11}	5	8.4
5	Single	25	47	6×10^{-11}	5	1.8
0	Continued	0	0	7.5×10^{-13}	10	30
1	Continued	32	72	3×10^{-11}	10	15
5	Continued	47	94	6×10^{-11}	10	6.8

Table 23.4 Effect of various classes of anti-static agent [8]

Material treated with	Static charge (arbitrary units) 50% r.h.; winding at 180 m/min		
	Viscose rayon	Acetate	Nylon
(Untreated)	47	60	128
Hygroscopic salts	17–38	0–29	3–19
Polyalcohols	45–46	22–33	92–98
Soaps	35–48	21–32	64–88
Sulphonated fatty compounds	34–52	16–32	32–85
Non-ionogenic products	31–42	18–43	22–78
Cation-active products	32–54	15–38	31–62

conducting polymer. For example *DuPont* incorporated streams of colourless polymer in their anti-static nylon carpet fibres. Metal fibres, e.g *Bekinox* stainless steel fibres, which are made with diameters from 2 to 22 μm, have high conductivity.

A more extensive discussion of the chemistry, effectiveness and durability of the many ways of reducing static is given by Holme *et al*. [4].

23.4 Generation of charge

Henry [28–30] has summarised the chief hypotheses that have been put forward to explain the separation of charge on materials in contact. None of them has been convincingly proved to be the sole mechanism, and he suggests that probably all the mechanisms operate to varying degrees in different cases. Whenever two surfaces are brought into contact, it is likely that some charge transfer across the surface will occur, but the conditions that affect it need to be worked out. Some of the charge transfer will result from the equilibrium distribution of charged particles between the surfaces and some from kinetic effects due to such transient influences as temperature differences. It may be noted that the highest observed charges (1500 $\mu C/m^2$) would be explained by the transfer of relatively few charges: one electronic charge for every

$100\,nm^2$ ($10\,nm \times 10\,nm$) would be sufficient. This area would cover many hundreds of atoms.

It is therefore a general rule that, unless the electrical states of two materials are extremely well balanced, there will be a large transfer of charge when their surfaces are brought in contact. The theories discussed below as a justification for this generalisation suggest that charge densities of $10^5\,\mu C/m^2$ would be commonplace. These values are far in excess of what is observed in practice, where the charge levels are reduced by leakage after separation of the surfaces. It is very difficult to get two surfaces in perfect electrical balance, and, even if it were achieved, the balance would be very easily disturbed by the slightest change of conditions. Charge generation is therefore very difficult to avoid.

There is one possible exception to this rule. Charge separation does require the *movement* of some free charges (electrons or ions). If, in an extremely good insulator, there are no mobile ions or electrons at all, then the charge separation will not occur, although charges may be deposited on the material. This may explain why polypropylene fibres appear to cause fewer static problems than some other synthetic fibres, despite their very high resistance.

The various possible mechanisms of charge transfer, which were discussed in more detail in previous editions of this book, are as follows:

1. Difference in contact potential between two metals in contact, due to difference in energy levels of electrons.
2. Difference in energy levels involving insulators, complicated by the presence of forbidden bands and extra levels on the surface [31, 32].
3. Activation by pressure making lower energy levels accessible and leading to charge reversal from positive to negative [32], as in Fig. 23.9. The reverse is not observed.
4. Presence of mobile cations on an acidic surface or mobile anions on a basic surface. Medley [33] observed this effect due to salt linkages, $R—COO^{-+}H_3N$, in keratin. On treatment with HCl, this changes to R—COOH $Cl^{-+}H_3N$, giving a mobile Cl^- ion. Treatment with NaOH gives $R—COO^{-+}Na\ H_2N + H_2O$, with a mobile Na^+ ion. On separating keratin from filter paper, the charge reversed depending on the treatment.
5. Asymmetric rubbing leads to thermal gradient, due to action being distributed along a length of one surface and at one place on the other. Charged mobile particles will move from hot to cold.
6. Symmetrical rubbing may give local asymmetry due to high spots on the surfaces. This is illustrated by a distribution of opposite charges over the surface of a polyethylene sheet when it is rubbed against another sheet [17]. In another example, different charges are found when a fibre is drawn from a lock of wool with or against the scales [24].
7. A double layer on a surface may be rubbed off on to another surface.
8. Piezo-electric polarisation due to pressure may lead to charge separation. In wool, pressure leads to the root end becoming negative and the tip end positive, which Martin [24] suggests may be the cause of the charging of wool withdrawn from a lock.

9. A pyro-electric effect at hot spots. Martin [24] found that wool became negatively charged at the root end on immersion in liquid air.

Henry [28–30] combines the first three mechanisms in an instructive example, which is simplified in that it considers the transfer of only one type of particle and uses classical mechanics, which will not be valid if electrons are involved. For electrons, quantum mechanics should be used. A charged particle between two surfaces is repelled by short-range forces when it is very near one of the surfaces, but it is attracted to the surface by the induced 'image' electrostatic forces when it is at a greater distance away. The combination of these forces results in the potential energy diagram shown in Fig. 23.14(a).

We consider unit area with n_1 ions on the first surface, which is at a temperature T_1, and n_2 ions on the second surface at a temperature T_2. The number of ions crossing the barrier $(V_m - V_1)$ per unit area per unit time will be proportional to $n_1 T_1^{\lambda} \exp[-(V_m - V_1)/k\,T_1]$. The index λ varies according to the particular theory in statistical mechanics employed and need not be specified here. Quantum mechanics would give a less simple energy term, owing to the possibility of the passage of particles through the barrier by means of the tunnel effect. There will be a similar loss of ions from the second surface over the barrier $(V_m - V_2)$. The difference in transfer rates will cause a separation of charge and will give rise to an electrostatic field, which will change the potential energy diagram. This will continue until the electrostatic field is such as to equalise the rates of transfer from each side. If E_1 and E_2 are then the electrostatic potentials at the surfaces, and E_m that at the position of maximum total energy, and if V_m is also now taken at this position (Fig. 23.14(b)) the rate changes to $n_1 T_1^{\lambda} \exp\{[-(V_m - V_1) + e\,(E_m - E_1)]/k\,T_1\}$, where e is the charge on the ion. There is an analogous expression for the reverse direction. Equilibrium will occur when the two rates are equal. An external electric field F, which also changes the height of the barrier, can be added to the model.

The analysis continues so as to predict the charge densities $\pm Q$ on surfaces separated by a distance D. We write $(V_1 - V_2) = (W_2 - W_1) = \Delta W$, where W_1 and W_2 are the amounts of work needed to remove the type of ion concerned from the surfaces into a vacuum and $V + eE = U$. The value of Q is given by:

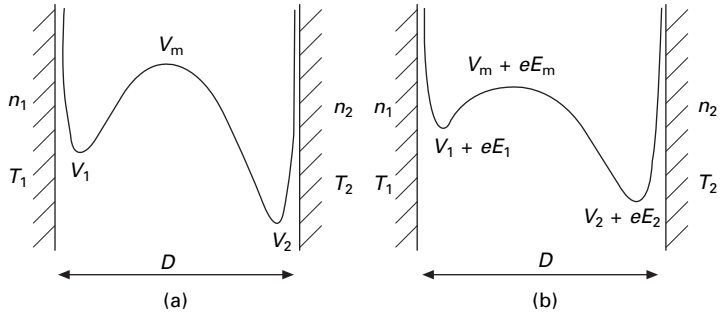

23.14 Potential energy of charged particles between two surfaces: (a) in absence of electrostatic field; (b) at equilibrium, with electrostatic field.

$$4\pi eDQ = -\Delta W + kT\log_e\left(\frac{n_2}{n_1}\right) + \Delta T/T\left(\lambda kT + U_m - \frac{U_1 + U_2}{2}\right) - eDF \tag{23.1}$$

In this expression, $-\Delta W$ represents the difference in energy levels, that is, the contact potential of mechanisms 1 and 2. The second term represents the effect of the different concentrations, n_1 and n_2, on the two surfaces, that is, mechanism 3. The third term gives the effect of the difference in temperature, ΔT, between the two surfaces, that is, mechanisms 4 and 5. Of this term, the first part within the brackets is an effect similar to thermal diffusion, while the other terms derive from the potential energy 'hump' that has to be overcome. The final term in the expression represents the effect of an external field, which gives rise to an additional charge density sufficient to produce an equal and opposite field. This example illustrates how the various effects combine together. The other mechanisms listed may also come in as additional effects.

Charges as great as those which would be predicted on these theories, amounting to more than $10^5\,\mu C/m^2$, are rarely observed in practice. Leakage, through either the air or the material, usually occurs and limits the observable charge. This fact makes experimental investigation of charge generation difficult. Leakage also explains the absence of a difference in magnitude of the charge obtained from the distance apart in the electrostatic series and the apparent abruptness with which reversals of charge occur. Whereas the original charge separation may vary continuously from a high positive to a high negative value as conditions change, the observed charge will drop in a step from a constant positive value to a constant negative value, as is illustrated in Fig. 23.15.

23.5 Leakage of charge

23.5.1 Leakage in air

As discussed above, the inherent magnitude of charge separation is much greater than observed charges, unless the two surfaces are almost perfectly balanced. The

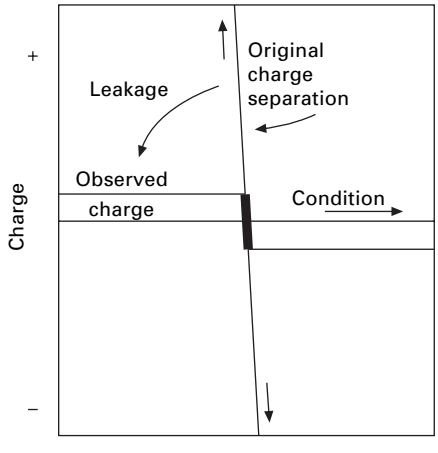

23.15 Original and observed charge separation.

observed charges depend primarily on the extent to which the charge can leak away and this can happen in a variety of ways.

When the material is completely non-conducting, leakage through the air is the only factor that limits the static charge and it is an important factor in materials with low conductivity. The breakdown potential of air at atmospheric pressure is 30 kV/cm, and this means that the maximum charge which can exist on a plane surface is about 30 μC/m^2. For a sheet with two surfaces, 60 μC/m^2 should be possible, but, in fact, uneven charging and irregularity of the surface usually prevent more than half this amount from being observed. If the material is passing over a rod, the leakage will occur through the air back to the rod, as shown in Fig. 23.16. The presence of other neighbouring conductors may cause a concentration of lines of force, as shown in Fig. 23.17, resulting in a discharge to the conductor and leaving a smaller charge density on the material. This has been found by Medley [26], who has discussed the conditions necessary to cause the greatest discharge. The field strength will also be influenced by the shape of the specimen and by the presence of neighbouring charges. For example, single fibres can support high surface charges (about 150 μC/m^2) owing to the rapid decrease of field strength as the lines of force diverge from the fibre. Where fibres are grouped together, as in a roving, however, such high fibre-surface charges are not possible, since the combined field at the outside of the roving would then exceed the dielectric strength of the air.

It is the limitation of charge by conduction in air that results in the constant portion of the curves of charge versus relative humidity or conductance of the material. There may even be a slight increase (as in Fig. 23.6) since, under some conditions, the dielectric strength of air is greater at a higher humidity. Near atmospheric pressure,

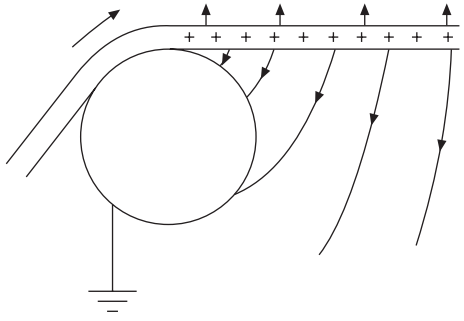

23.16 Electrostatic field causing leakage through air back to rod.

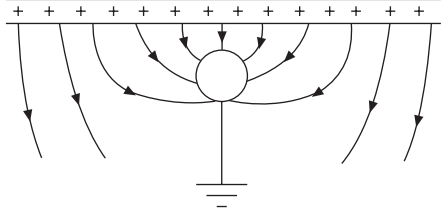

23.17 Concentration of lines of force due to neighbouring conductor.

the dielectric strength of air decreases as the pressure drops, which results in a decrease in the observed charge (Fig. 23.10), but in a good vacuum the dielectric strength is high and the observed charges are high. The particular advantage of Medley's technique [27] of backing a thin film of polymer with mercury (see Section 23.3.2) is that the field due to the charge decreases rapidly as the separation of the surfaces increases. In a sufficiently narrow gap, the ions present cannot accelerate enough for ion multiplication by collision to occur; consequently, the breakdown strength increases. At atmospheric pressure, this increase in dielectric strength occurs when the gap is reduced to a few microns, but at low pressures it occurs at greater thicknesses. Thus in the initial stages of the separation, while the field is high, the dielectric strength is also high.

Anything that increases the dielectric strength of the atmosphere, such as saturation with carbon tetrachloride, results in an increase of the limiting charge that can be obtained. Conversely, lowering the resistance of the air by ionising it reduces the limiting charge. Static eliminators, which apply a high voltage to metal points, work on this principle. Alternatively, radioactive material will ionise the air.

To make a complete quantitative analysis of the charge left on the separated material after leakage has occurred, one would need to work out the distribution of electric field in the system and the currents that would flow as a result of the electric field. Working out the field is a complex problem owing to the disturbing influence of dielectrics and conductors in the system. The mathematical difficulty is further increased when current flows, since this alters the charge distribution and consequently alters the electric field producing the current.

The electric fields are determined not only by the charge on the insulator but by image charges in the neighbouring conductor. Medley [12], neglecting the effect of the dielectric constant of the material and using an approximate image system, worked out the field due to an approximately uniform charge distribution on a thin sheet of material separated from a conducting cylinder and parallel to a conducting plane. It can then be seen where the dielectric strength of the air is exceeded. By analysis or successive approximation, a modified charge distribution, taking account of the leakage in air, can be worked out.

In practice, an approximate value can be obtained by assuming that just beyond the point of separation, or just beyond a conductor whose influence is being considered, the charge density is reduced to a uniform value, σ_a, giving a field equal to the dielectric strength of air, E_{crit}. For a plane surface, by the application of Gauss's theorem, this gives:

$$\sigma_a = \frac{2\varepsilon E_{crit} \cos\theta}{\alpha} \tag{23.2}$$

where ε = permittivity of air ≈ permittivity of vacuum, α = ratio of the normal flux density to the average normal flux density on both sides of the surface, and θ = angle between lines of force and the normal to the surface.

High values of θ will be dominant, giving cos = 1 at 90°. The ratio α will be limited to values between 0 and 2, and, unless there are marked disturbing effects due to dielectrics or conductors near the charged surface, it will be approximately equal

to 1. Thus $(\cos\theta/\alpha) \sim 1$. With $\varepsilon_0 = 8.85$ pF and $E_{crit} \sim 4$ MV/m, this indicates a maximum charge density of the order of 10 μC/m^2 in accord with the usual observations. It will be lower when the electric field is concentrated and higher when special precautions are taken to limit the discharge.

23.5.2 Leakage in the material

As soon as the resistance of the material becomes low enough for appreciable current to flow through it, the observed charge starts to decrease. Since a small increase in humidity causes a large increase in conductance, the curve of charge against relative humidity then drops rapidly, as is shown in Figs 23.6–23.8.

Once again, exact analysis is difficult, but the influence of the material may be illustrated diagrammatically. In a perfect insulator (Fig. 23.18(a)), no current flows through the material and a charge, limited by air leakage, remains on the surface. In a moderate insulator (Fig. 23.18(b)), the charge left after leakage through the air can spread out from the surfaces where it first appears. This gives an electric field acting back along the material, since at a distance the effect of the double layer is negligible.

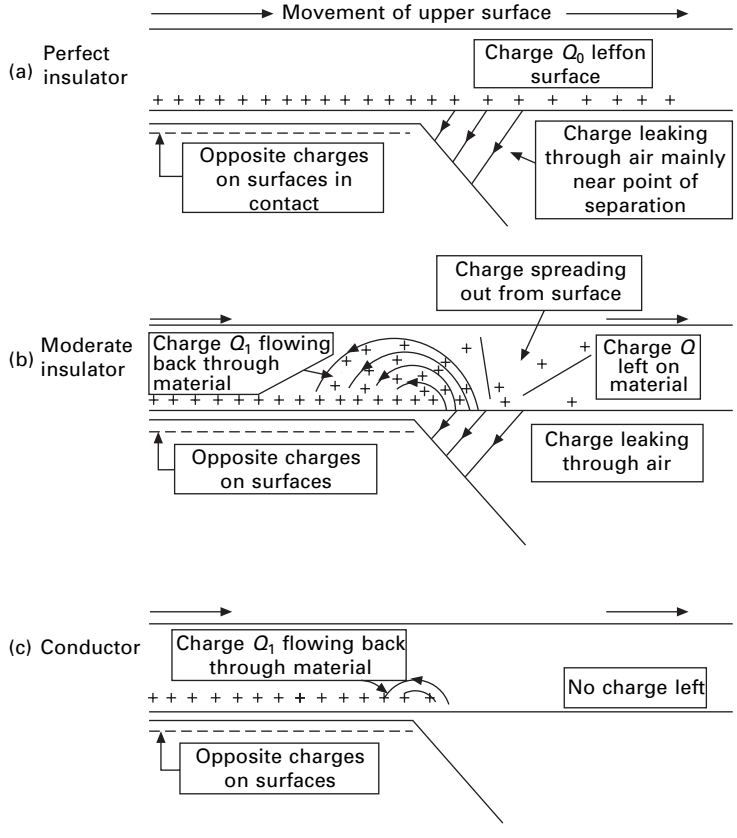

23.18 Leakage of charge in (a) perfect insulator, (b) moderate insulator and (c) conductor.

Some charge will flow back behind the point of separation and become a source of charge for the double layer at the surfaces in contact. In a good conductor (Fig. 23.18(c)), there will be a large backward current and the charge will never get far beyond the point of separation but will, in effect, be circulating near the surfaces in contact, and never penetrating deeply into the material.

The currents will flow in the reverse direction to the movement of the material that is carrying charge forward. Consequently, the greater the speed of the material, the smaller will be the reduction of charge for a given conductance. This means that the higher the speed of a process, the more likely is the occurrence of static charges.

If we consider unit width of material (Fig. 23.19), of thickness t and conductivity k, moving with a velocity v, and having a charge per unit area σ (not necessarily all on the surface), then the rate of transport of charge past a given point owing to the movement of the material is σv. If there is an electric field E, with a component ($E \sin\phi$) in the opposite direction to the motion, the current flowing will be ($E \sin\phi \cdot kt$). The net rate of transfer of charge is therefore ($\sigma v - E \sin \phi \cdot kt$).

In the steady state, this must be equal at all points along the material, and a relation between σ and $E \sin \phi$ is thus established. If σ' is the limiting charge per unit area left on the material at a long distance from the point of separation, we must have:

$$\sigma' v = \sigma v - E \sin \phi \cdot kt \tag{23.3}$$

$$\sigma' = \sigma - E \sin \phi \frac{kt}{v} \tag{23.4}$$

Using this relation, and deriving values of E from the approximate image system, Medley [12] worked out, by successive approximations, the charge distribution in the steady state for material coming off a cylinder of unit diameter. This shows that, owing to the influence of the induced charge on the cylinder, a maximum in the charge on the material occurs some distance beyond the point of separation and thus most of the current will finally reach the cylinder by discharge across the gap, rather than by conduction behind the point of separation. This effect is less marked when the ratio of thickness of material to diameter of cylinder is greater.

We may obtain an approximate expression for σ' in the following way. For surface charge on a dielectric material remote from conductors, the field in the dielectric is ($\sigma/2\ \varepsilon_r\ \varepsilon_0$). We may therefore put $E \sin \phi = \Phi\sigma/2\varepsilon_0$, where it follows from the geometry of Fig. 23.20 that $\Phi = (2 - \alpha) \tan \phi/\varepsilon_r$ and is a dimensionless function

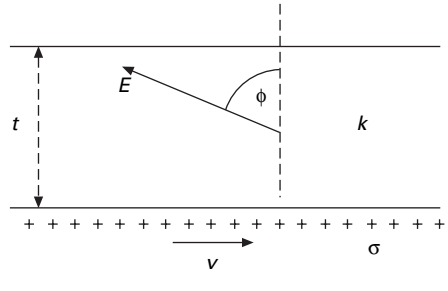

23.19 Field in specimen.

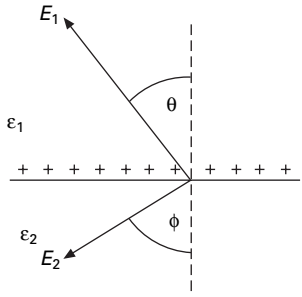

23.20 Effect of surface charge. If σ is the surface density of charge and E_1 and E_2 are electric fields making angles θ and ϕ with the surfaces of two media of permittivity ε_1 and ε_2, then by Gauss's theorem: $\varepsilon_1 E_1 \cos\phi + \varepsilon_2 E_2 \cos\phi = \sigma$. Hence:

$$\phi = \frac{\varepsilon_1 E_1 \cos\theta}{\frac{1}{2}(\varepsilon_1 E_1 \cos\theta + \varepsilon_2 E_2 \cos\phi)} = \frac{2\varepsilon_1 E_1 \cos\theta}{\phi}$$

$$= 2\,\varepsilon_r\,\varepsilon_0\,E_1\cos\theta/\sigma,$$

where ε_r is the relative permittivity of medium 1 and ε_0 is the permittivity of a vacuum.

depending on the relative permittivity and the field distribution in the particular system.

Substituting in equation (23.3), we get:

$$\sigma' = \sigma\left(1 - \frac{\Phi k t}{2\varepsilon_0 v}\right) \tag{23.5}$$

Near the point of separation, σ will drop to the value σ_a, limited by air discharge given by equation (23.2), and we have[2]:

$$\sigma' = \sigma_a\left(1 - \frac{\Phi k t}{2\varepsilon_0 v}\right) = \frac{2\varepsilon_0 E_{crit}\cos\theta}{\alpha}\left(1 - \frac{\Phi k t}{2\varepsilon_0 v}\right) \tag{23.6}$$

It follows from this equation that the charge remaining on the material is a fraction of the maximum value determined for different systems by the value of (kt/v). It can be noted that kt is the conductance (reciprocal of resistance) per unit width per unit length. The charge will drop to half the maximum value when $(kt/\varepsilon_0 v)$ equals $1/\Phi$. Considering that values of (kt/v) cover a range of at least a million to one, the results given in Tables 23.2 and 23.5 support this view and indicate that $1/\Phi$ lies between 1 and 7.

[2]The various expressions quoted here will only be correct in a consistent set of units. In SI units, this means that the conductivity k should be in $\Omega^{-1}\,m^{-1}$, the thickness t in m, and the velocity v in m/s. The permittivity ε_0 is in the usual units (F/m or $kg^{-1}\,m^{-3}\,s^4\,A^2$) and has the value 8.85×10^{-12} F/m. The product (kt/v) will have the units $\Omega^{-1}\,m^{-1}\,s$, which also, as should be the case, are equal to $kg^{-1}\,m^{-3}\,s^4\,A^2$. We may note that $kt/2v$ will have the same units if k is expressed in $\Omega^{-1}\,cm^{-1}$ and t in cm, with v in m/s.

Table 23.5 Critical conditions for reduction of charge [12]

$\frac{kt}{v}$ or $\frac{ka}{2v}$	Values of fraction of maximum charge for systems below						
(Ω^{-1} m^{-1} s)	A	B	C	D	E	F	G
1.3					0.71	0.56	0.67
1.6	0.91	0.80	0.96	0.91			
6.3	0.45	0.52	0.67	0.65			
12.6	0.30	0.30			0.24	0.25	0.19

System	25 μm Nylon strip on platinum cylinder			
	Width (cm)	Load (mN)	Cylinder diameter (cm)	Speed (cm/s)
A	1	150	0.12	0.5
B	1	150	0.12	10
C	2	50	1.25	0.5
D	2	50	1.25	10

Single fibres, 0.1 cm platinum cylinder

	Material	Diameter (μm)	Speed (cm/s)
E	Nylon	20	0.5
F	Nylon	20	10
G	Wool	45	10

Equation (23.6) will cease to hold when kt/v becomes large, and the expression approaches zero and then becomes negative. The derivation is only valid when the current flow is relatively small.

As ε_r increases, the line of force would tend to concentrate in the dielectric material, which would increase ϕ. So, as a rough approximation, $\tan \phi = \varepsilon_r \tan \theta$, which indicates that $\Phi \approx (2 - \alpha) \tan \theta$. For $\theta = 20°$ and $\alpha = 1$, this would make $1/\Phi$ equal to 2.8, in agreement with the experimental results.

For a cylindrical specimen of radius a, equation (23.5) changes to:

$$\sigma' = \sigma\left(1 - \frac{\Phi k a}{4\varepsilon_0 v}\right) \tag{23.7}$$

23.5.3 An alternative leakage equation

The expression $E \sin \phi = \Phi\sigma/2\varepsilon_0$ above (21.11) is an approximation because the charge causing the electric field E will be not the unreduced value σ but some average of values between σ, near to the point of separation, and σ', at a remote position. This is the source of error in the derivation, which makes the equation invalid for large values of kt/v. If we adopt the other extreme possibility, we put $E \sin \phi = 2\pi\sigma'\Phi$. This leads to:

$$\sigma' = \sigma\left(1 + \frac{\Phi k t}{2\varepsilon_0 v}\right)^{-1} \tag{23.8}$$

A comparison of the predictions of the two equations (23.5) and (23.8) is shown in Fig. 23.21. The actual behaviour should lie between the predictions of the two equations, as indicated by the dotted lines.

23.5.4 The action of a surface coating

It has already been mentioned that, when the material is a good conductor, the leakage does not penetrate deeply into the material. Consequently, a thin permanent conducting layer on the surface of a fibre would reduce static charges, but Medley [12] has pointed out that the action of a surface dressing may be slightly different from this.

A liquid dressing may not separate the two materials but may instead form a wedge-shaped film at the point at which they diverge from one another, as shown in Fig. 23.22. This liquid will act as a leaky dielectric, and dissipation of charge will occur owing to current flow across it. The time constant of a condenser is independent of its size and shape, and the decay of charge is given by the relation $\sigma = \sigma_0 \exp(-tk/\varepsilon)$ where σ_0 is the initial charge density, σ is the charge density at time t, ε is the permittivity of the liquid, and k is its conductivity. If v is the speed of the material and δ the length of the wedge, the time for a given portion of material to pass the liquid is δ/v, and therefore:

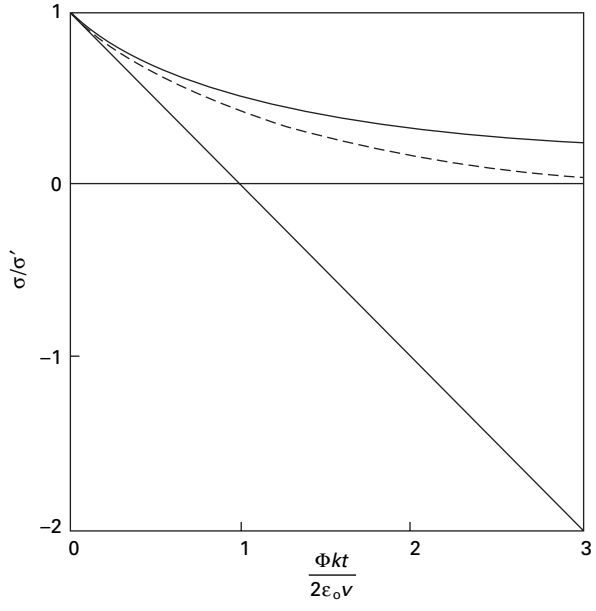

23.21 Comparison of prediction of equations (23.5) and (23.8), with indication (dotted) of likely real relation.

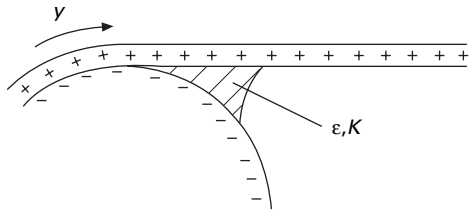

23.22 Wedge-shaped film at point of separation.

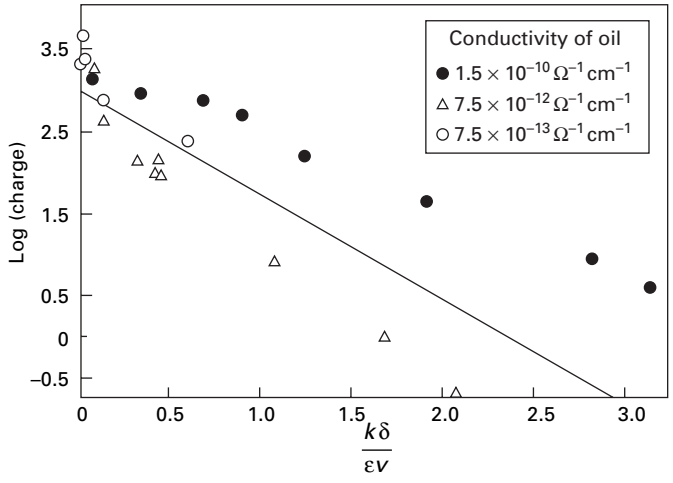

23.23 Reduction of charge on wool fibre due to conducting oils [12]. The line represents equation (23.10). Charge is in arbitrary units.

$$\sigma = \sigma_0 e^{-k\delta/\varepsilon v} \tag{23.9}$$

$$\log_e \frac{\sigma}{\sigma_0} = -\frac{k\delta}{\varepsilon v} \tag{23.10}$$

Figure 23.23 shows an experimental check of this relation for varying rubbing speeds and three different mixtures of liquid paraffin and Lubrol MO.

It will be seen from equation (23.9) that the condition for marked reduction of electrification is $\varepsilon v < k\delta$. It may be noted that the quantity $k\delta/\varepsilon v$, equal to $k\delta/\varepsilon_r\varepsilon_0 v$, is a dimensionless parameter.

It follows from this view of the action of an anti-static agent that it need not be present on the fibres but can be present on the guide or roller in order to give the wedge-shaped film. Medley [12] found that a porous cast-iron roller, impregnated with *Empilan* A (conductivity of $10^{-7}\,\Omega^{-1}\,cm^{-1}$), produced negligible static in worsted drawing, in contrast to the behaviour of an ordinary roller. This procedure does not, of course, meet the need for a permanent anti-static dressing to prevent the troubles due to static in use.

If the liquid is not a conductor, leakage will not occur, and the observed charges may even increase (as in Table 23.3), owing to the greater dielectric strength of the

liquid than that of air. This will reduce discharge in the region near the point of separation where the field is greatest.

Graham [34] has taken a rather different view of the action of anti-static agents. Figures 23.24 and 23.25 show the effect of five liquids on the charge given when nylon is rubbed over brass. He suggests that if it is thick enough, the liquid film prevents the contact potential between the two surfaces from becoming effective and that, if separation then occurs within the film, no charge will result. He associates the more effective action of the liquids with the higher dielectric constants to their greater degree of shielding. For this mechanism to be effective, the liquid film must be reasonably isotropic. With the surface-active agents, Fig. 23.25, the molecules are regularly oriented, and reversals in their effect occur as increasing amounts are applied. The reversals correspond to successive monomolecular layers and will be associated with the surfaces changing from polar to inert groups and vice versa. With triethanolammonium oleate, the regularity breaks down with larger amounts, but it persists to thick layers with potassium oleate.

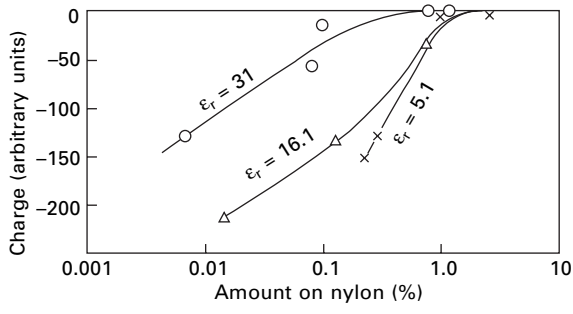

23.24 Effect of relative permittivity ε_r of surface dressing on charge. After Graham [34].

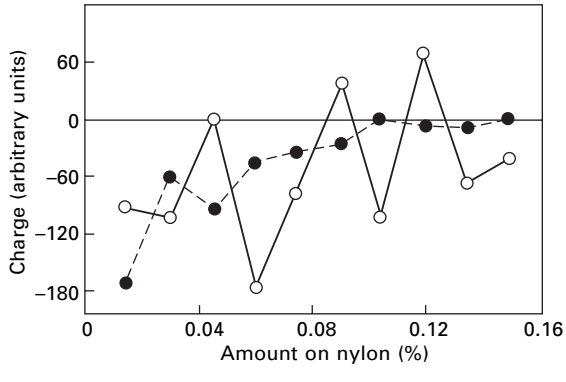

23.25 Effect of surface activity on charge: ○ potassium oleate; ● Dotted line: triethanolammonium oleate. After Graham [34].

23.6 References

1. *Brit. J. Appl. Phys.*, 1953, Supplement No. 2: 'Static Electrification' (report of Conference).
2. *J. Text. Inst.*, 1957, **48**, P4: 'Static Electricity in Textiles' (report of Conference).
3. D. F. Arthur. *J. Text. Inst.*, 1955, **46**, T721 (review of literature).
4. I. Holme, J. E. McIntyre and Z. I. Shen *Textile Progress*, **28**, No. 1, 1998.
5. W. H. Rees. *J. Text. Inst.*, 1954, **45**, P612.
6. P. S. H. Henry. *Brit. J. Appl. Phys.*, 1953, Suppl. No. 2, S78.
7. H. Sagar. *J. Text. Inst.*, 1954, **45**, P206.
8. K. Götze, W. Brasseler and F. Hilgers. *Melliand Textilber.*, 1953, **34**, 141, 220, 349, 451, 548, 658, 768.
9. P. E. Secker and J. N. Chubb. *J. Electrostatics*, 1984, **16**, 1.
10. J. F. Keggin, G. Morris and A. M. Yuill. *J. Text. Inst.*, 1949, **40**, T702.
11. M. Hayek and F. C. Chromey. *Amer. Dyest. Rep.*, 1951, **40**, 164.
12. J. A. Medley. *J. Text. Inst.*, 1954, **45**, T123.
13. V. E. Gonsalves and B. J. van Dongeren. *Text. Res. J.*, 1954, **24**, 1.
14. A. E. Seaver. *J. Electrostatics*, 1995, **35**, 231.
15. W. J. Durkin. *J. Electrostatics*, 1995, **35**, 215.
16. M. S. Ellison. *J. Textile Inst.*, 1991, **82**, 512.
17. P. S. H. Henry. *Brit. J. Appl. Phys.*, 1953, Suppl. No. 2, S31.
18. W. R. Harper. *Proc. Roy. Soc.*, 1951, **A205**, 83.
19. S. P. Hersh and D. J. Montgomery. *Text. Res. J.*, 1955, **25**, 279.
20. R. G. C. Arridge. *Brit. J. Appl. Phys.*, 1967, **18**, 1311.
21. P. A. Smith, G. C. East, R. C. Brown and D. Wade. *J. Electrostatics*, 1988, **21**, 81.
22. W. Tsuji and N. Okada. Cited by I. Skurada in *Handbook of Fiber Science and Technology*, Vol. IV, *Fiber Chemistry*, M. Lewin and E. M. Pearce (Editors), Marcel Dekker, New York, USA, 1985, p. 580.
23. A. Cohen. *Ann. Phys.*, 1898, **64**, 217.
24. A. J. P. Martin. *Proc. Phys. Soc.*, 1941, **53**, 186.
25. J. A. Medley. *Nature*, 1950, **166**, 524.
26. J. A. Medley. *Brit. J. Appl. Phys.*, 1953, Suppl. No. 2, S23.
27. J. A. Medley. *Brit. J. Appl. Phys.*, 1953, Suppl. No. 2, S28.
28. P. S. H. Henry, *Brit. J. Appl. Phys.*, 1953, Suppl. No. 2, S6.
29. P. S. H. Henry, *Sci. Prog.*, 1953, No. 164, 617.
30. P. S. H. Henry. *J. Text. Inst.*, 1957, **48**, P5.
31. F. A. Vick. *Brit. J. Appl. Phys.*, 1953, Suppl. No. 2, S1.
32. V. E. Gonsalves. *Text. Res. J.*, 1953, **23**, 711.
33. J. A. Medley. *Nature*, 1953, **171**, 1077.
34. G. W. Graham. *Nature*, 1951, **168**, 871.